Cold Plasma: Dynamics and Consequences* In Geospace

(* Selected)

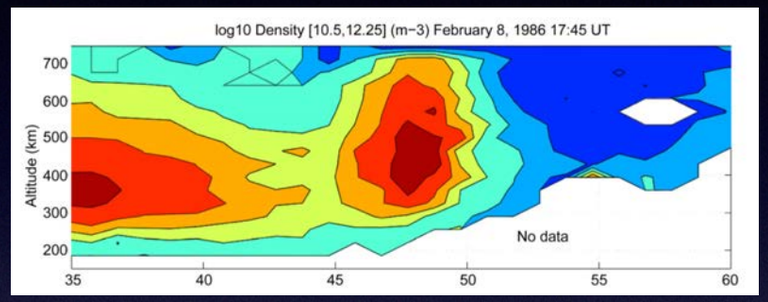

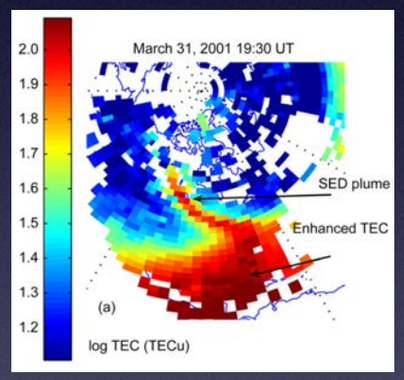

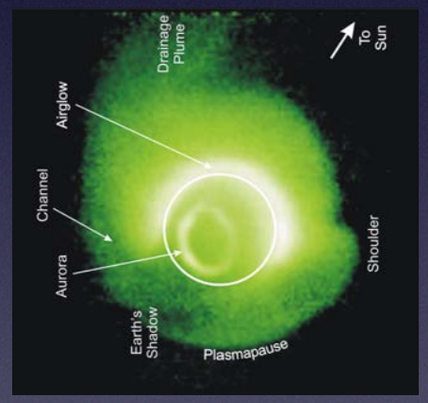

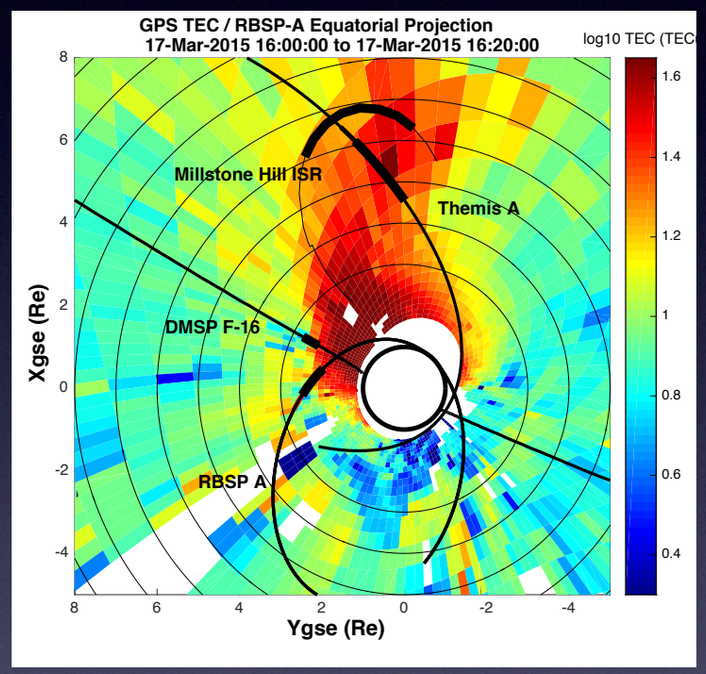

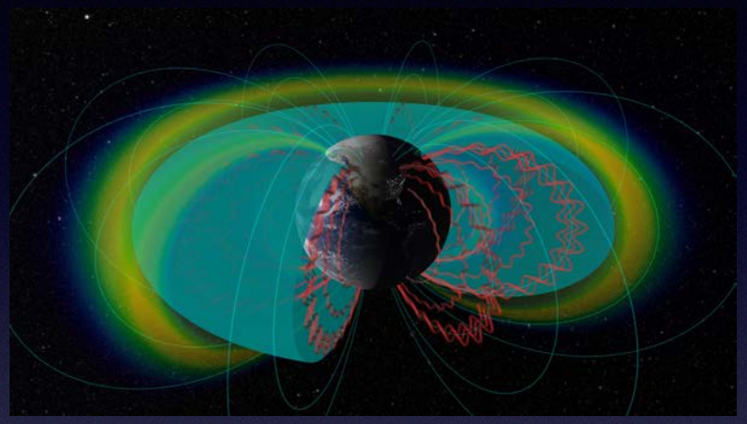

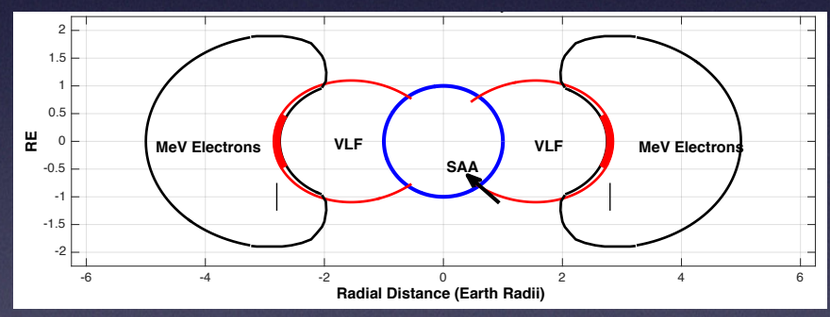

Special thanks to:
J. C. Foster, A. J. Coster, S.-R. Zhang, W. Rideout, B. Walsh, D. Welling
MIT Haystack Observatory Atmospheric and Geospace Sciences group
DMSP, IMAGE, Van Allen Probes, THEMIS, MMS teams

P. J. Erickson
MIT Haystack Observatory

CEDAR/GEM
Santa Fe, NM June 23, 2016

Outline

NB: This talk focuses on cold plasma starting its life with energies 0.1 to a few eV

- Basics of Ionospheric Cold Plasma Production
- Geospace Plasma Structuring
- Cold Plasma Influences In Geospace:

1. Ionosphere-Magnetosphere Feedback
2. Cold Plasma Effects At The Magnetosphere Boundary
3. Radiation Belt Dynamics: Cold Plasma Influence

Outline

- Basics of Ionospheric Cold Plasma Production
- Geospace Plasma Structuring
- Cold Plasma Influences In Geospace:

1. Ionosphere-Magnetosphere Feedback
2. Cold Plasma Effects At The Magnetosphere Boundary
3. Radiation Belt Dynamics: Cold Plasma Influence

Cold Plasma Sources

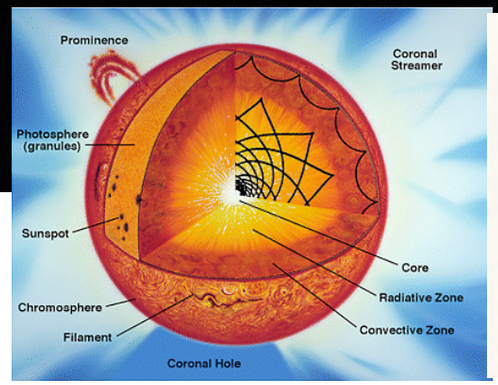

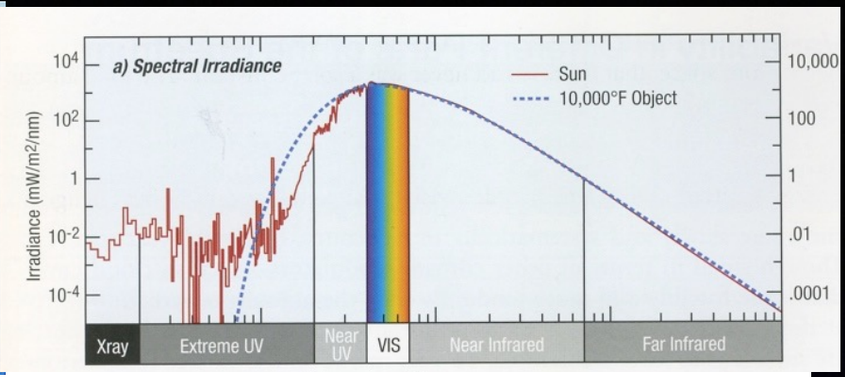

$$q(z) = [\text{density}]\,[\text{cross-section}]\,[\text{flux at z}]$$
$$= n(z)\sigma[F_0 e^{-\tau(z)/\mu_0}],$$

$\mu_0 \equiv \cos\chi_0$ ← Solar zenith angle

$\tau(z) \equiv \sigma \int_z^\infty n(z)\,dz$ Absorption depth (sigma = absorption cross-section)

$n(z) = n_0 e^{-z/H}$ Isothermal atmosphere

Solve.. → $\tau(z) = \sigma n_0 H e^{-z/H}.$

Production rate $\ln q(z) = \ln(\sigma n_0 F_0) - \frac{z}{H} - \frac{\sigma n_0 H}{\mu_0} e^{-z/H}.$

Extrema: $\frac{d}{dz}\ln q(z) = -\frac{1}{H} + \frac{\sigma n_0 H}{H\mu_0} e^{-z/H} = 0$

Max prod. rate: $\frac{\sigma n_0 H}{\mu_0} = e^{z/H}.$

So where production = loss, $z_{\max} = H \ln\left(\frac{\sigma n_0 H}{\mu_0}\right);$

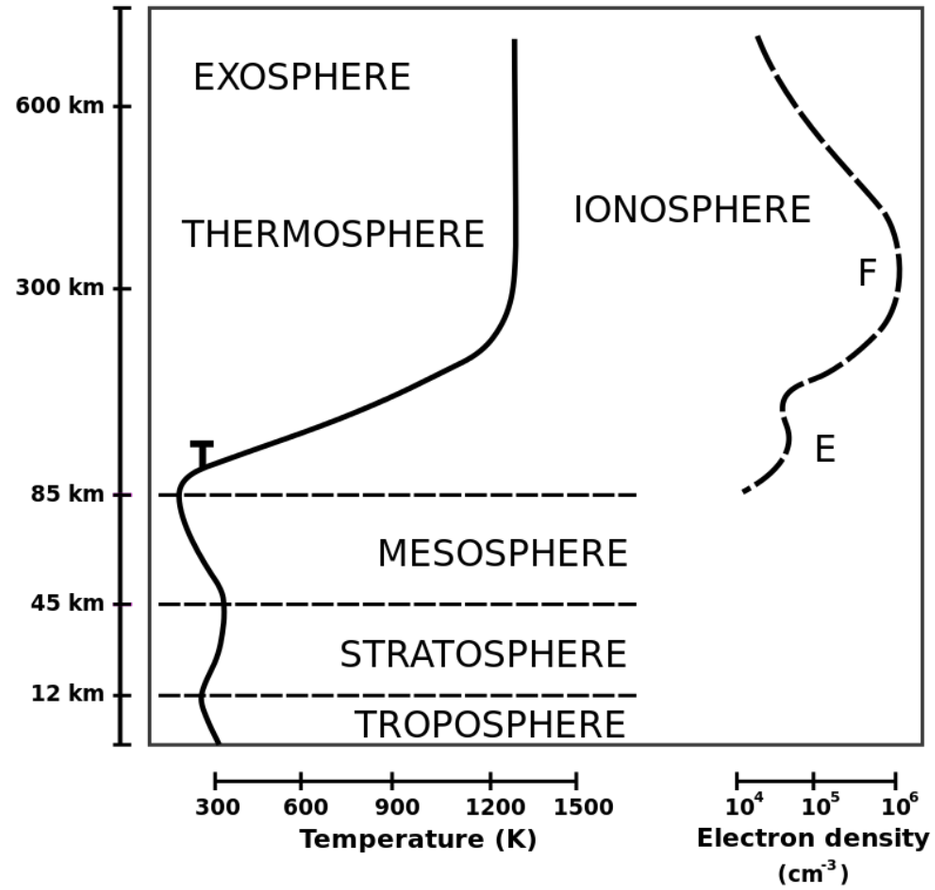

Cold Plasma Sources: Chapman Production Function

So where production = loss,

$$z_{\max} = H \ln\left(\frac{\sigma n_0 H}{\mu_0}\right),$$

(Above this, production > loss; below this, production < loss)

Production rate at this level is therefore

$$q(z_{\max}) = n_0 F_0 \sigma \frac{\mu_0}{\sigma n_0 H} e^{-1} = \frac{\mu_0 F_0}{H} e^{-1}.$$

Integrated production rate over whole atmosphere:

$$\int_0^\infty q(z)\,dz = \int_0^\infty n_0 F_0 \sigma e^{-z/H} \exp\left(-\frac{\sigma n_0 H}{\mu_0} e^{-z/H}\right) dz$$

Chapman Function

$$\int_0^\infty q(z)\,dz = F_0 \mu_0 \left[1 - \exp\left(-\frac{\sigma n_0 H}{\mu_0}\right)\right].$$

Cold Plasma Sources: Chapman Production Function

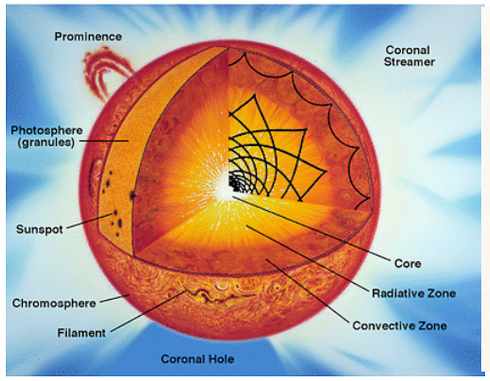

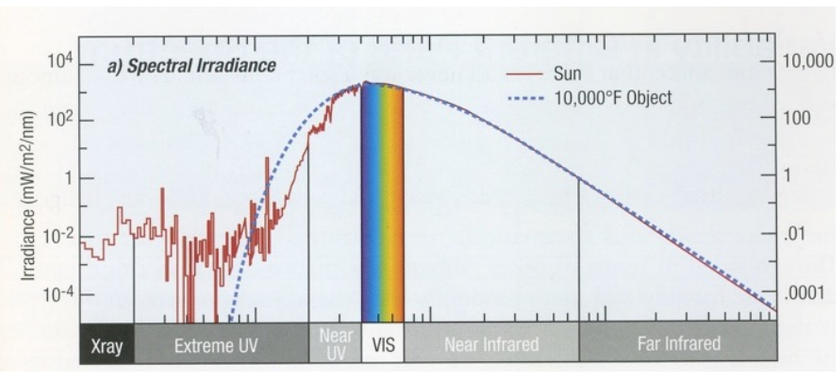

$$\int_0^\infty q(z)\,dz \quad = \quad F_0\mu_0\left[1-\exp\left(-\frac{\sigma n_0 H}{\mu_0}\right)\right].$$

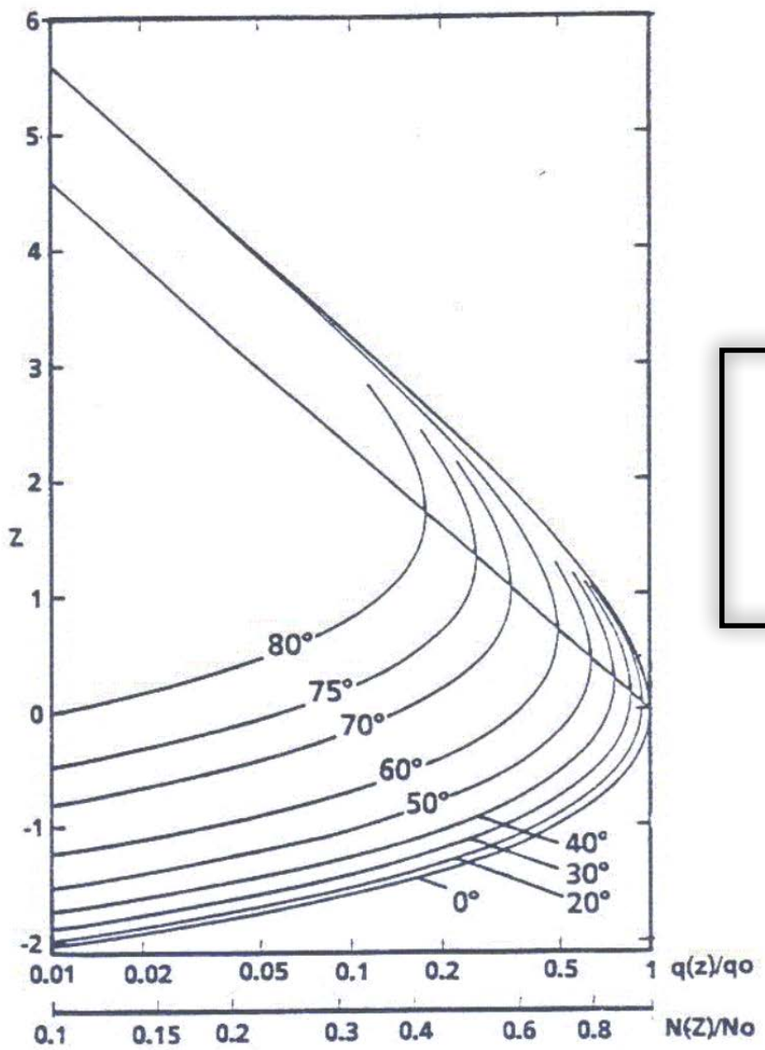

Figure 4.2.: The normalized photo ionization rate $q(z)/q_0$ and the electron density $N(z)/N_0$ according to Chapman's theory show the Chapman layer variations with altitude z and zenith angle χ. Notice that the horizontal axis is logarithmic.

Cold Plasma Sources: Chapman Production Function

Change in ion density: $$\frac{dN^+}{dt} = q - L$$ Loss $$L = \alpha\, n_e N^+$$

Poisson's equation: $$n_e = N^+$$

Change in Electron density: $$\frac{dn_e}{dt} = q - \alpha n_e^2$$

At equilibrium, $$\frac{dn_e}{dt} = 0 \text{ and } q = \alpha\, n_e^2 .$$

Chapman Electron Density Profile

$$n_e(\chi, z') = n_{em_0} \cdot e^{\frac{1}{2}\left(1 - z' - \sec(\chi)\cdot e^{-z'}\right)}$$

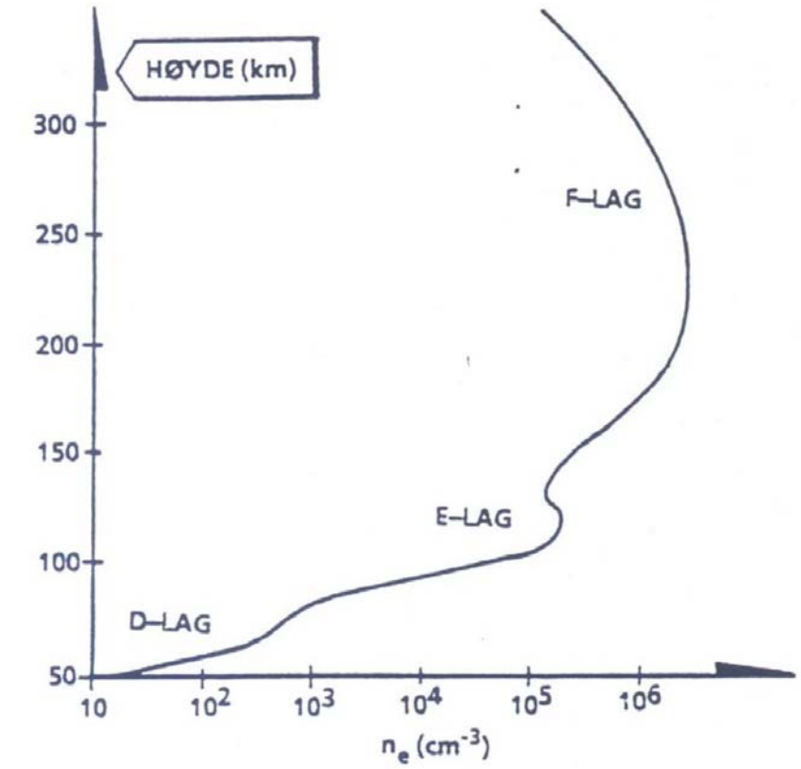

Figure 4.3.: Typical electron density profile in the normal ionosphere

Cold Plasma Climatology: The Ionosphere

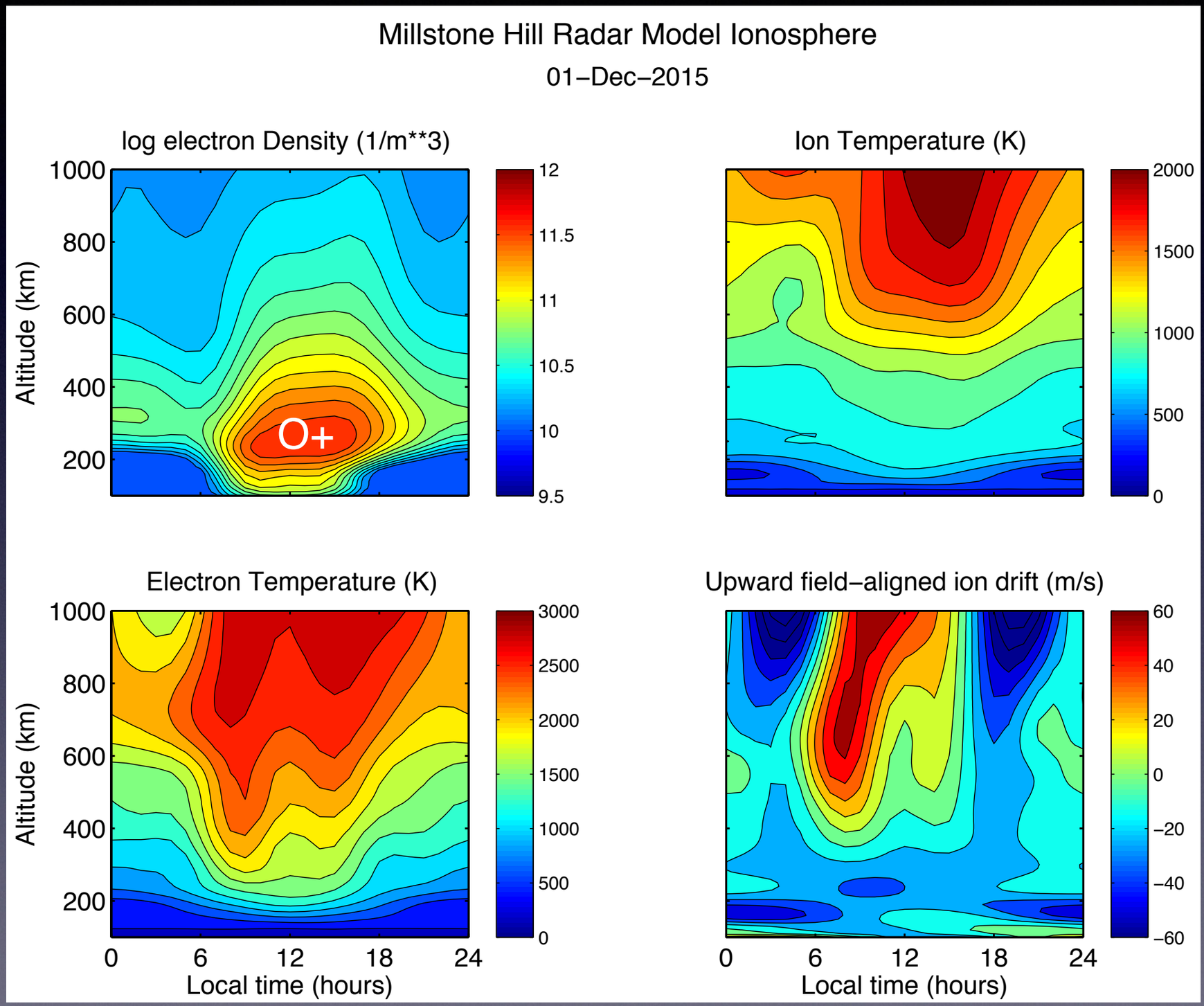

Zhang, Holt

Cold Plasma Climatology: The Ionosphere

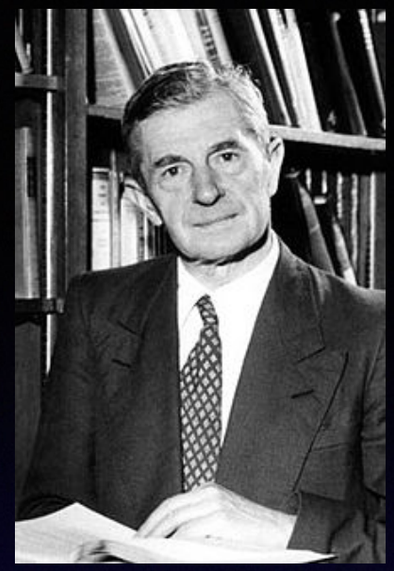

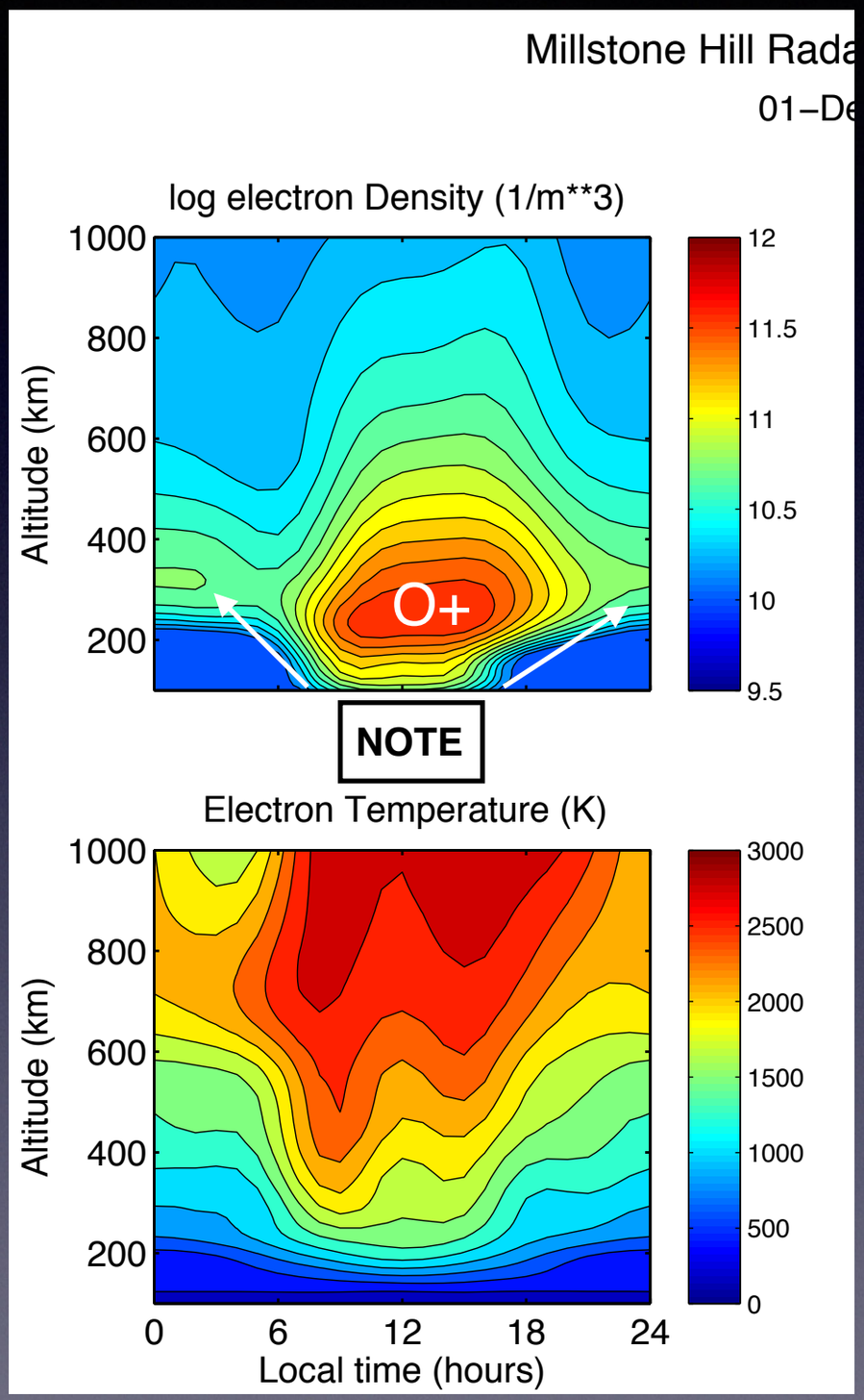

Chapman Profile

Chapman

$$n_e(\chi, z') = n_{em_0} \cdot e^{\frac{1}{2}\left(1 - z' - \sec(\chi) \cdot e^{-z'}\right)}$$

Marconi Says He Sent
10,000 Across the Atlantic

(CONTINUED FROM PAGE ONE)

his entire satisfaction with the operation of the system. Between five and ten thousand words were handled today.

"I feel confident that the system will continue to work satisfactorily," Marconi said. "There has not been the slightest hitch today. We can handle about thirty words per minute at present and have Western Union and C. P. R. connections with the station. Messages are being handled without any delay."

Several messages were filed by press representatives but replies had not been received when the party left for town. Mr. Marconi said these messages could not be sent till tomorrow, owing to accumulation of work.

ACCEPTING BUSINESS IN BRITISH CAPITAL.

LONDON, October 17—Marconi's wireless opened for business here today, charging the ordinary 6½d per word, with a minimum of 5s. 6d. as against the cable rate of one shilling, without the minimum

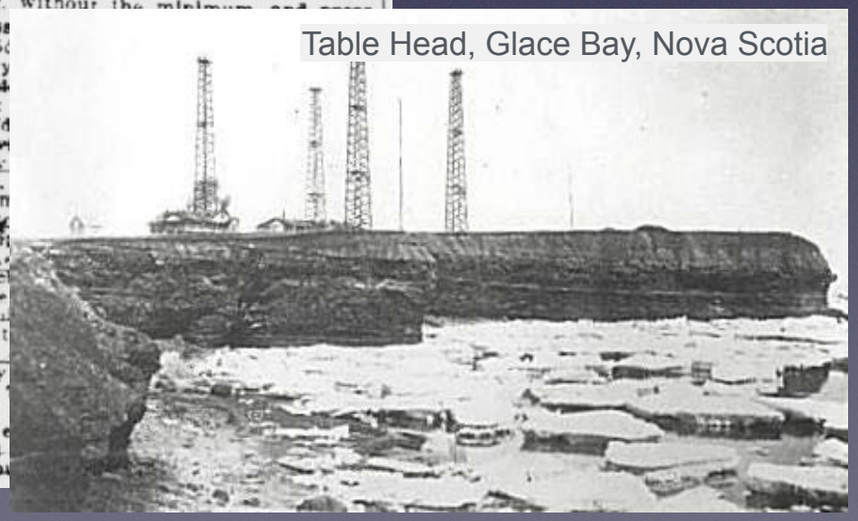

Table Head, Glace Bay, Nova Scotia

The Plasmasphere

REVIEWS OF GEOPHYSICS AND SPACE PHYSICS, VOL. 11, NO. 1, PP. 133–154, FEBRUARY 1973

On What Ionospheric Workers Should Know about the Plasmapause-Plasmasphere

D. L. CARPENTER AND C. G. PARK

Radioscience Laboratory, Stanford University
Stanford, California 94305

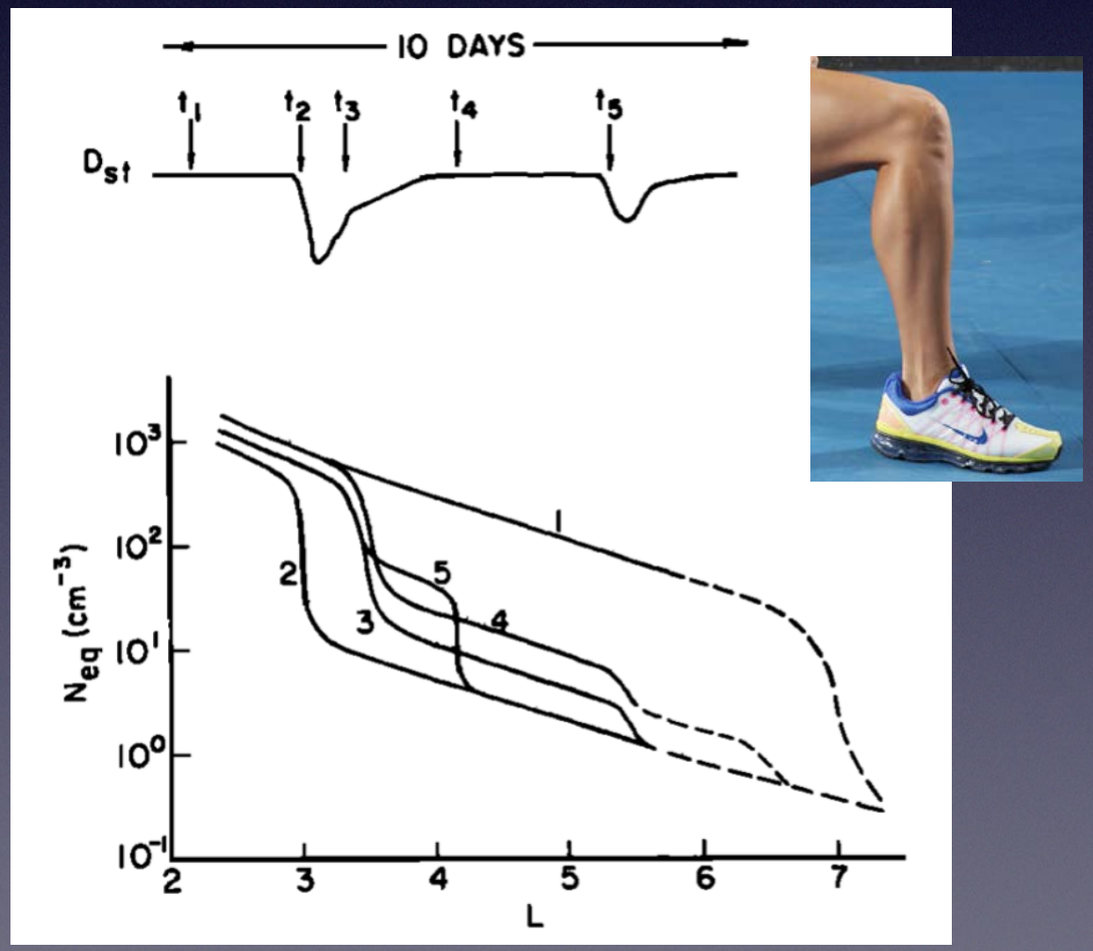

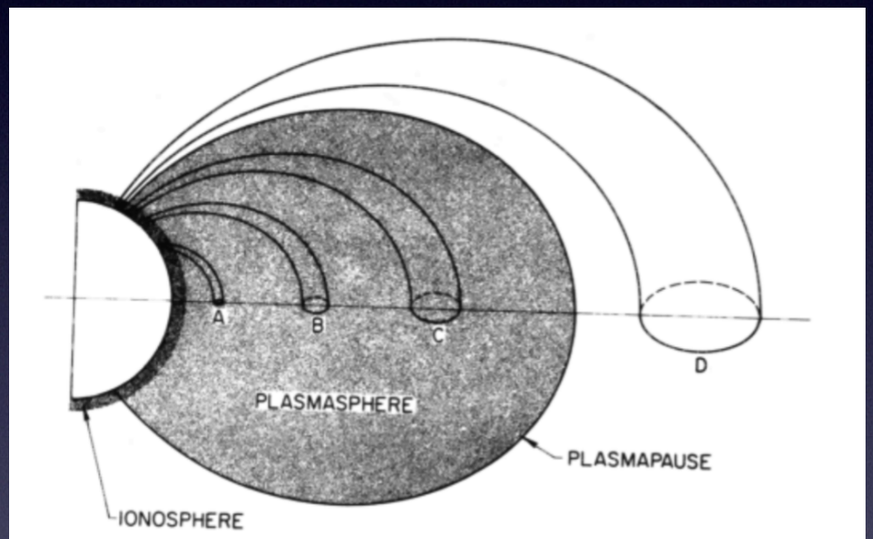

Fig. 1. Sketch of a magnetic-meridian cross section of the earth and its plasma environment showing the regular ionosphere extending to roughly 1000 km (heavy shading) and the overlying plasmasphere (medium shading). The plasmasphere is shown to terminate at the plasmapause, an abrupt magnetic field aligned boundary at which the number density of electrons decreases sharply within a distance of a fraction of an earth radius. Four magnetic flux tubes labeled A, B, C, and D are shown for illustration. The tubes are of equal cross section at 1000-km altitude and are used in illustrating the problem of interchange of thermal ionization between the ionosphere and the overlying region.

Plasmaspheric Wind

$$0 = \mathbf{E} + \mathbf{u}_n \times \mathbf{B} + \frac{1}{\nu_{in}}[\mathbf{J} \times \mathbf{B} + \rho \mathbf{g} - \nabla p] \times \mathbf{B}$$
$$- \frac{1}{en}\mathbf{J} \times \mathbf{B} - \frac{m_e}{e^2 n}\left(\nu_{ei} + \nu_{en} + \frac{m_e}{m_i}\nu_{in}\right)\mathbf{J}$$
$$+ en\frac{(\nu_{en} - \nu_{in})}{\nu_{in}}[\mathbf{J} \times \mathbf{B} + \rho \mathbf{g} - \nabla p]$$

Imbalance between pressure gradient, gravitational, centrifugal, and inertial forces

e.g. Lemaire and Schunk, 1992

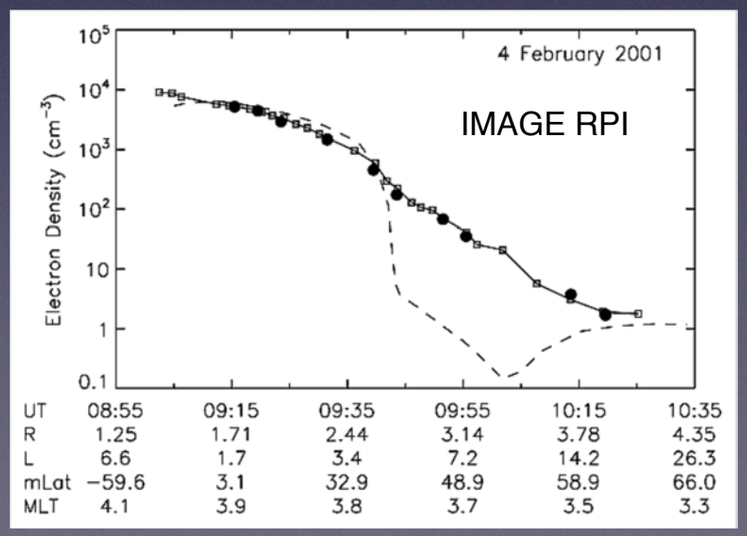

IMAGE EUV 30.4 nm
He+ Density

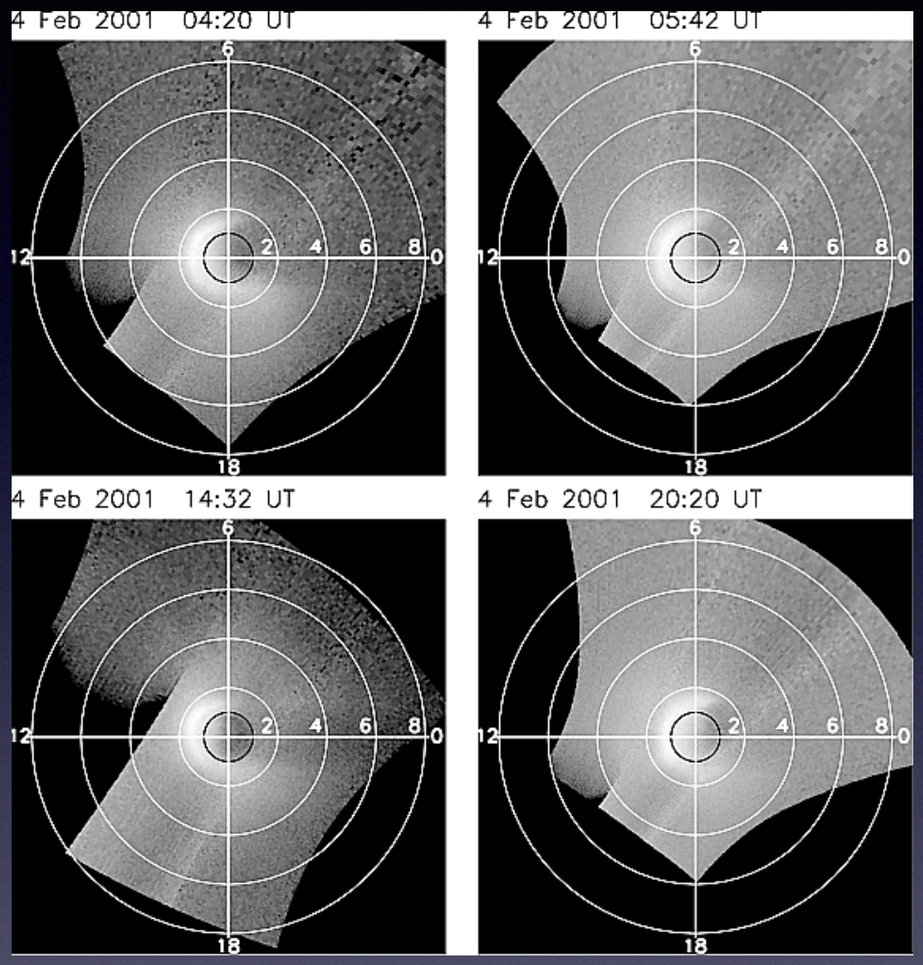

"Such smooth transition is possible if the magnetospheric convection is very weak so that the corotation dominates to a large radial distance." (Tu et al, 2007)

Ionospheric Plasma Structure: Transport Consequences

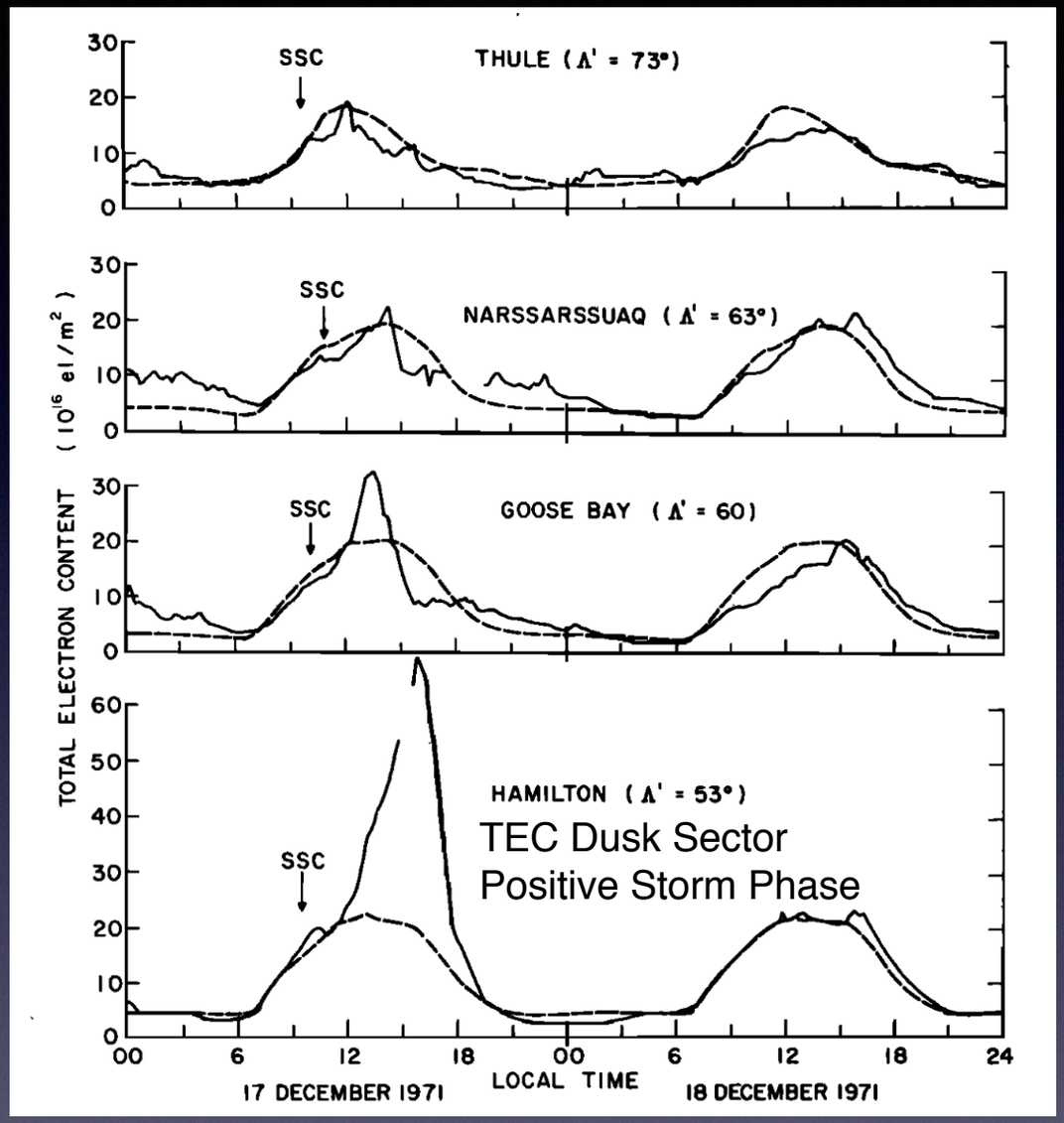

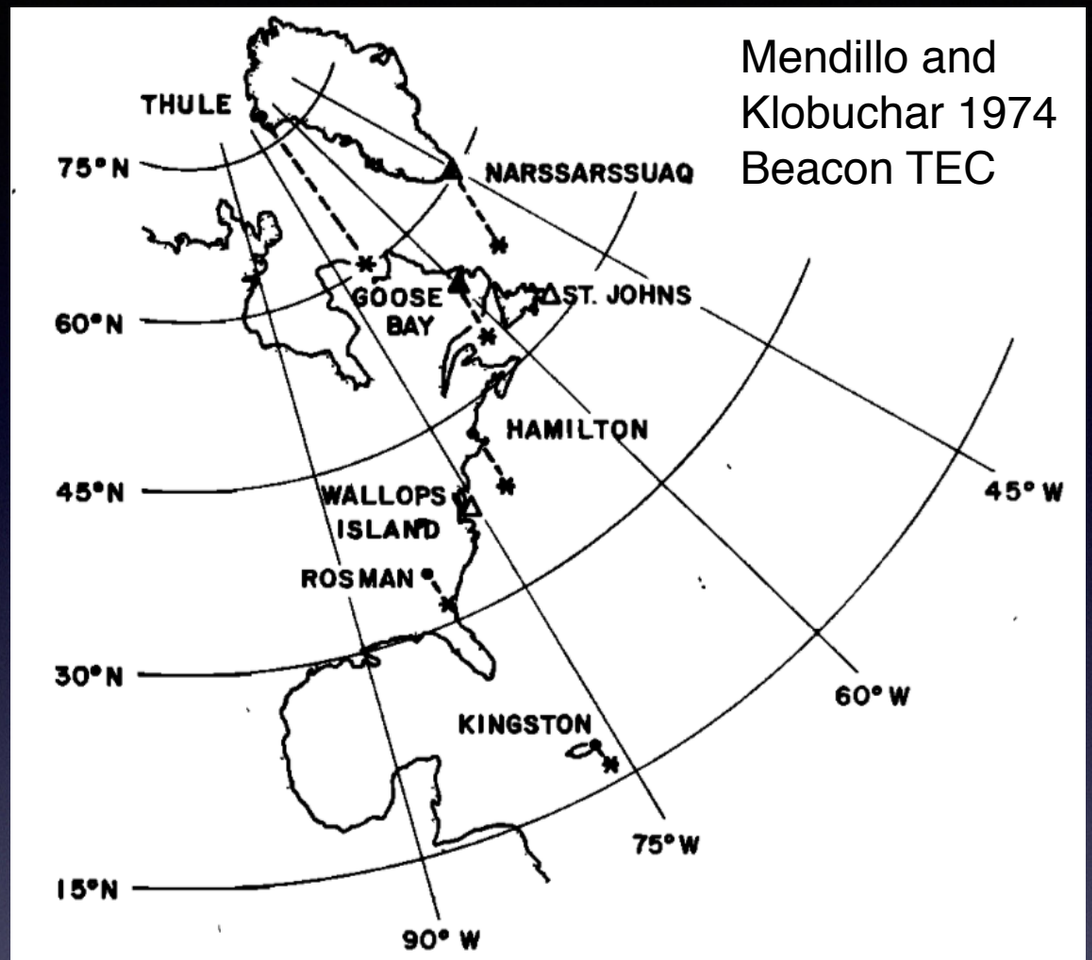

Fig. 1. Locations of TEC observing stations (solid dots), their 420-km subionospheric points (asterisks) for ATS 3 at 70°W, and the nearby ionosonde stations (open triangles).

- Unusually high, localized electron density columnar content
- Follows storm onset
- Latitude dependence

Ionospheric Plasma Structure: Transport Consequences

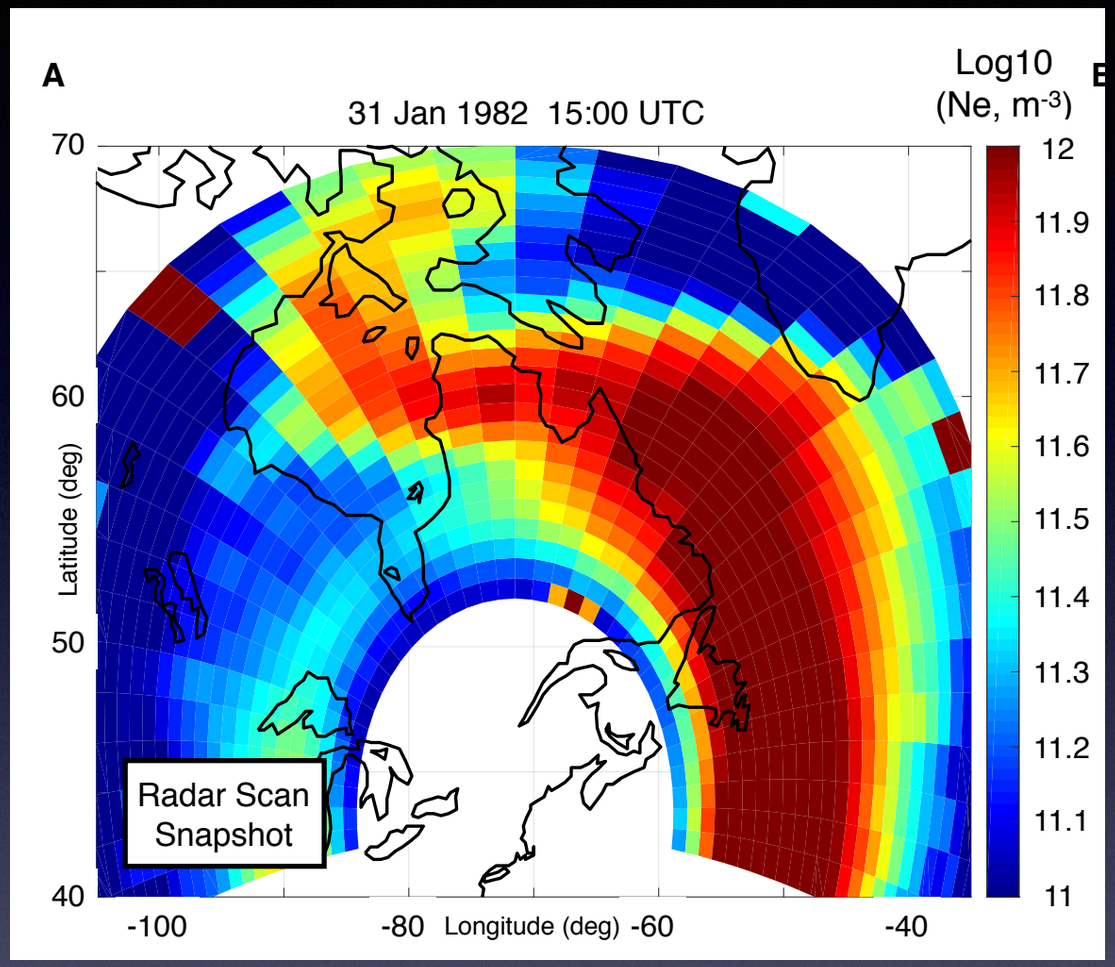

Millstone Hill Radar scans
Foster 1993

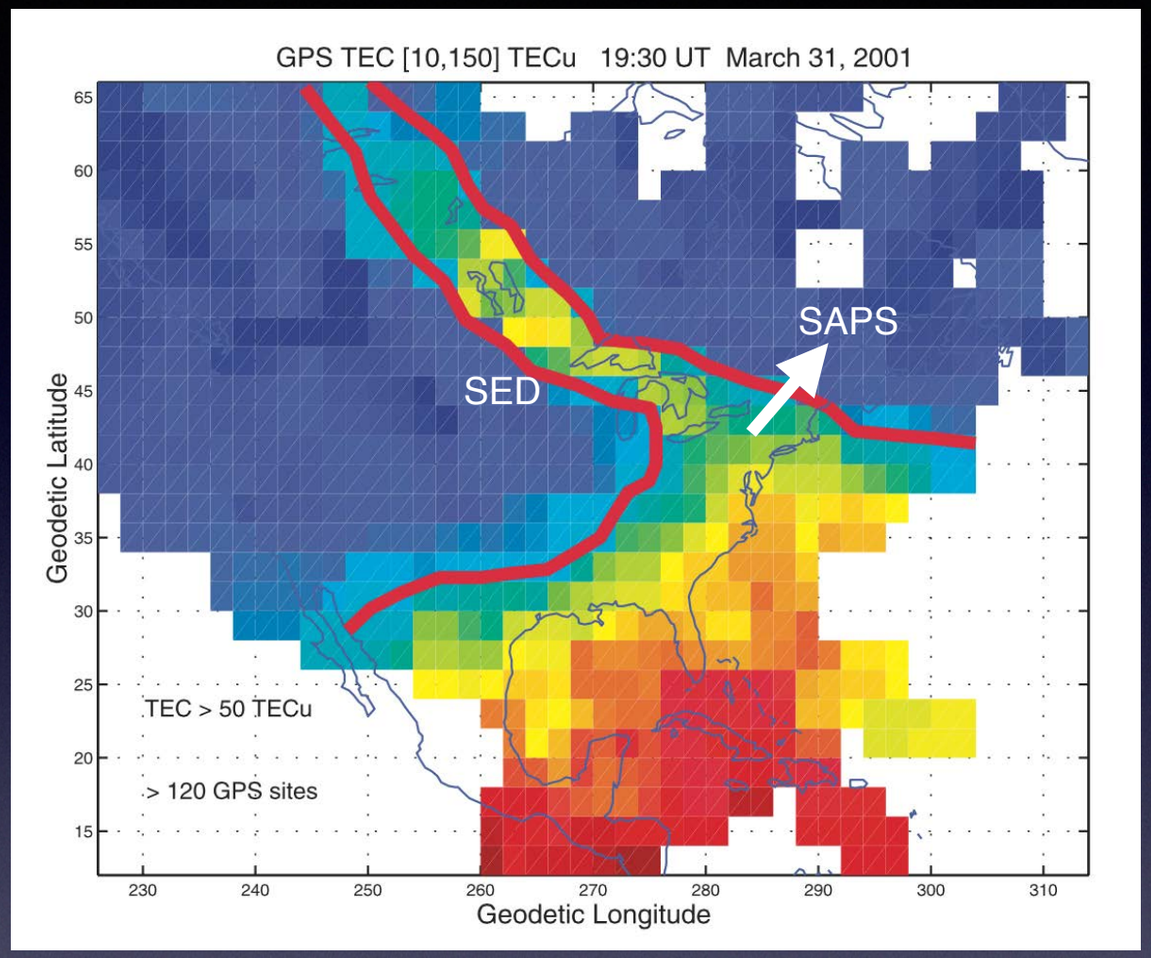

Foster et al 2002
GPS TEC

- Large density
- Predominantly O+
- Transport from lower latitudes towards noontime cusp

Sub Auroral Cold Plasma Structuring Agents: SAPS

Storm time FACs
Iijima and Potemra, 1978

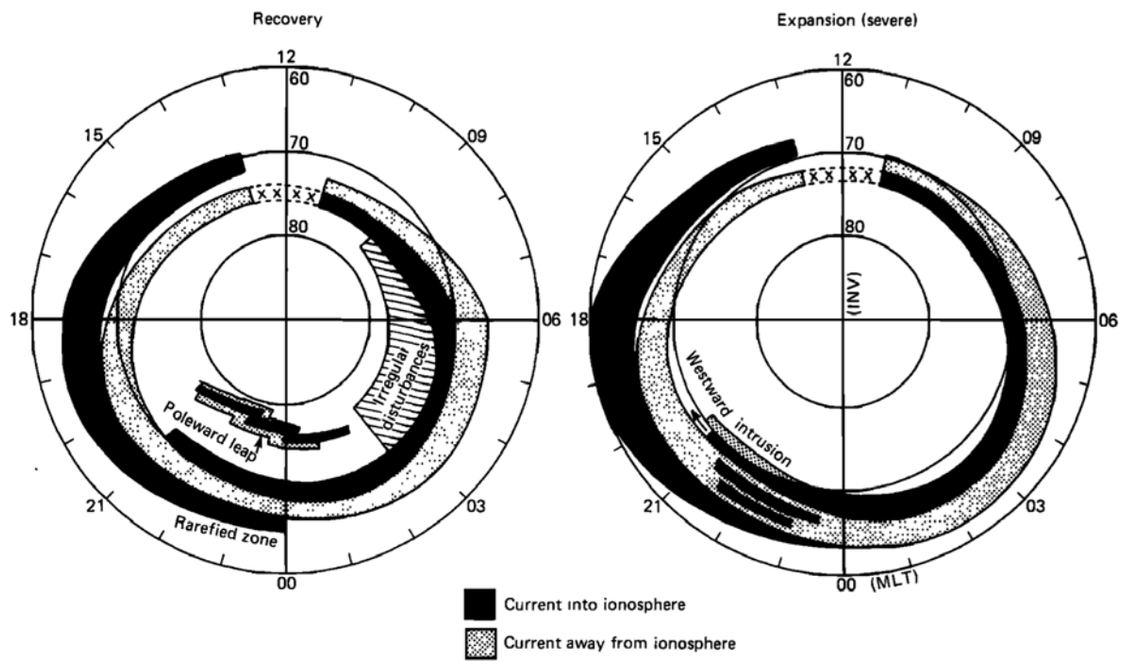

Fig. 15. Schematic diagram illustrating substorm-associated changes superimposed upon the basic distribution of field-aligned currents.

Region 2: $\nabla \cdot \mathbf{J} = 0$ $\quad j_{\parallel} = \nabla p \times \nabla V$

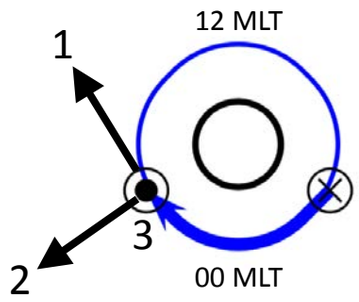

1: Azimuthal pressure gradient
2: Radial flux tube volume gradient
3: 1 x 2 = parallel current closure

Vasylunias, 1970

Electric fields in the ionosphere
(Ohm's Law)

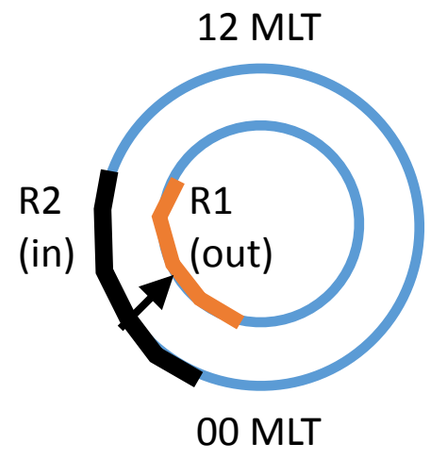

SAPS:
Current closure through
low conductance ionosphere =
potential created =
poleward E field in dusk sector

Storms + Substorms
Without Borders GC Session:
Thursday PM

Kp = 6 event
F10.7 = 233
DsT -100 nT

Millstone Hill UHF Radar
Azimuth Scan (4 deg El)
Log Electron Density m^-3 [10, 12.5]
1980-10-11 03:47:27 UTC

Plasmasphere Boundary Layer
(Carpenter and Lemaire, 2004)

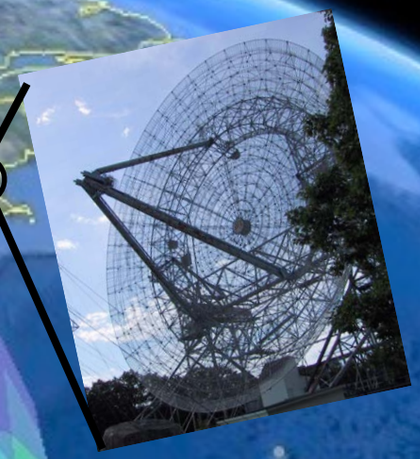

42.6 N, 288.5 E
54 MLAT
L ~ 2 to 4

39°52'41.15" N 81°05'52.87" W elev 278 m

Eye alt 6087.89 km

Kp = 6 event
F10.7 = 233
DsT -100 nT

Millstone Hill UHF Radar
Azimuth Scan (4 deg El)
Line-of-sight Ion Velocity [0,800] m/s
1980-10-11 03:47:27 UTC

Plasmasphere Boundary Layer
(Carpenter and Lemaire, 2004)

42.6 N, 288.5 E
54 MLAT
L ~ 2 to 4

39°52'41.15" N 81°05'52.87" W elev 278 m

Eye alt 6087.89 km

Sub Auroral Cold Plasma Structuring Agents: SAPS

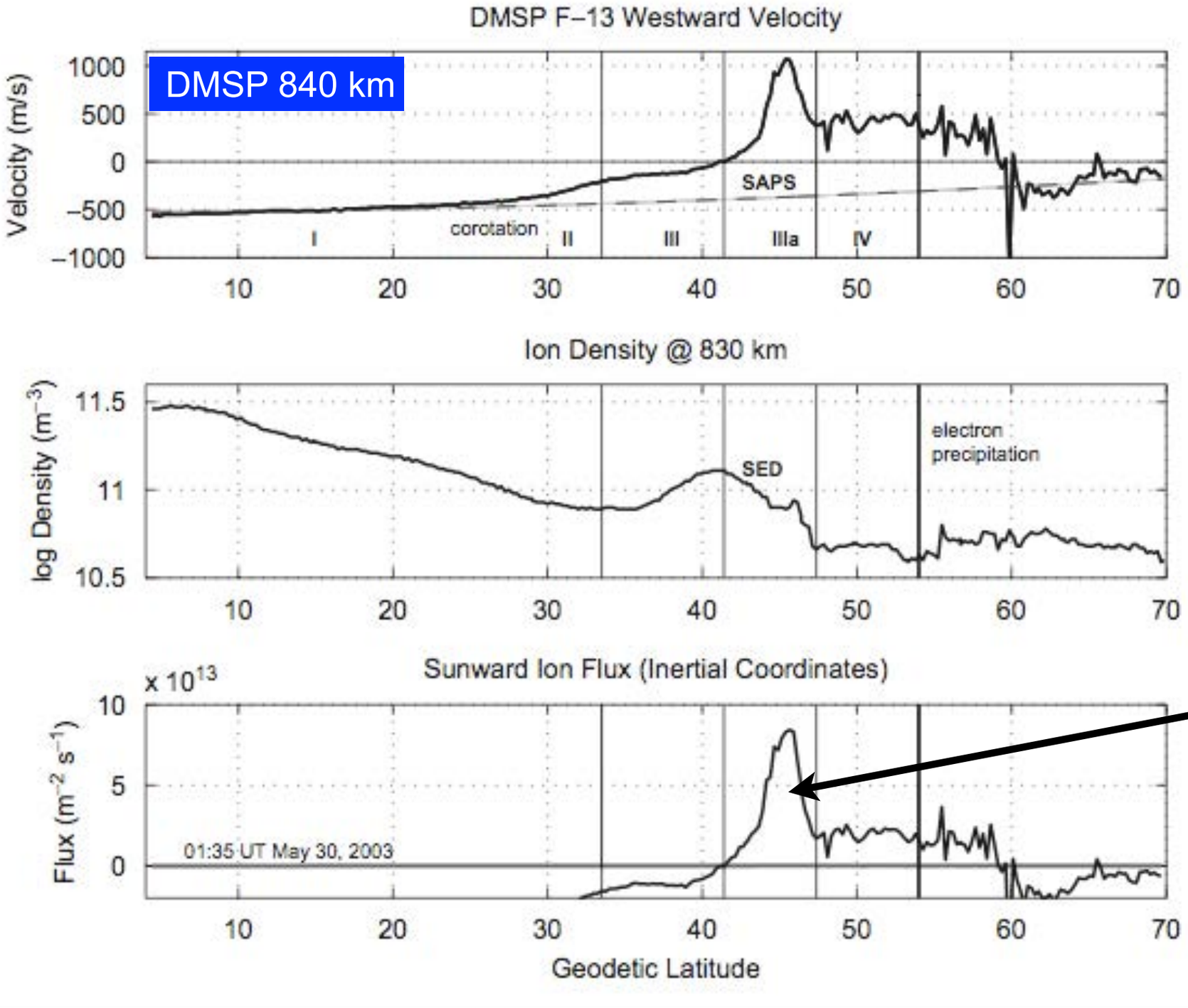

Sunward ion flux caused by SAPS/SED overlap

Foster et al, 2007

DMSP data and plots in Madrigal

- http://cedar.openmadrigal.org
- Presently 2016-2007
- Soon back to 1982
- ~5 days behind realtime
- Workshop planned for Oct. 2016 at Boston College (pje@haystack.mit.edu or patricia.Doherty@bc.edu)
- Data files divided by UT day, satellite, and 3 types:
  - flux/energy values
  - ion drift / magnetometer / electron density
  - plasma temp / O+ fract / vehicle pot

Many DMSP efforts also by NOAA, UTD, APL, etc.

Cold, Heavy Plasma Outflows

Important source for
ring current, plasma sheet
(it's not all solar wind plasma)

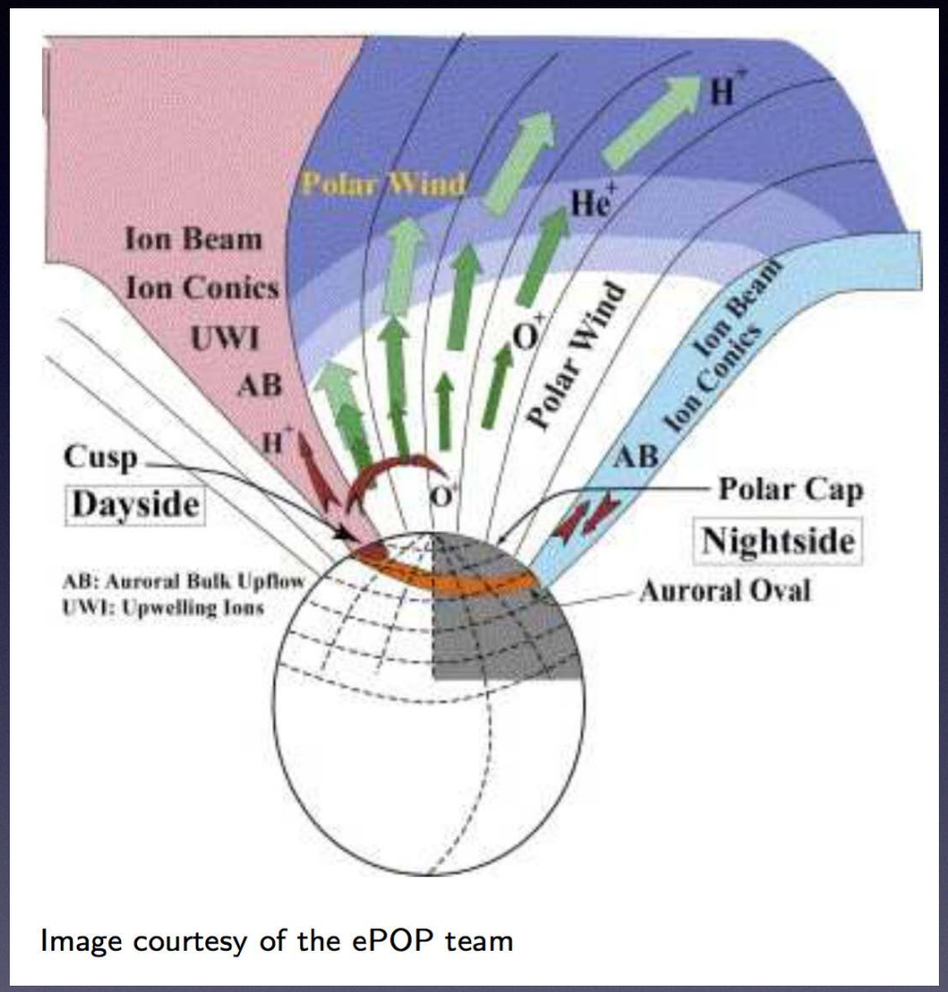

Image courtesy of the ePOP team

To high latitudes / cusp

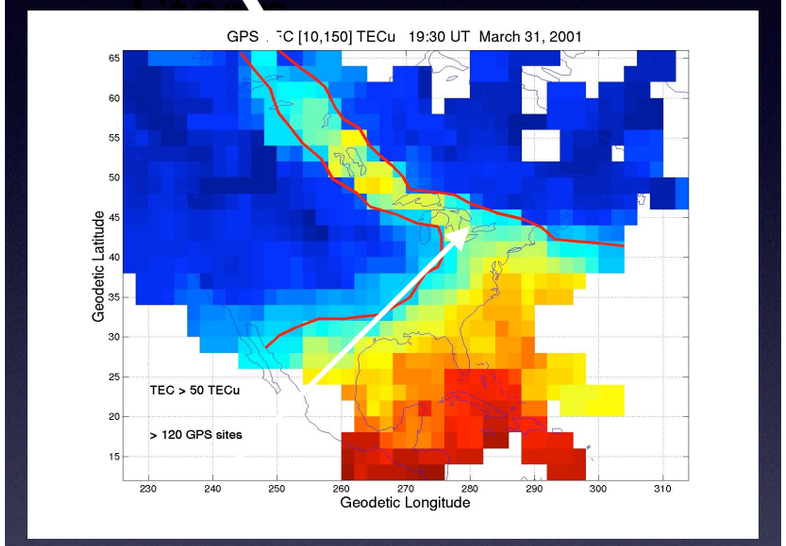

400 m/s @ 400 km

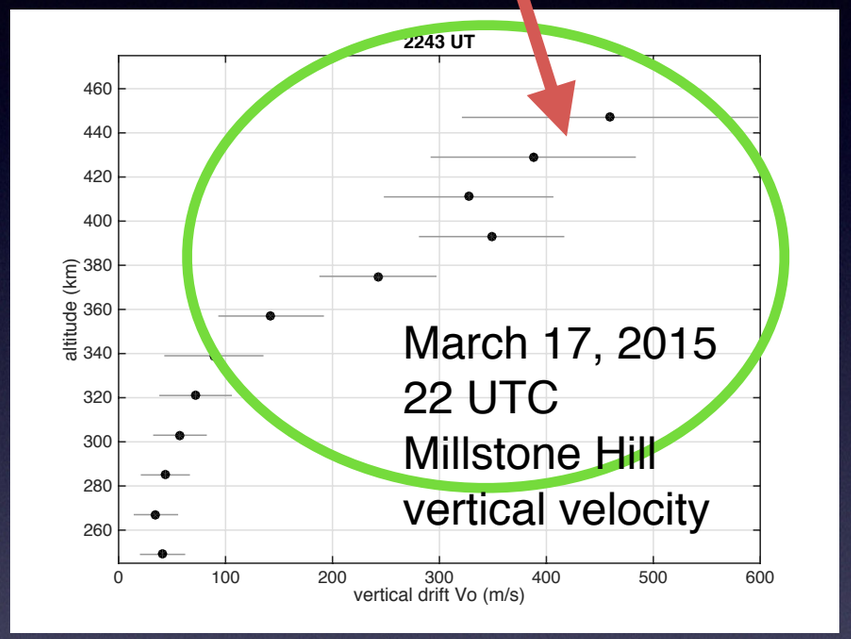

S.-R. Zhang, MIT Haystack
See Friday AM Thermosphere Cooling/ Heating

High latitude/cusp
Auroral bulk outflow, etc.
Heating, energization

Mid Latitude / SAPS
Associated vertical flow
Heating? Energization?

Cold, Heavy Plasma Outflows

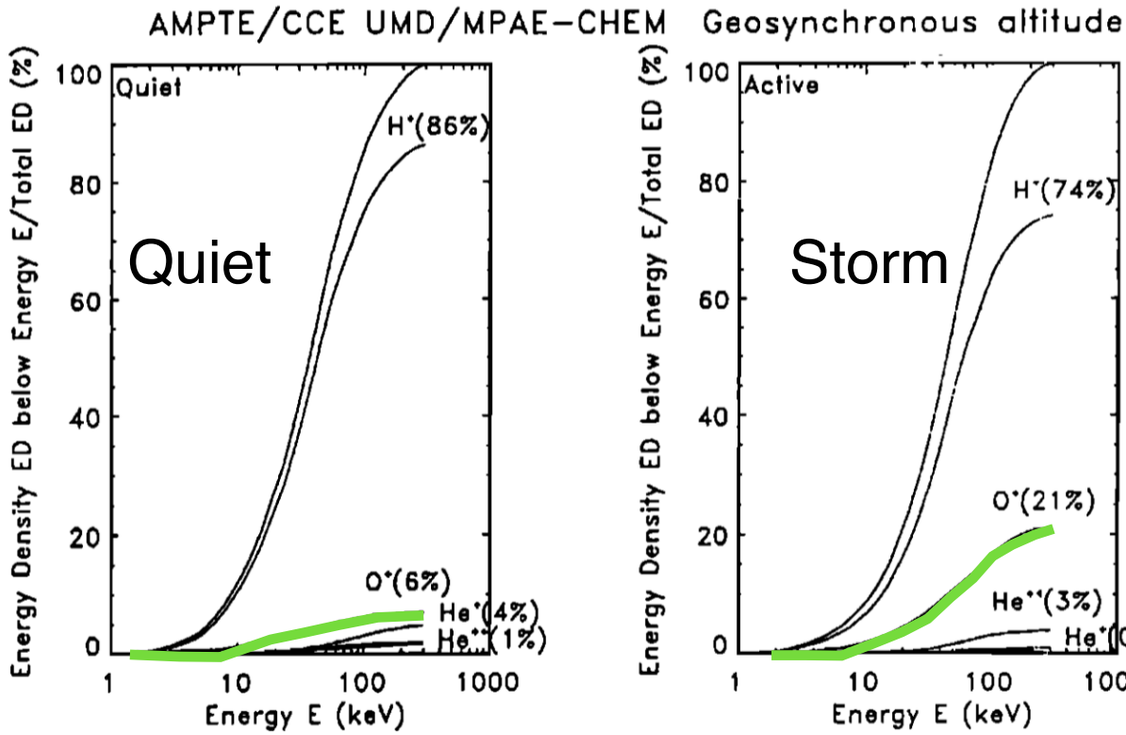

Ring Current Ion Composition

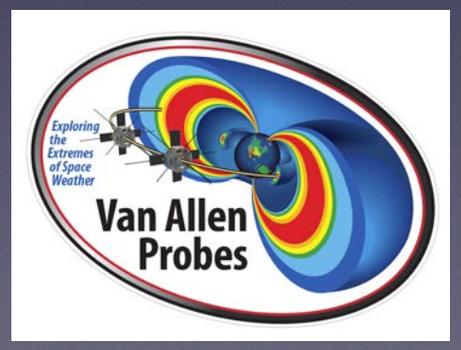

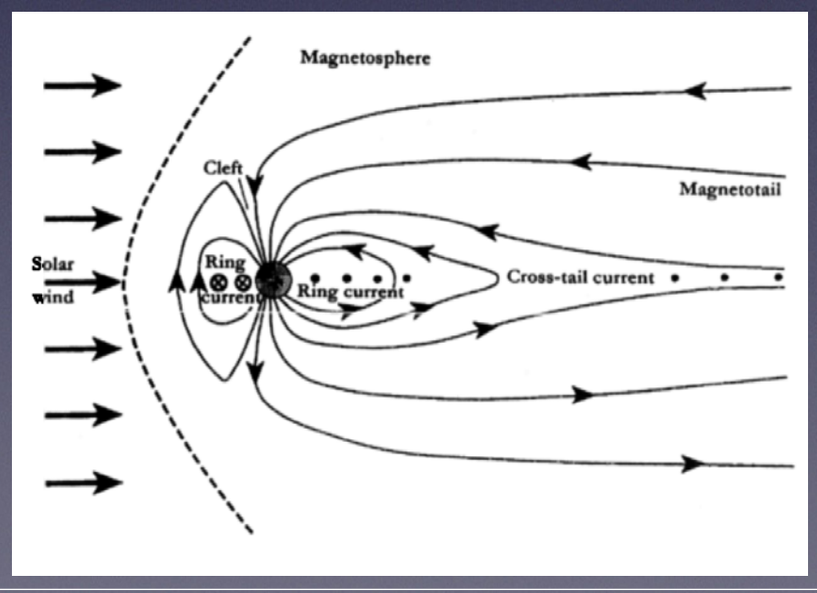

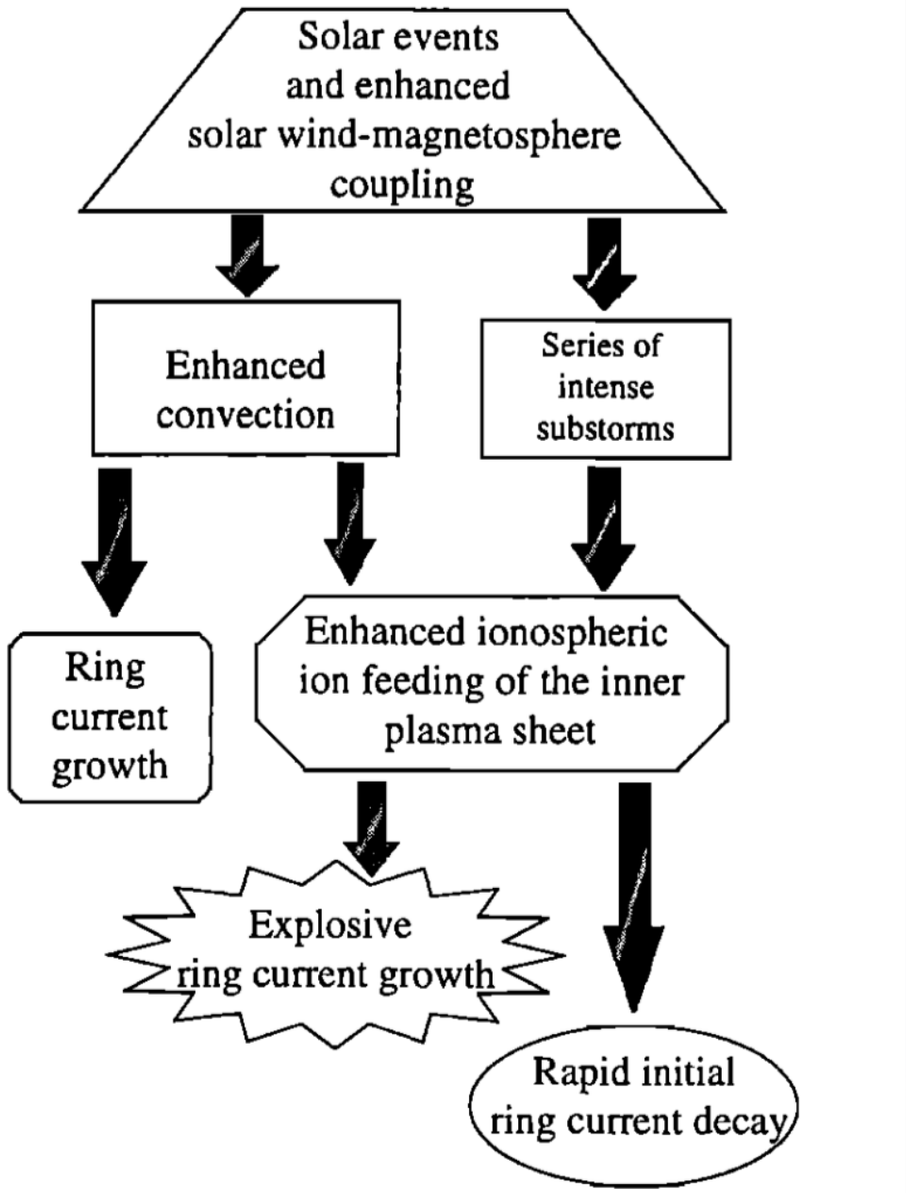

Plasmaspheric Plumes

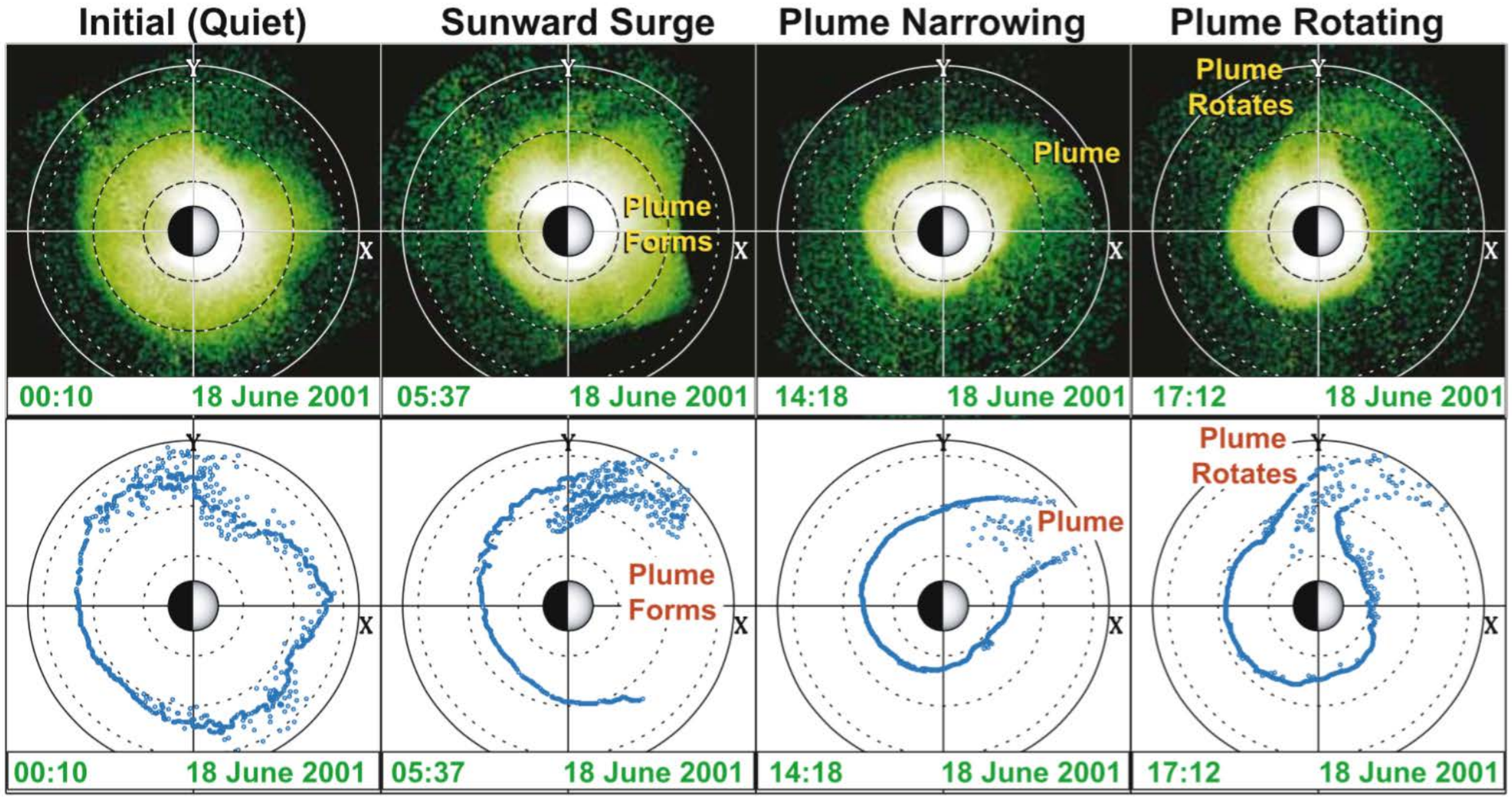

Fig. 5 (*Top row*) EUV plasmasphere images on 18 June 2001, depicting erosion of the plasmasphere and formation and rotation of a plume. Each panel displays the equatorial plasmaspheric He^+ distribution versus X and Y (in SM coordinates). *Color* indicates column abundance (in arbitrary units). The Sun is to the right (positive X) and the Earth is the *half-shaded circle* in the center. *Dotted circles* are drawn at $L = 2$, 4, and 6; the *solid circle* indicates geosynchronous orbit. (*Bottom row*) The *blue circles* are manually extracted points from the EUV image directly above, showing the outer boundary of the plasmasphere. (Adapted from Goldstein 2006)

Darrouzet et al Sp. Sci. Rev. 2009

Plasmaspheric Plumes

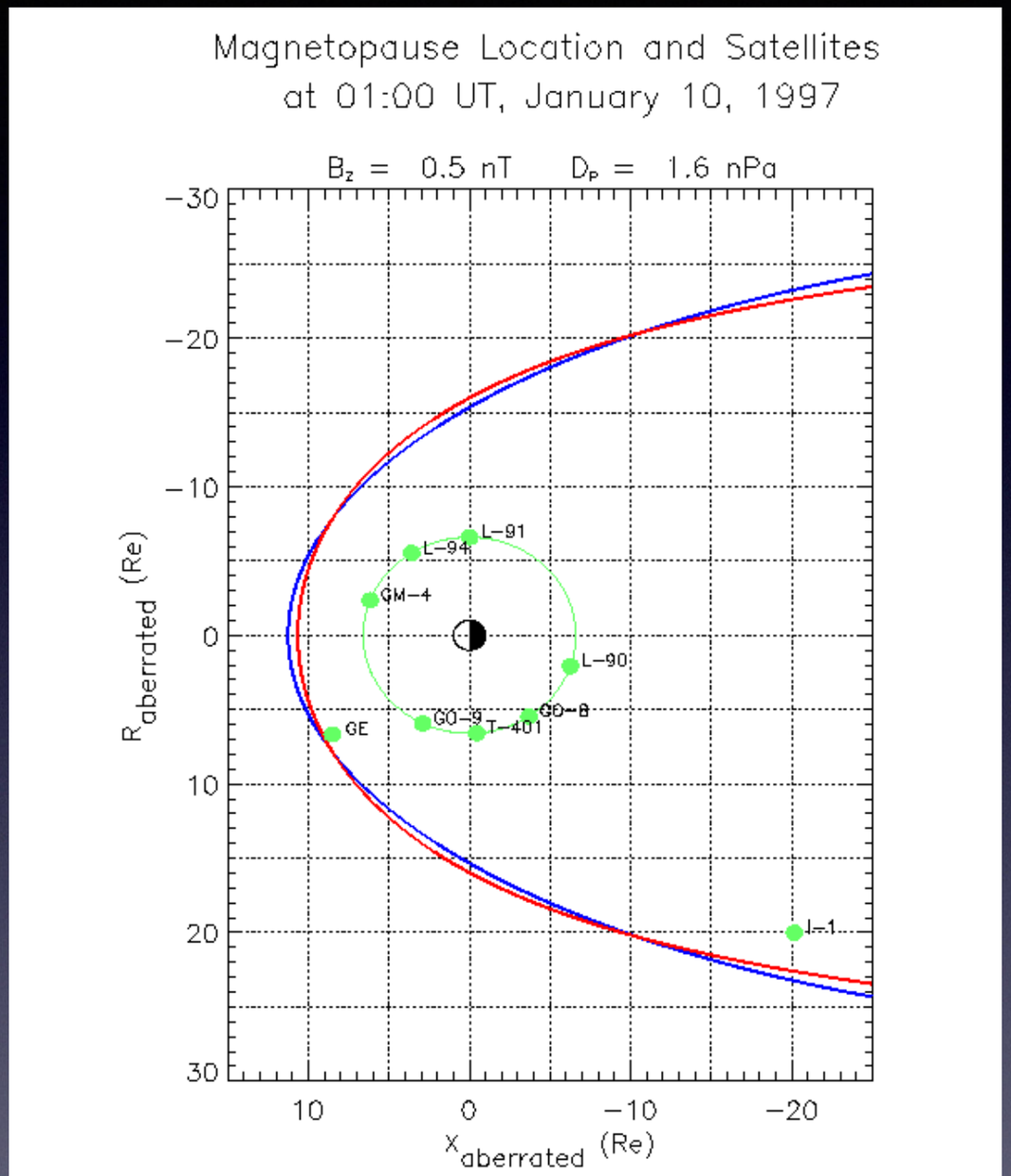

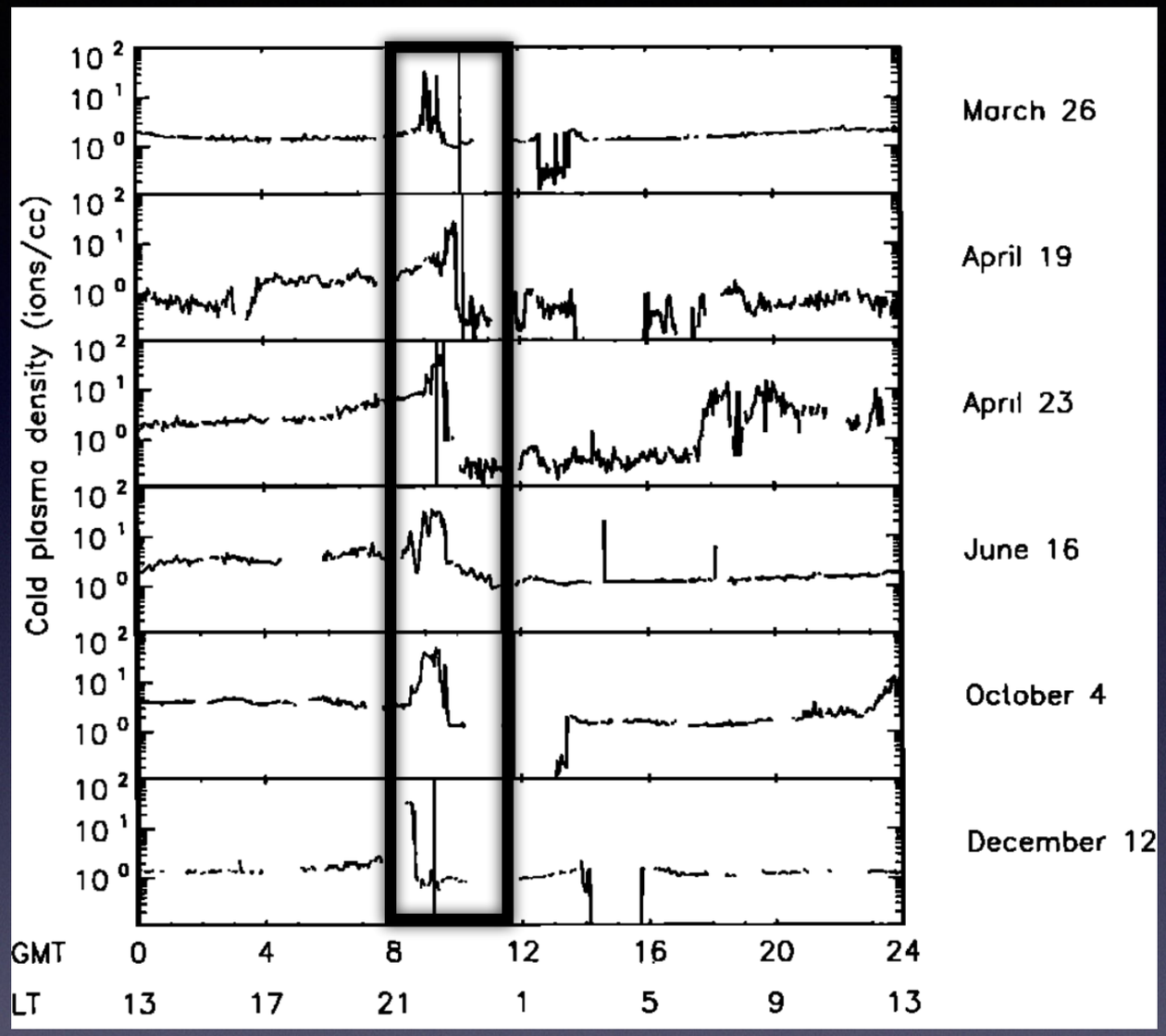

Ober et al 1997
Geosync
(LANL MPA)

Electrodynamics Connections: Ionosphere, Plasmasphere

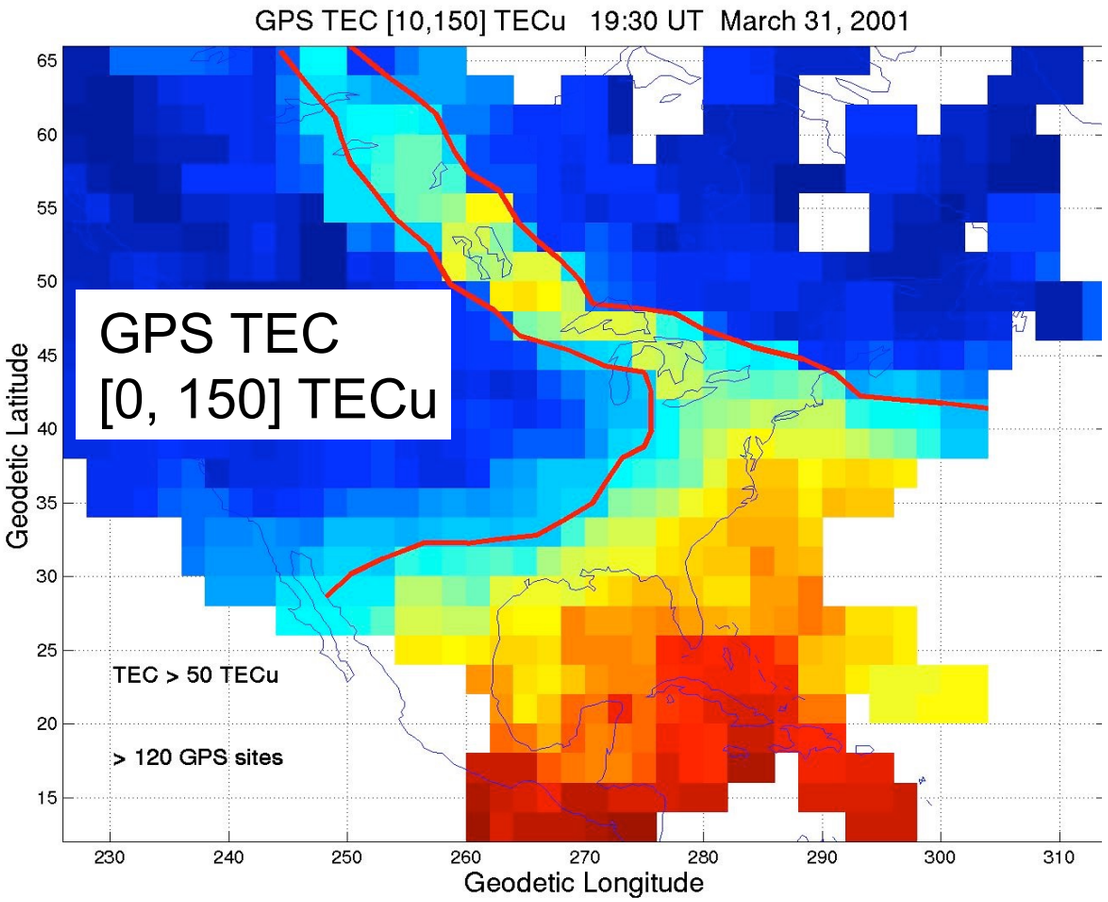

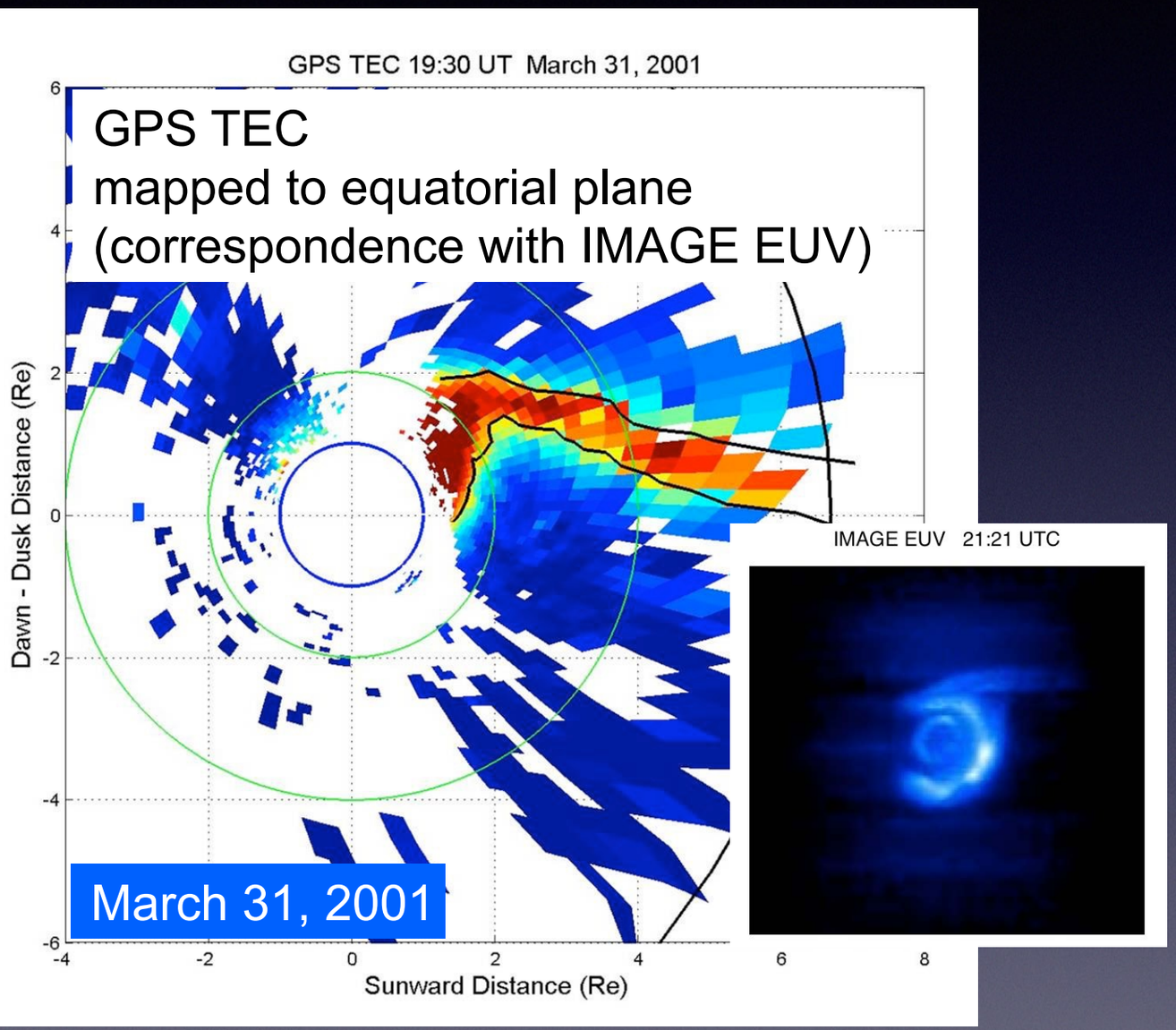

(e.g. Foster et al 2004)

Cold Plasma Redistribution: Multi-Scale Views

A

Radar Scan snapshot

31 Jan 1982 15:00 UT

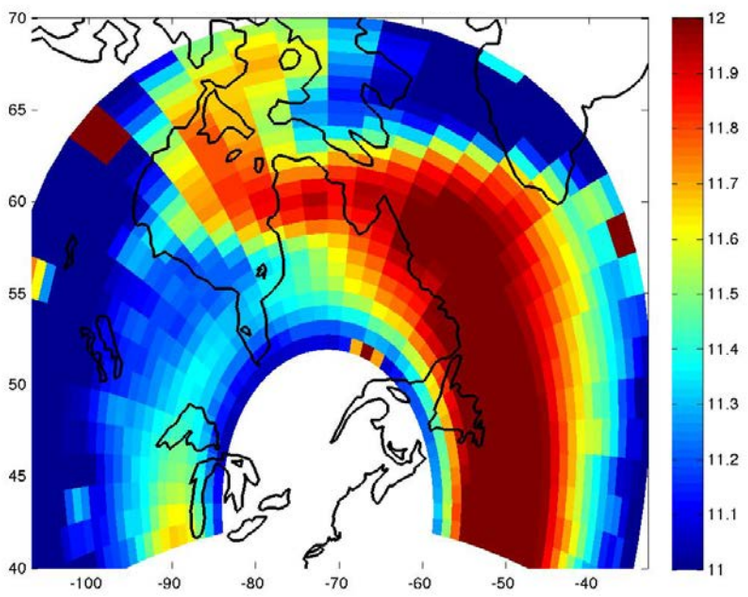

17 Jan2013 19:20 UT

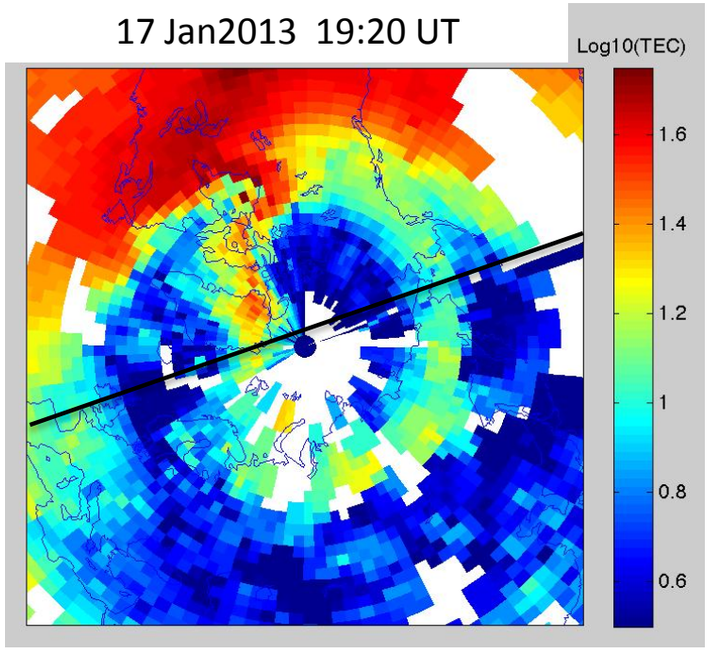

B

TEC TOI snapshot

C

IMAGE EUV Plume

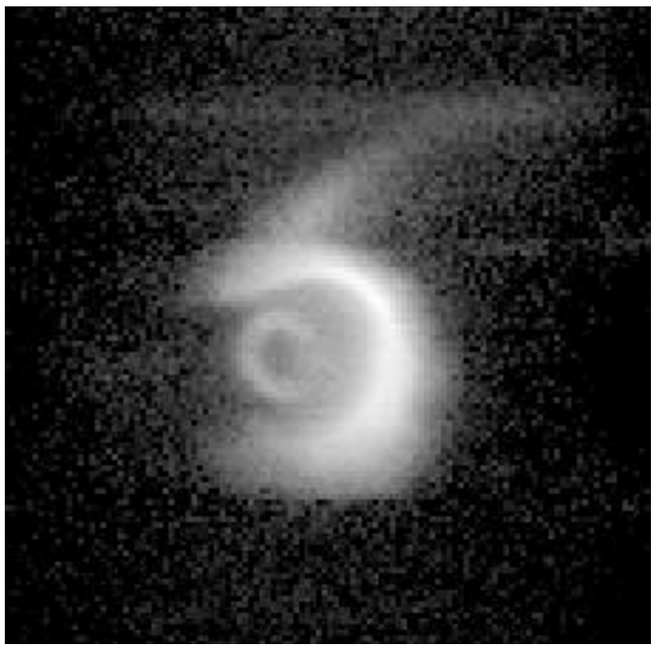

12 April 2001 03:49 UT

31 March 2001 19:30 UT

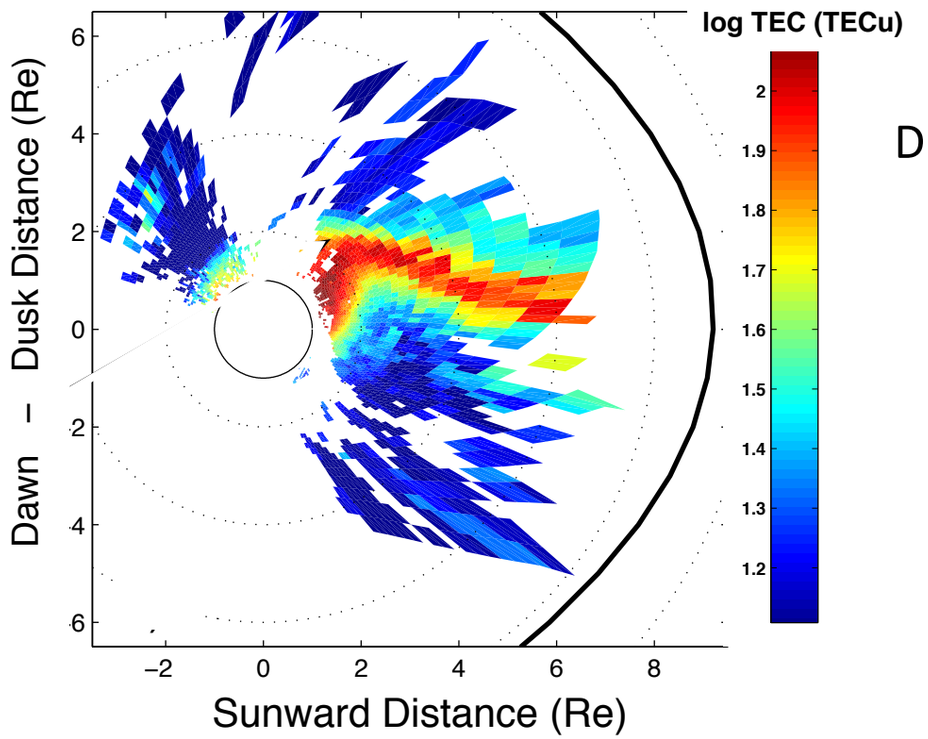

D

Outline

- Basics of Ionospheric Cold Plasma Production
- Geospace Plasma Structuring
- Cold Plasma Influences In Geospace:

1. Ionosphere-Magnetosphere Feedback
2. Cold Plasma Effects At The Magnetosphere Boundary
3. Radiation Belt Dynamics: Cold Plasma Influence

Cold Plasma Effects on Geospace: It's Not A Boundary Value Problem

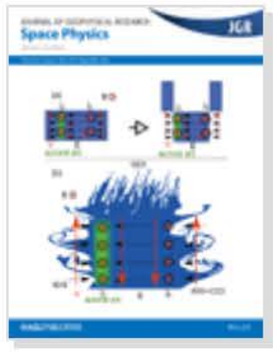

Commentary

The Ionospheric Source of Magnetospheric Plasma is Not a Black-Box Input for Global Models†

D. T. Welling ✉, M. W. Liemohn

Accepted manuscript online: 1 June 2016 Full publication history

DOI: 10.1002/2016JA022646 View/save citation

Cited by: 0 articles Check for new citations

Ring current not coupled

Ring current coupled to ionosphere-magnetosphere (R2 FAC pumps up outflow)

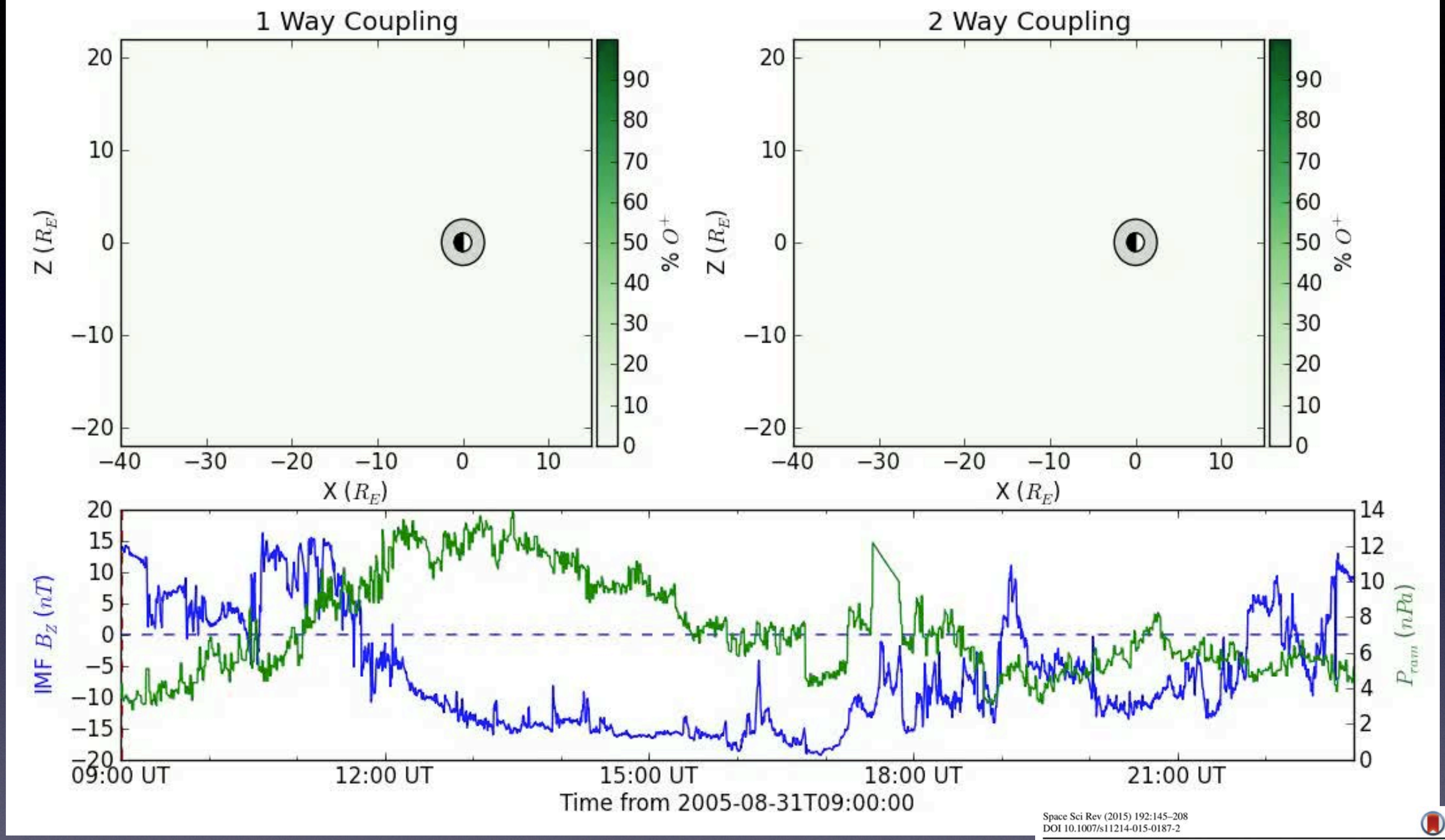

Welling, D. T., Jordanova, V. K., Glocer, A, Toth, G., Liemohn, M. W., & Weimer, D. R. (2015). The two-way relationship between ionospheric outflow and the ring current. *Journal of Geophysical Research: Space Physics*, *120*(6), 4338-4353. http://doi.org/10.1002/2015JA021231

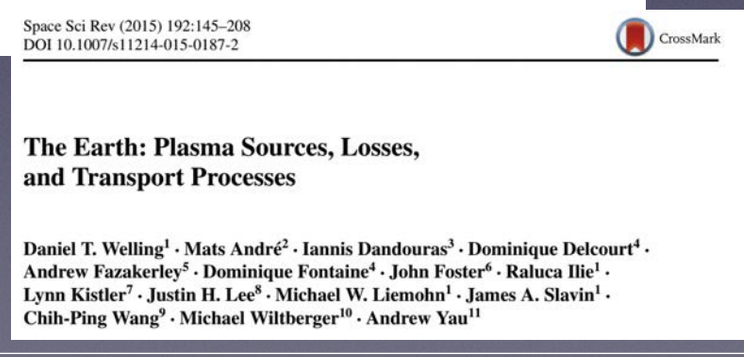
Space Sci Rev (2015) 192:145–208
DOI 10.1007/s11214-015-0187-2

CrossMark

The Earth: Plasma Sources, Losses, and Transport Processes

Daniel T. Welling[1] · Mats André[2] · Iannis Dandouras[3] · Dominique Delcourt[4] · Andrew Fazakerley[5] · Dominique Fontaine[4] · John Foster[6] · Raluca Ilie[1] · Lynn Kistler[7] · Justin H. Lee[8] · Michael W. Liemohn[1] · James A. Slavin[1] · Chih-Ping Wang[9] · Michael Wiltberger[10] · Andrew Yau[11]

Outline

- Basics of Ionospheric Cold Plasma Production
- Geospace Plasma Structuring
- Cold Plasma Influences In Geospace:

1. Ionosphere-Magnetosphere Feedback
2. Cold Plasma Effects At The Magnetosphere Boundary
3. Radiation Belt Dynamics: Cold Plasma Influence

Plasmasphere Erosion Flux

IMAGE EUV 30.4 nm He+
(representative only)

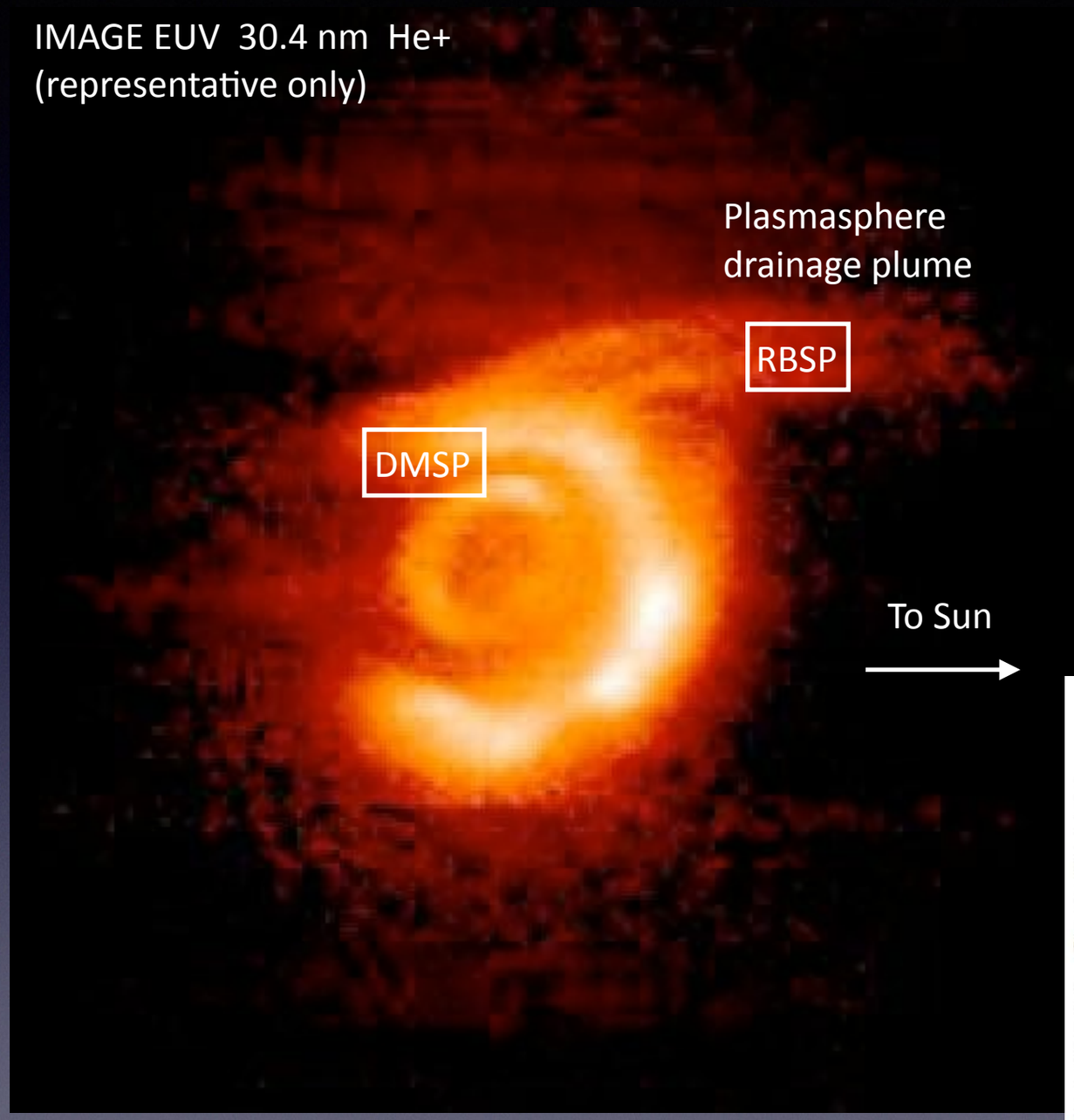

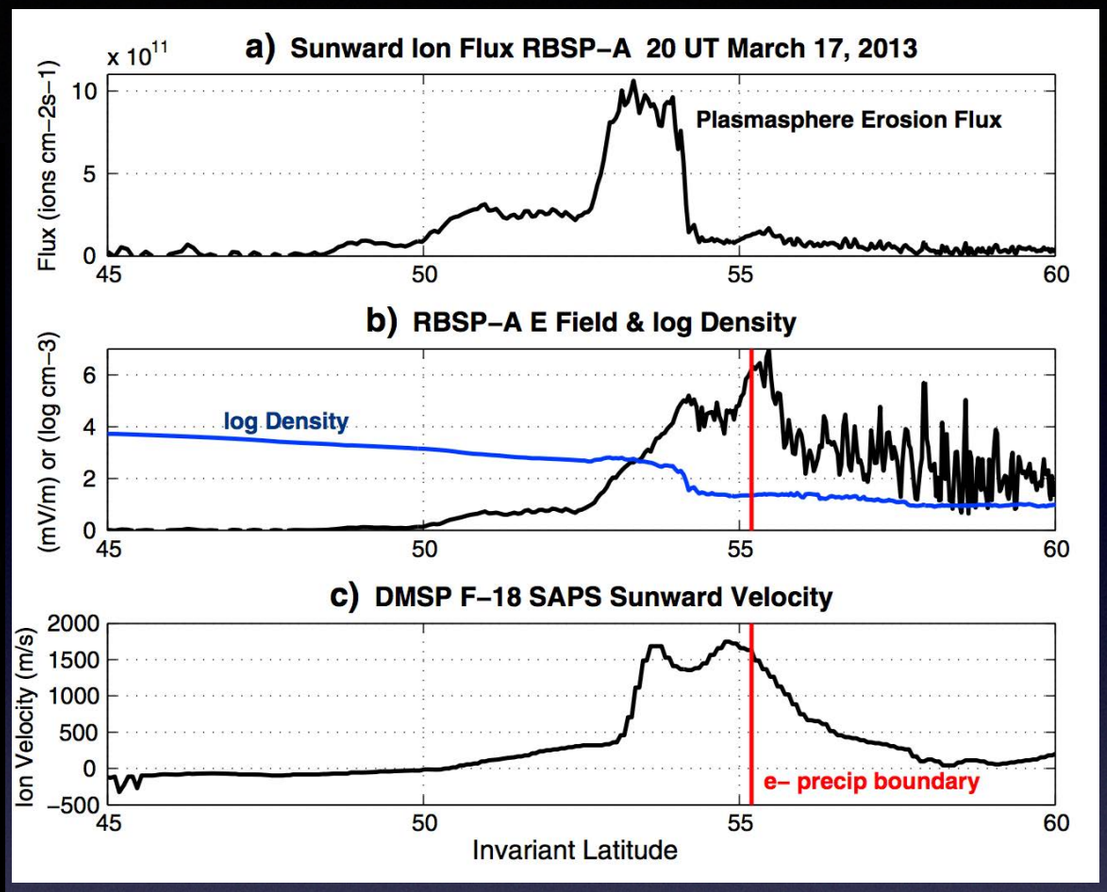

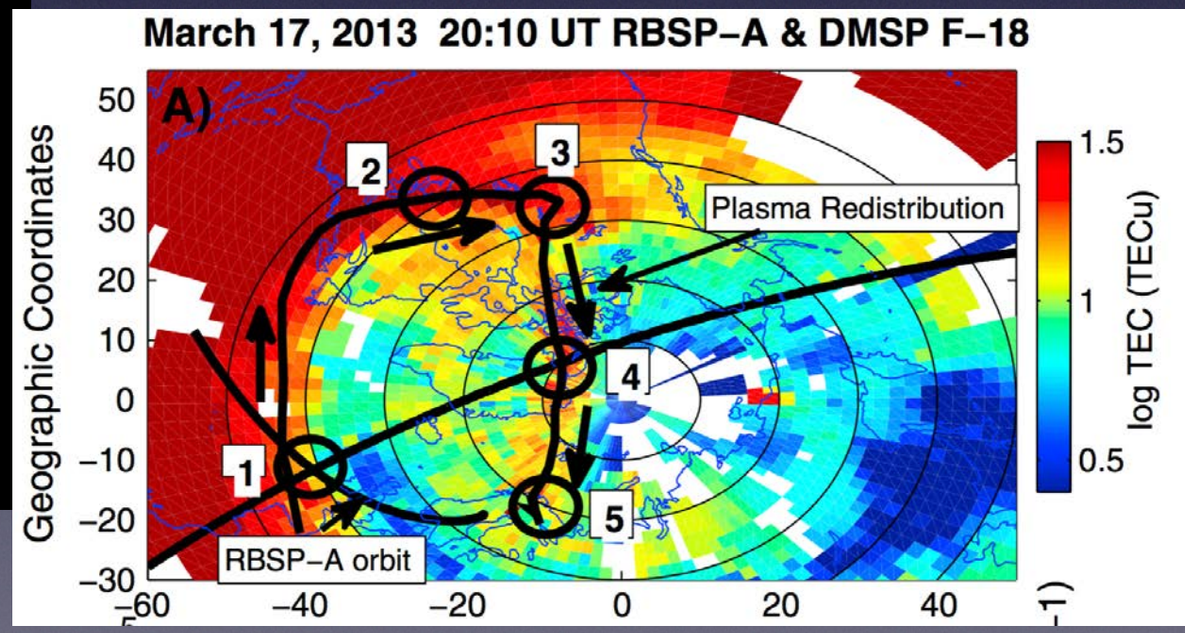

1.2E12 m^{-2} s^{-1} at RBSP (14 MLT)
2.0E13 m^{-2} s^{-1} at DMSP (20 MLT)
Total sunward fluence ~5E25 s^{-1}

Foster et al, 2014

Plasmaspheric drainage plumes: Mass-loading the magnetopause

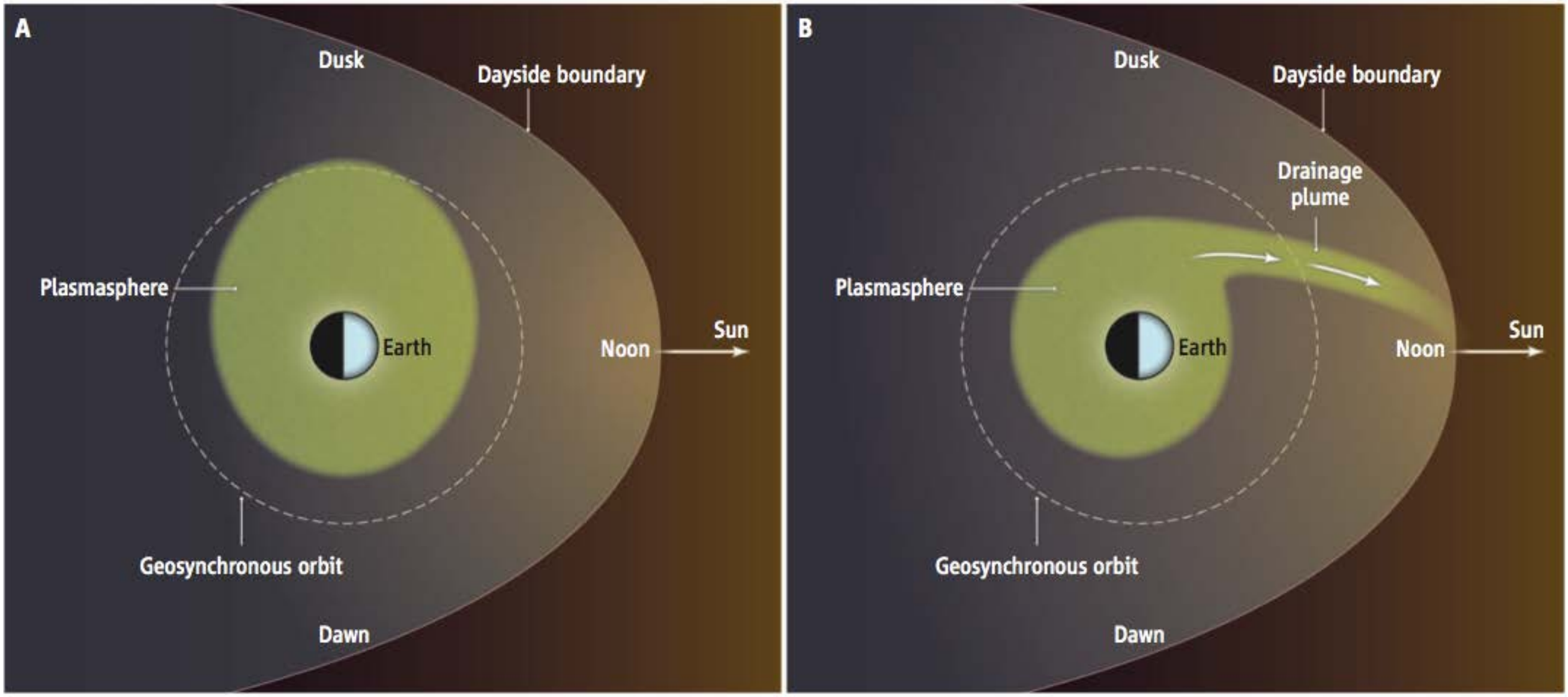

Pushing back. From a perspective high over the North Pole of Earth, the cold plasma in the equatorial plane of Earth's magnetosphere is sketched at two different times. (**A**) When solar-wind coupling is weak, the near-Earth reservoir (plasmasphere) is shown in green. (**B**) When coupling becomes stronger, the plume of sunward-convecting cold plasma eroding from the reservoir is seen. The cold plasma of the plume flows to the dayside boundary of the magnetosphere, where it interferes with the reconnection process. Space-based ultraviolet images of this cold-plasma movement can be seen in Goldstein (*7*).

Borovsky, Science, 2014

Plasmaspheric drainage plumes: Mass-loading the magnetopause

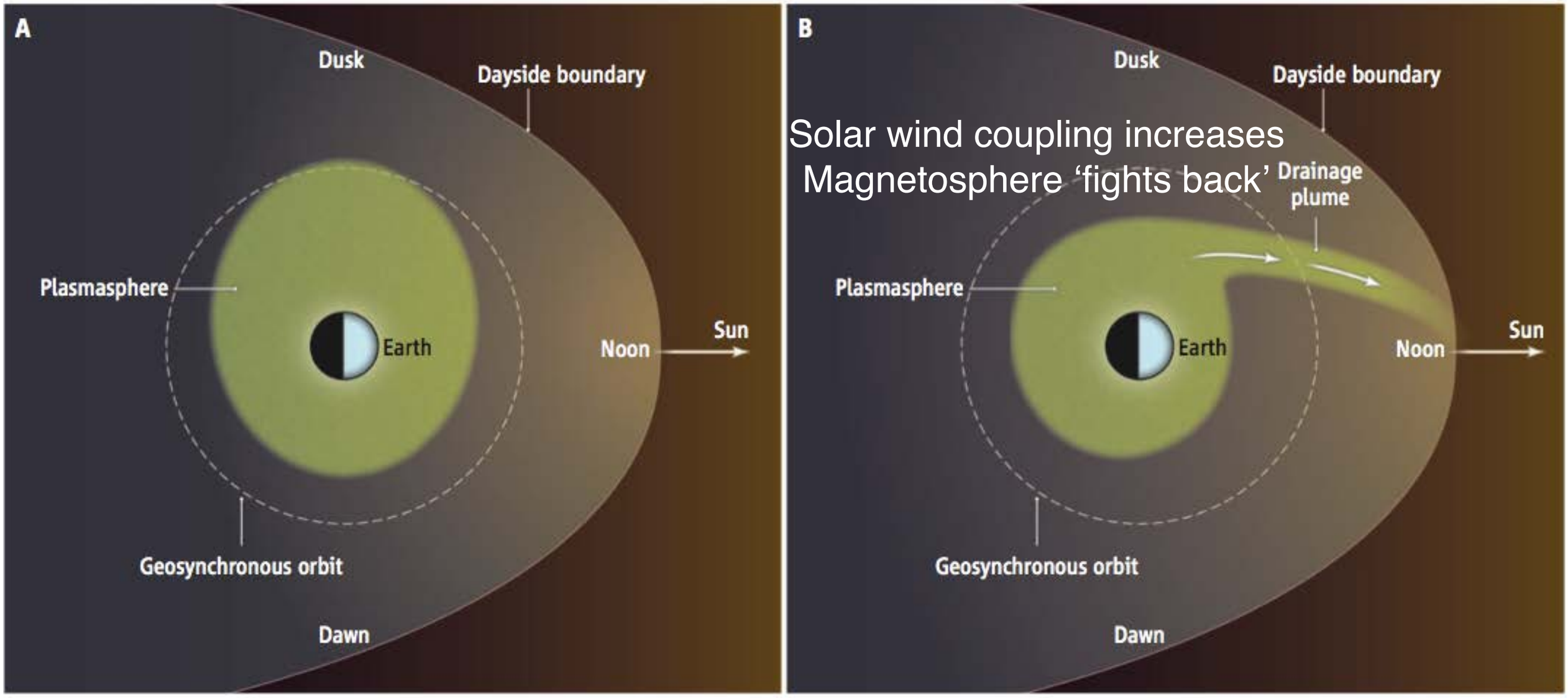

Pushing back. From a perspective high over the North Pole of Earth, the cold plasma in the equatorial plane of Earth's magnetosphere is sketched at two different times. (**A**) When solar-wind coupling is weak, the near-Earth reservoir (plasmasphere) is shown in green. (**B**) When coupling becomes stronger, the

. The
here,
ages

Plasmaspheric drainage plumes and solar-wind coupling

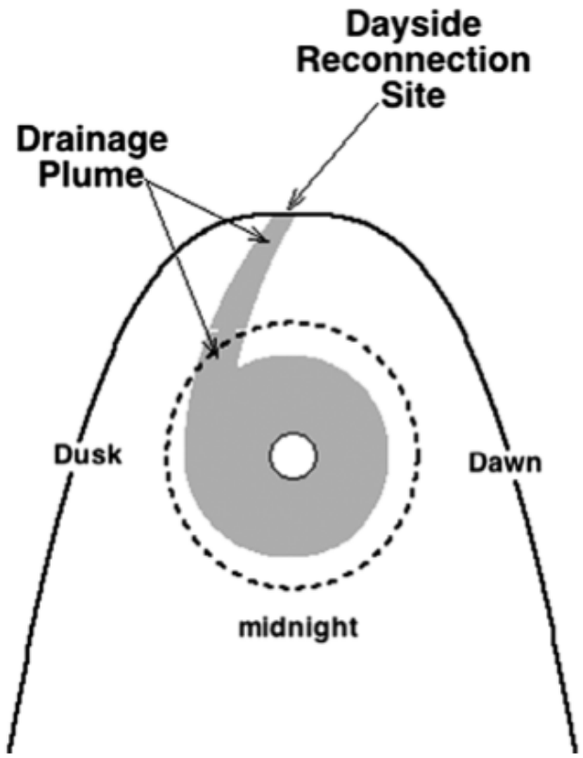

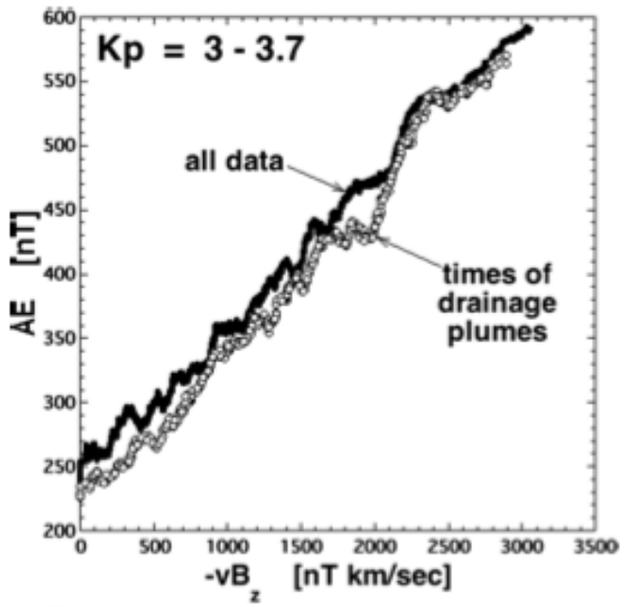

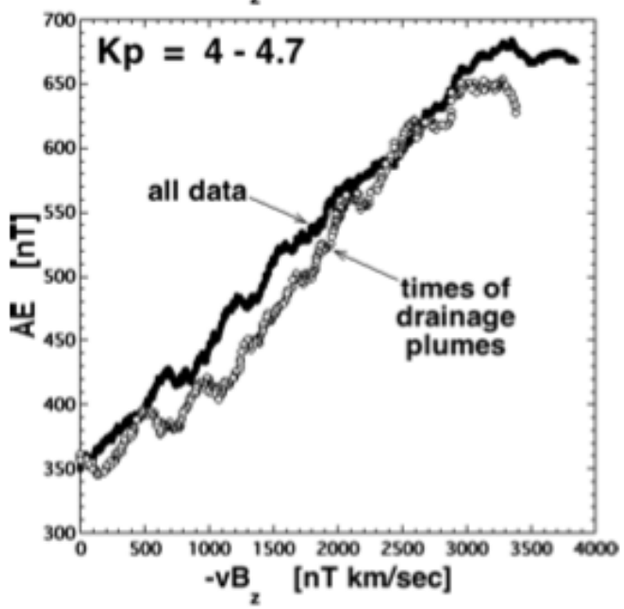

Presence of dense, cold plasma from dusk sector reduces solar-wind magnetosphere coupling (statistical study)

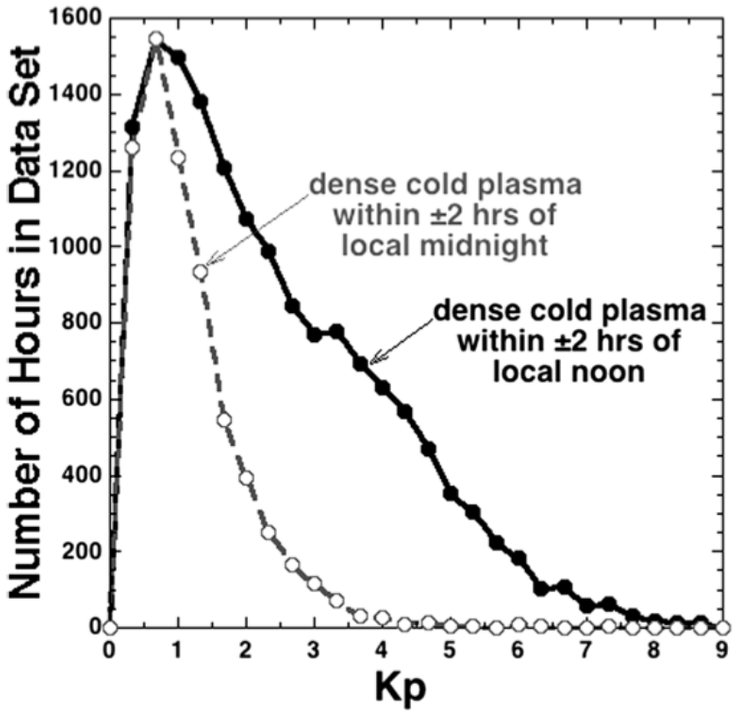

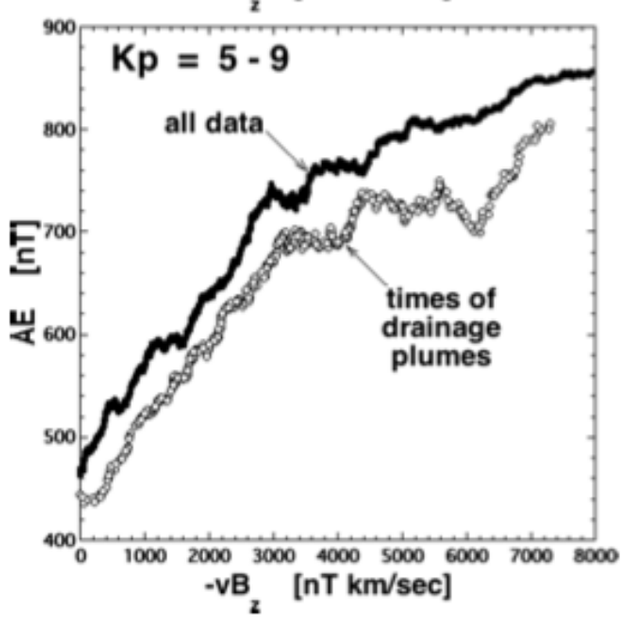

Borovsky and Denton, 2006

Geodetic GPS Total Electron Content Maps

17 Jan 2013

18:25 - 18:30 UT

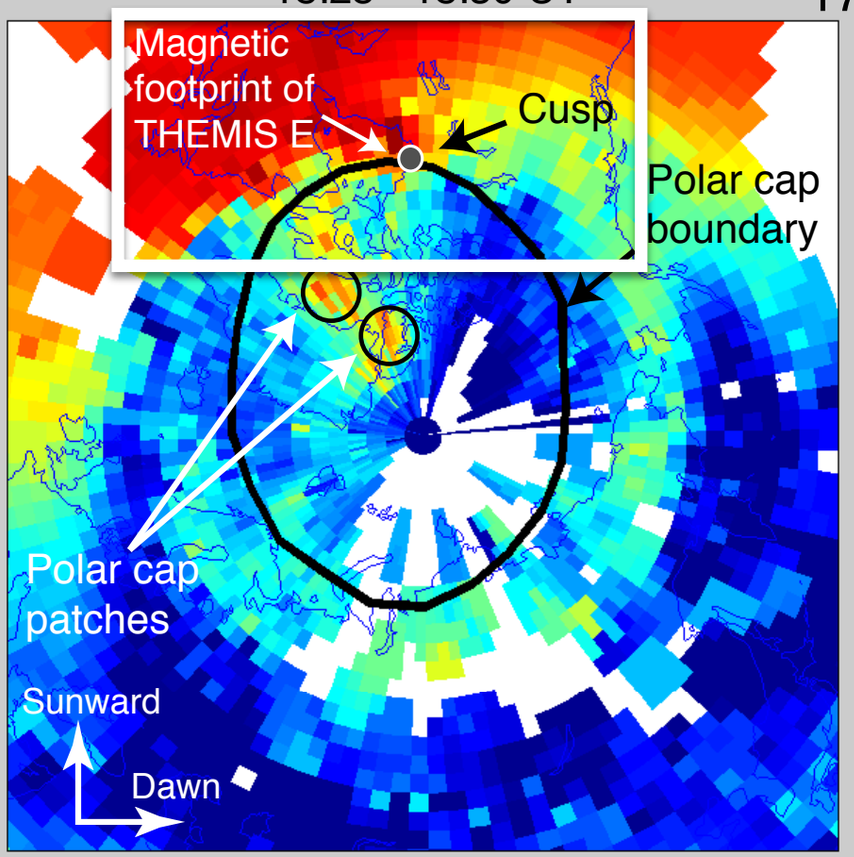

19:25 - 19:30 UT

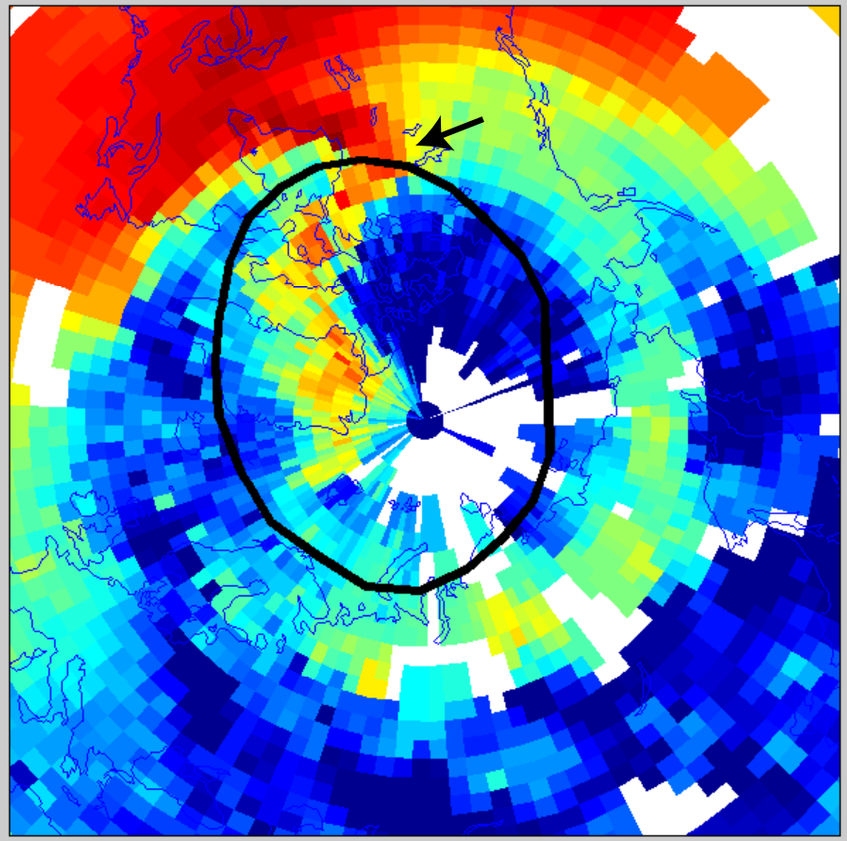

Log10(TEC)

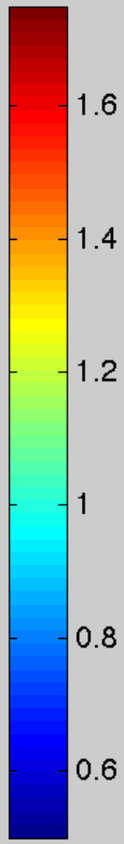

20:25 - 20:30 UT

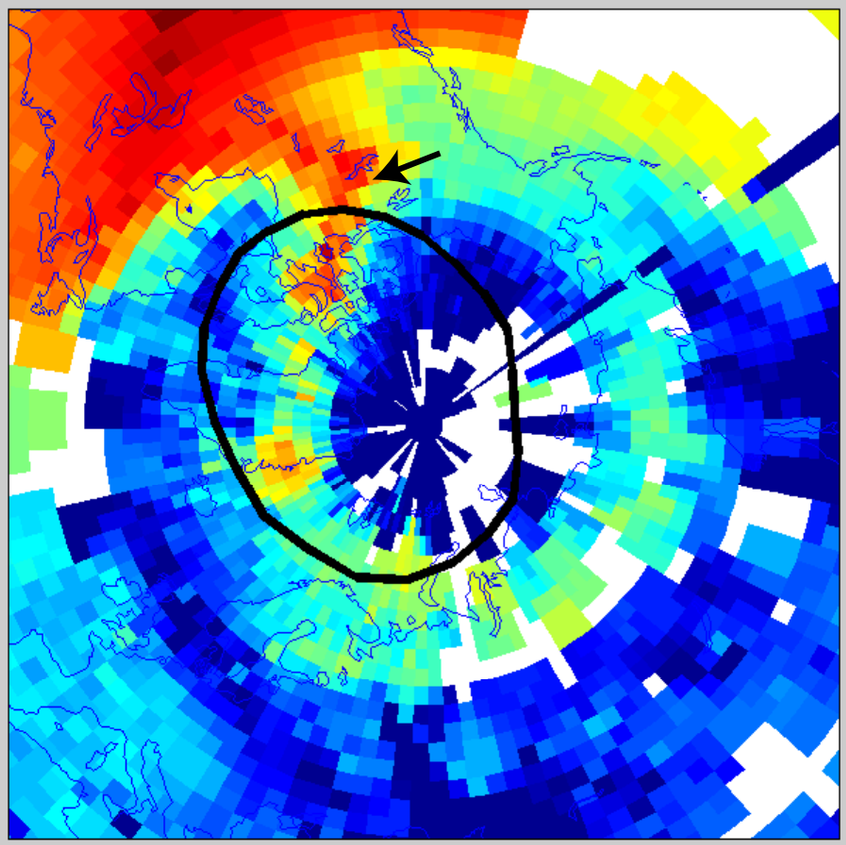

21:25 - 21:30 UT

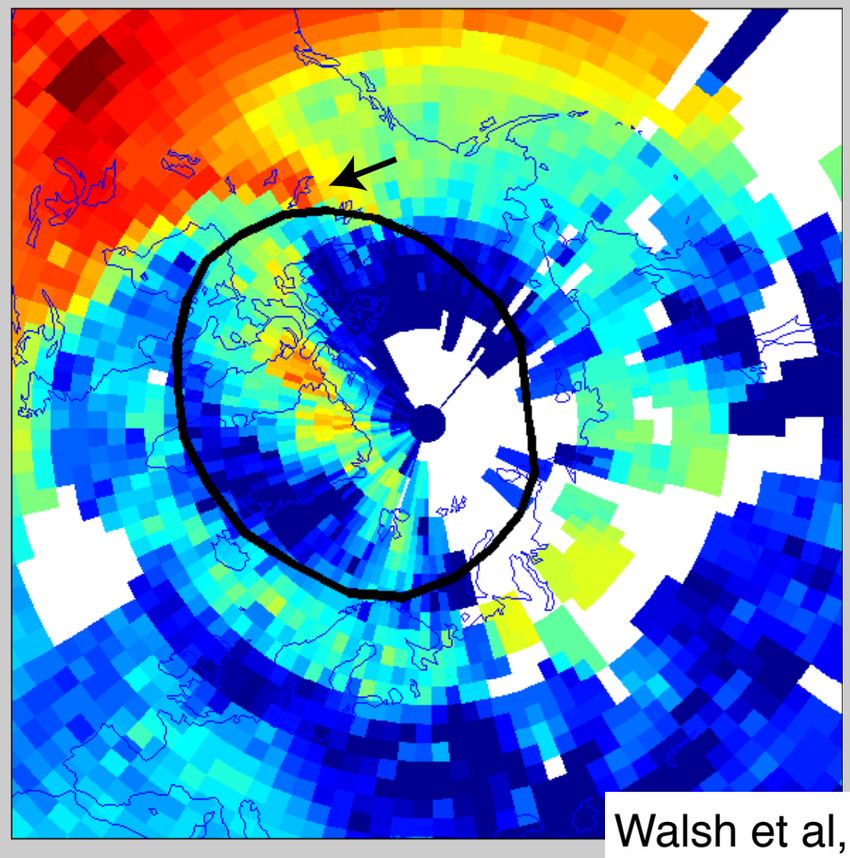

Walsh et al, Science, 2014

GPS Total Electron Content, January 17, 2013 19:00 UT

THEMIS-A
Merging

THEMIS A
THEMIS D
THEMIS E

Dusk
Sunward

YGSE (RE)

XGSE (RE)

log TEC (TECu)

Walsh et al, Science, 2014

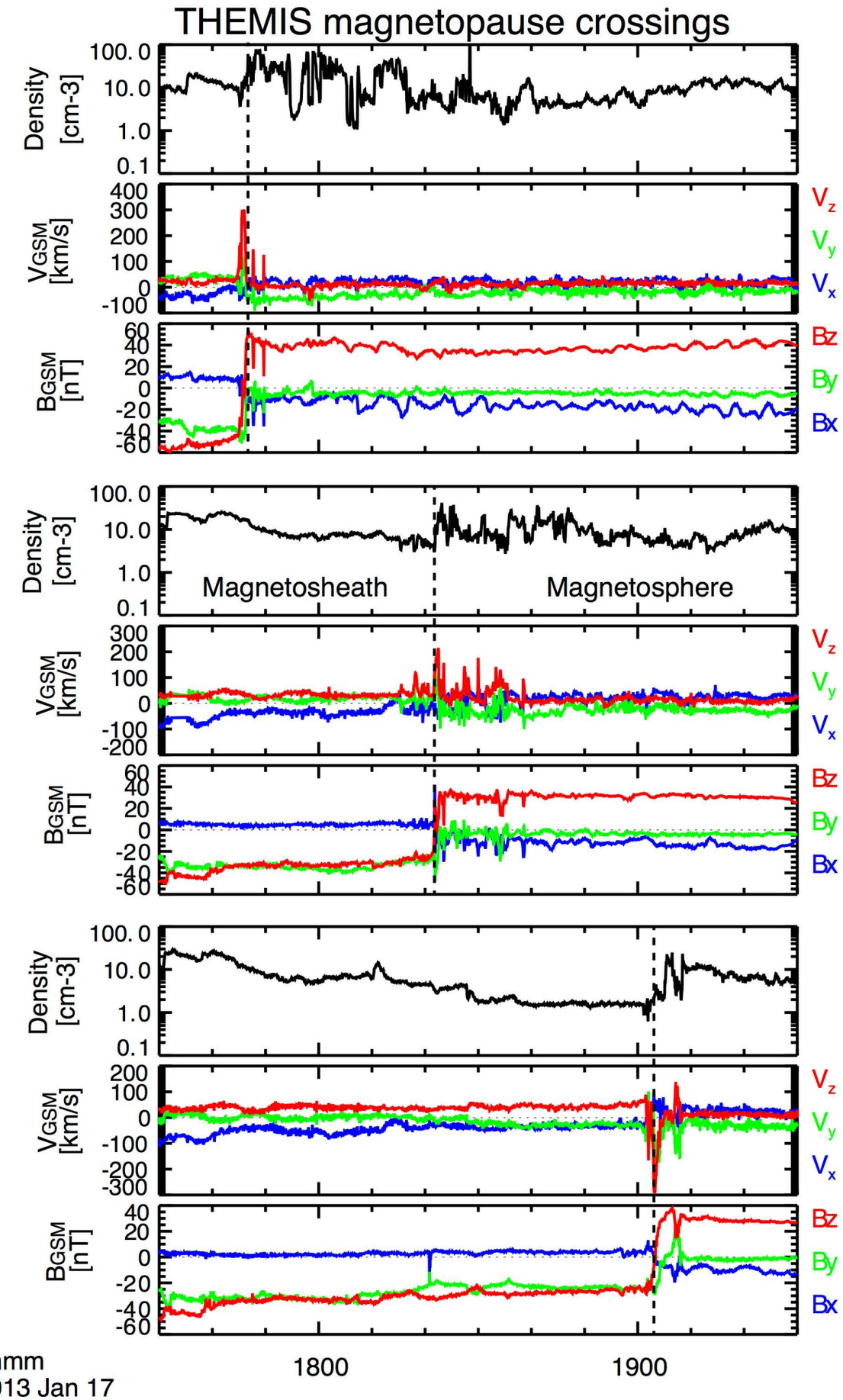

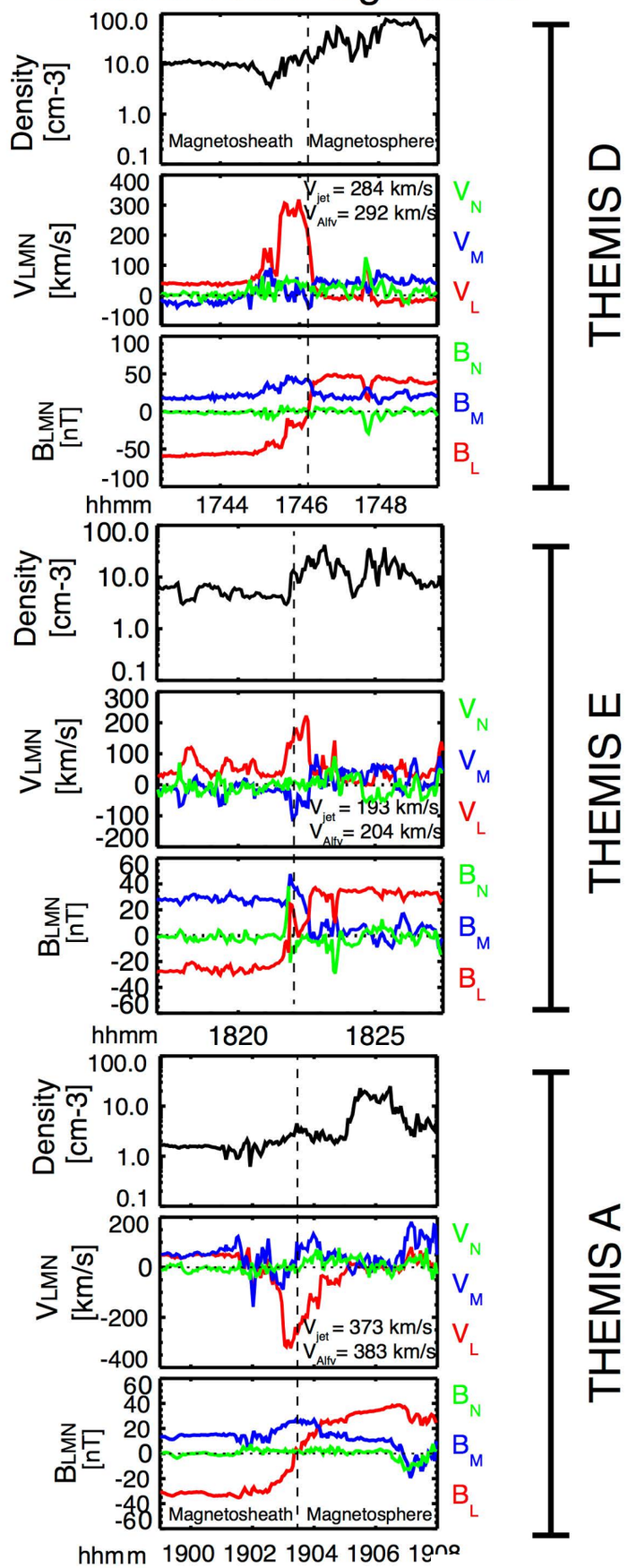

Walsh et al, Science, 2014

Reconnection signatures

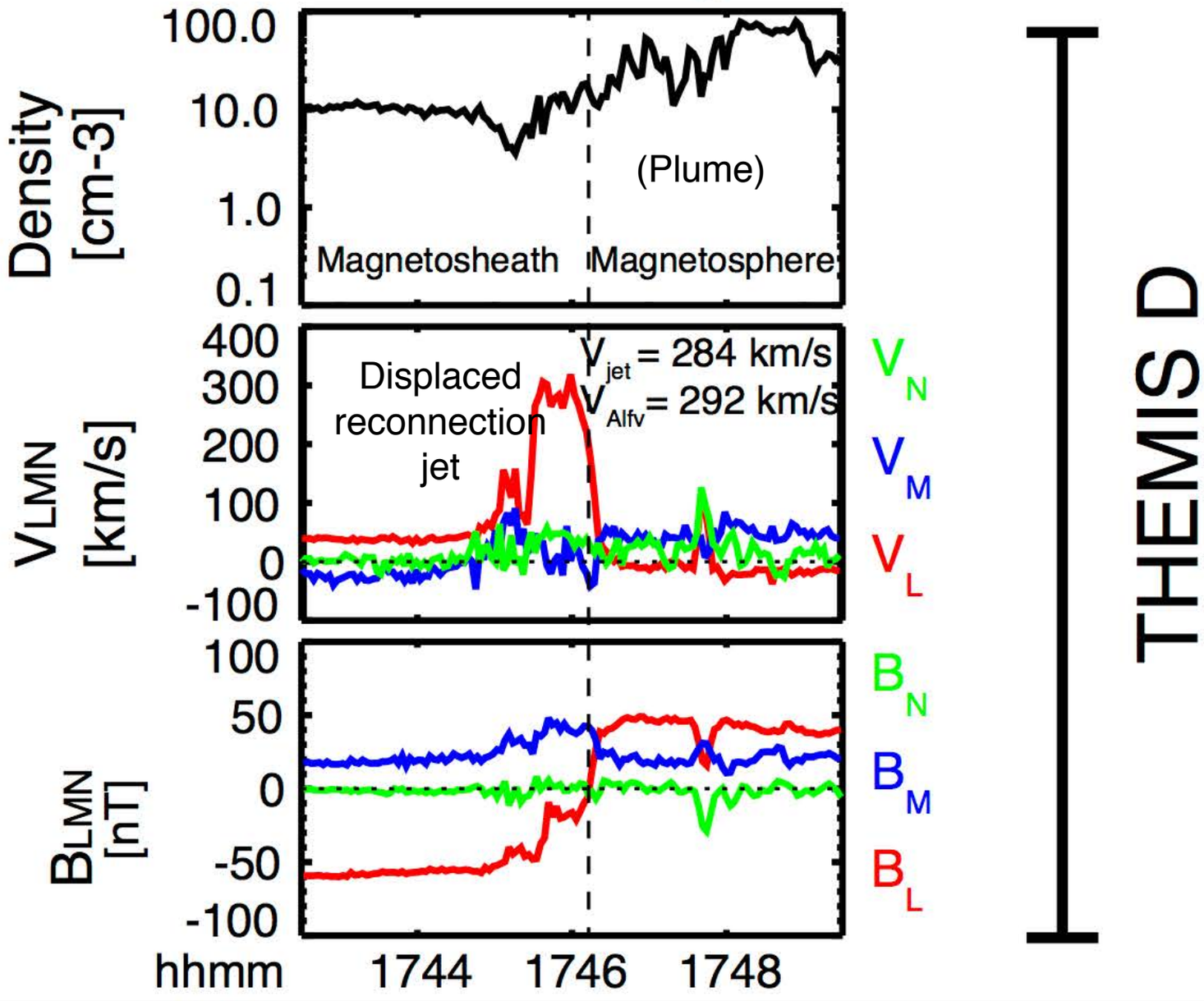

Walsh et al, Science, 2014

Geodetic GPS Total Electron Content Maps

18:25 - 18:30 UT

17 Jan 2013

19:25 - 19:30 UT

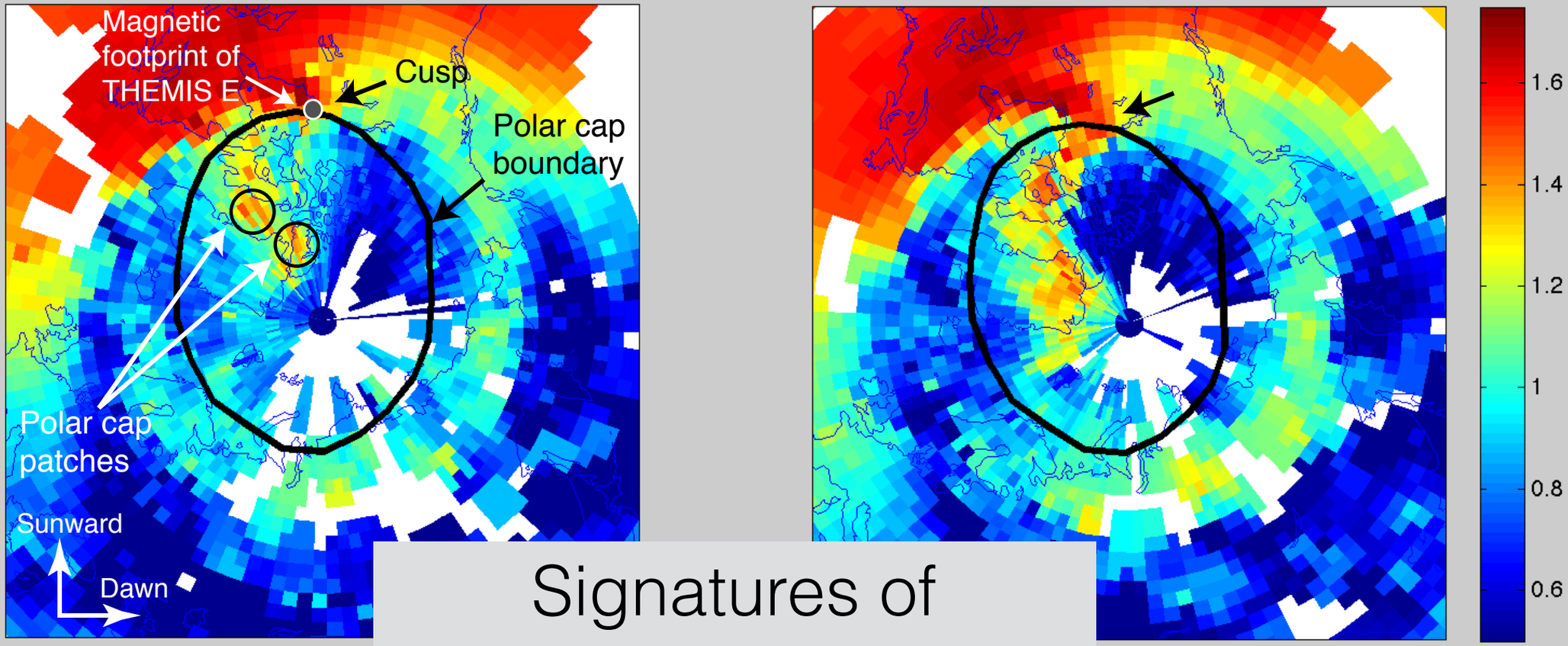

Signatures of variable reconnection: polar cap patches

20:25 - 20:30 UT

21:25 - 21:30 UT

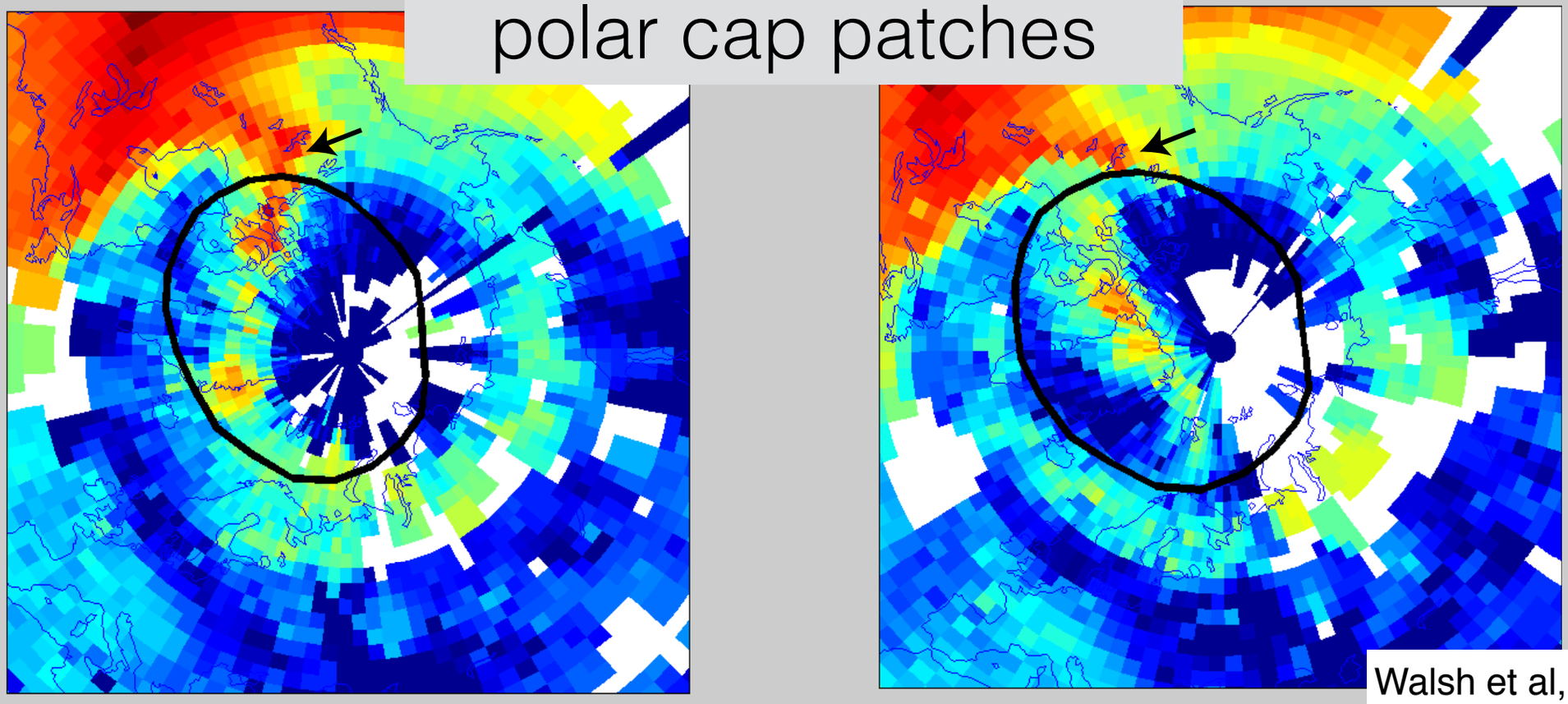

Walsh et al, Science, 2014

Outline

- Basics of Ionospheric Cold Plasma Production
- Geospace Plasma Structuring
- Cold Plasma Influences In Geospace:

1. Ionosphere-Magnetosphere Feedback
2. Cold Plasma Effects At The Magnetosphere Boundary
3. Radiation Belt Dynamics: Cold Plasma Influence

Earth's Radiation Belts

Protons (100+ MeV)
and HE electrons (100s keV)
(stable; CRAND)

Magnetically connected ionosphere / plasmasphere observations

Van Allen Probes (apogee at 5.5 to 6 Re; equatorial plane)

Electrons and Ions - H+, He+, O+ (highly variable; 10s eV - MeV+)

Particle Invariants

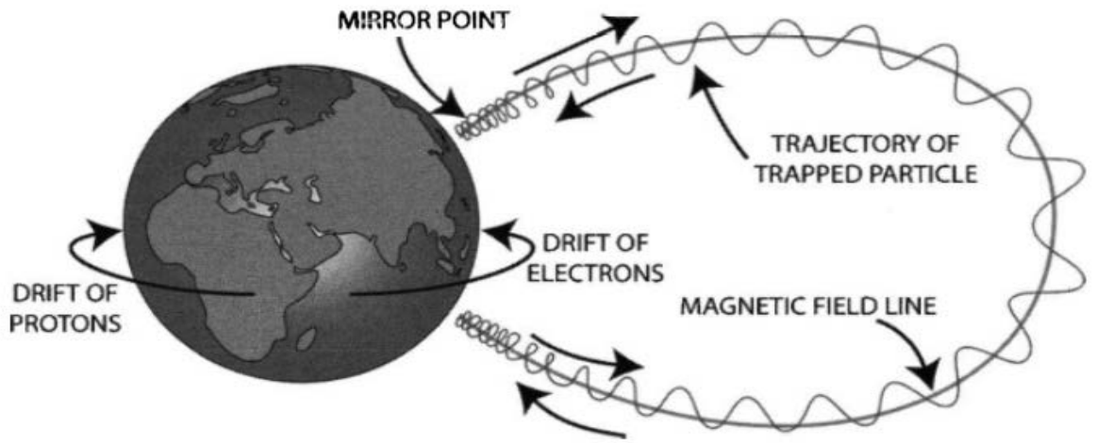

Characteristic time scales:
- Gyro: ~millisecond
- Bounce: ~0.1 - 1.0 s
- Drift: ~1 - 10 minutes

- Gyro motion:
  - V x B acceleration leads to gyro motion about field lines
  - frequencies ~kHz
  - associated 1st invariant μ, relativistic magnetic moment:

$$\mu = \frac{p^2 \sin^2 \alpha}{2 m_0 B}$$

pitch angle α: $\tan \alpha = \frac{V_\perp}{V_\parallel}$

- Three types of periodic motion of trapped particles
  - gyro motion
  - bounce motion
  - drift motion
- Each motion has an associated adiabatic invariant

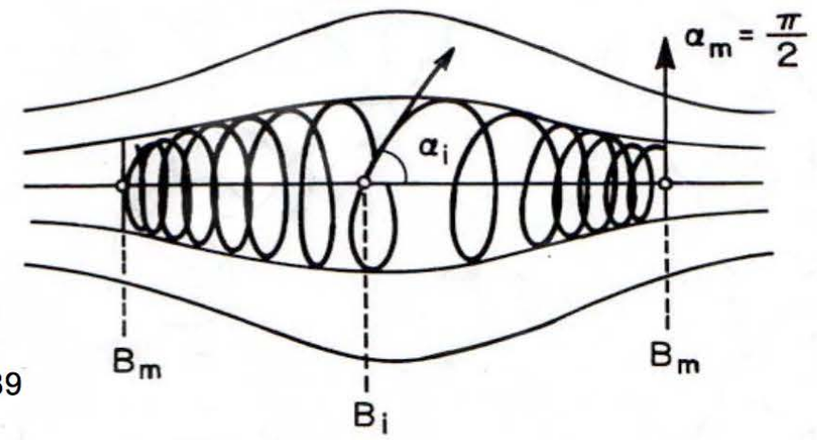

Spjeldvik and Rothwell, 1989

(D. Baker; W. Johnston GEM tutorial)

Wave-Particle Interactions

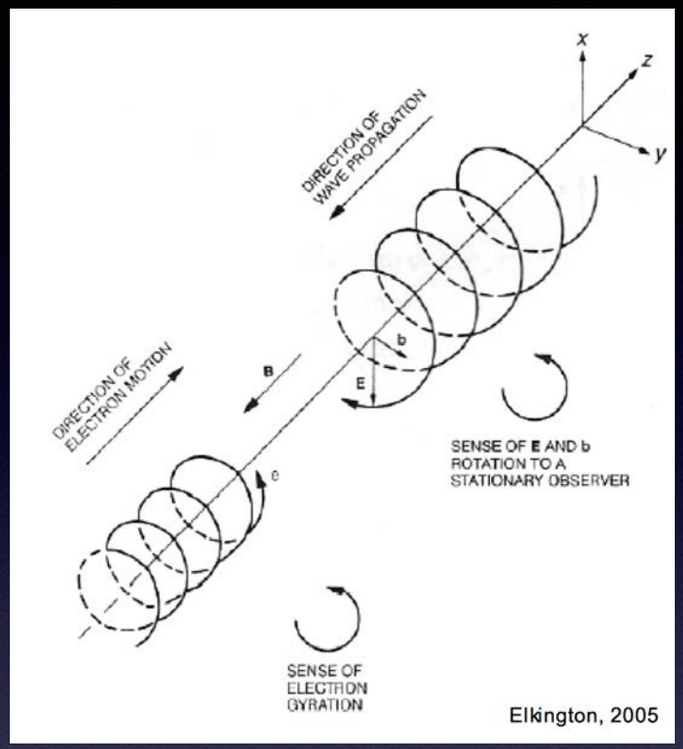

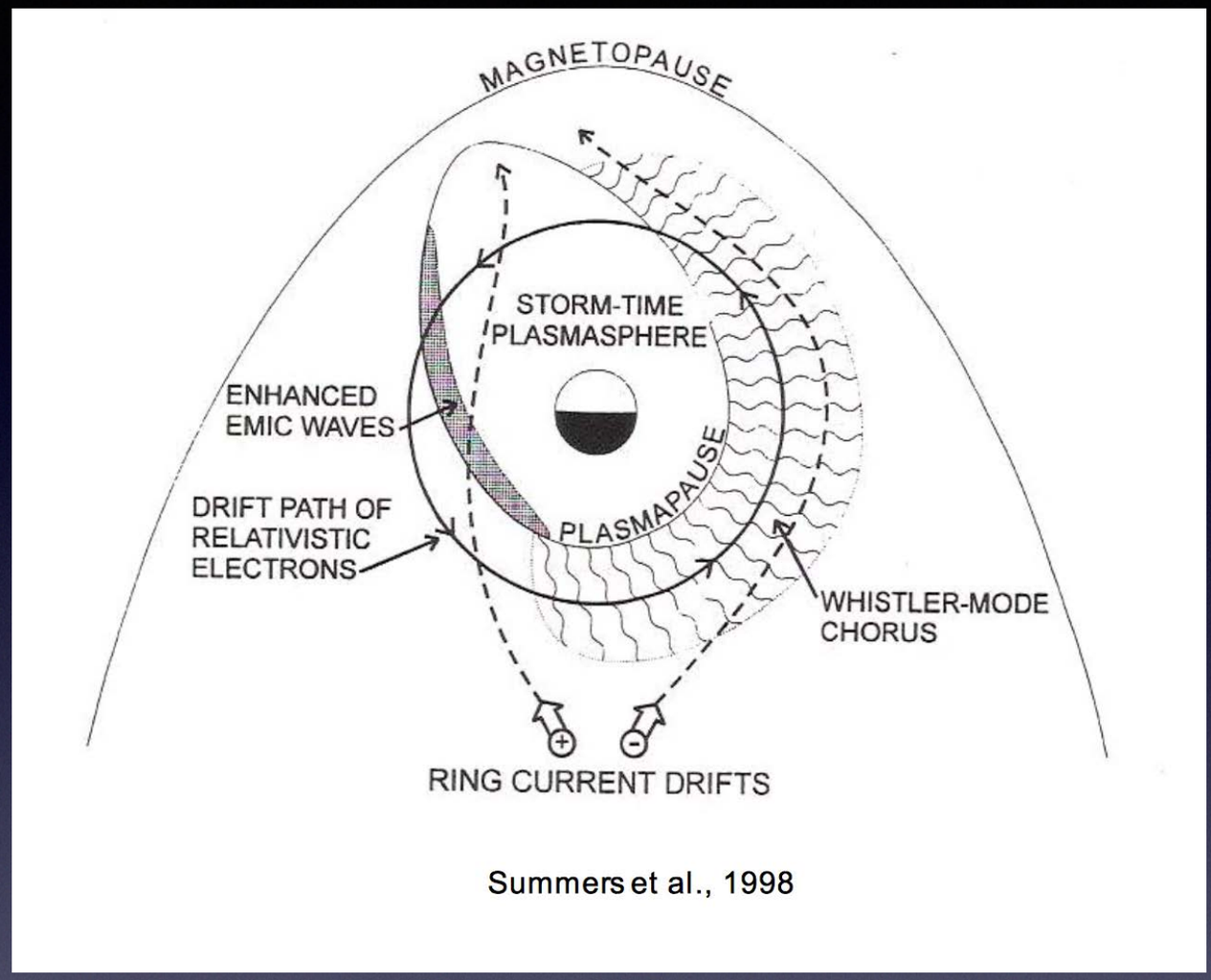

- Chorus / Whistlers
- ULF waves
- Magnetosonic waves
- EMIC waves
- Plasmaspheric Hiss [incoherent]

Resonance conditions can depend on ambient background plasma

Pitch angle, Coulomb scattering = Loss
Slow diffusion = Transport
Linear and non-linear processes involved

Diffusion Timescales

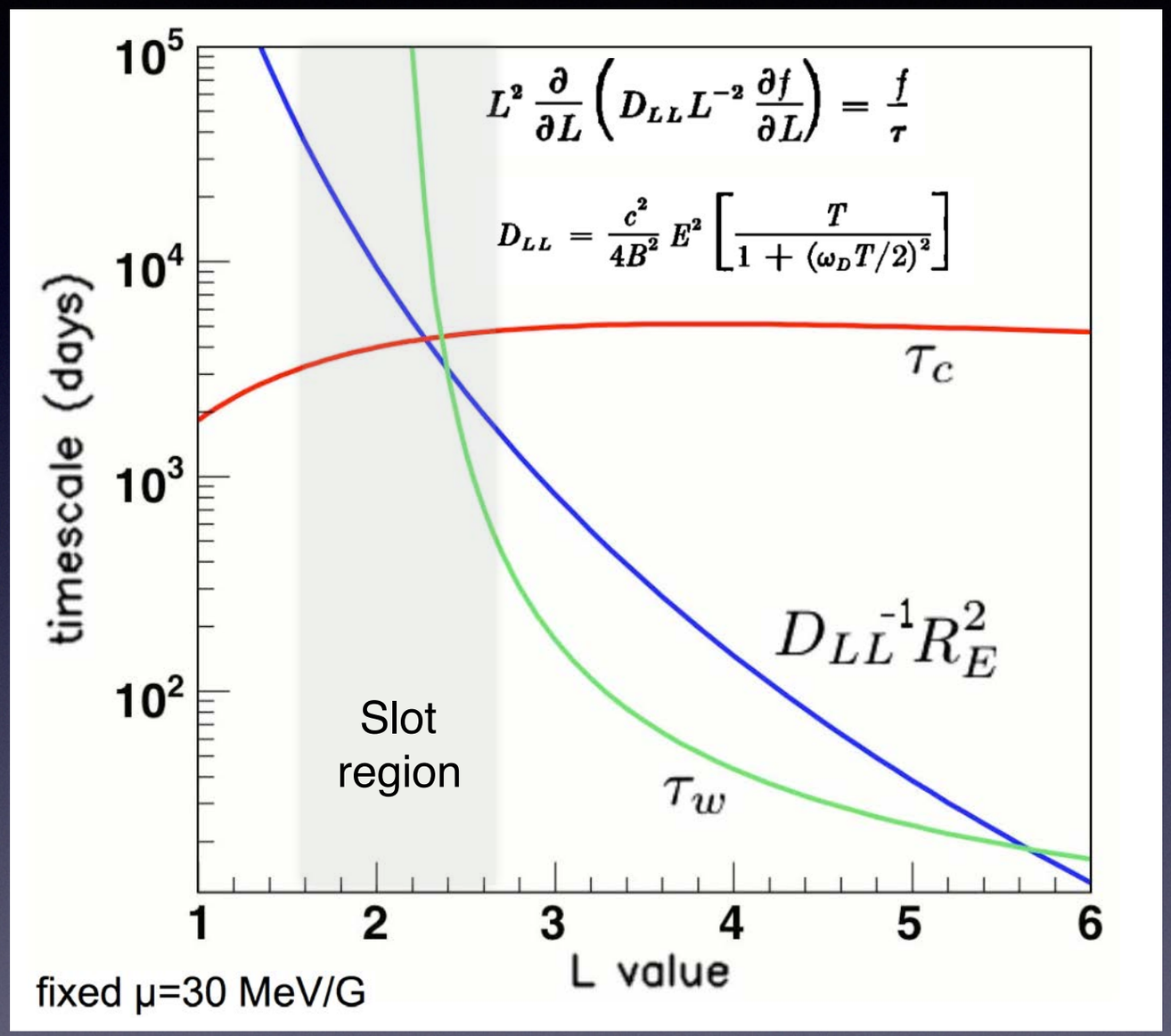

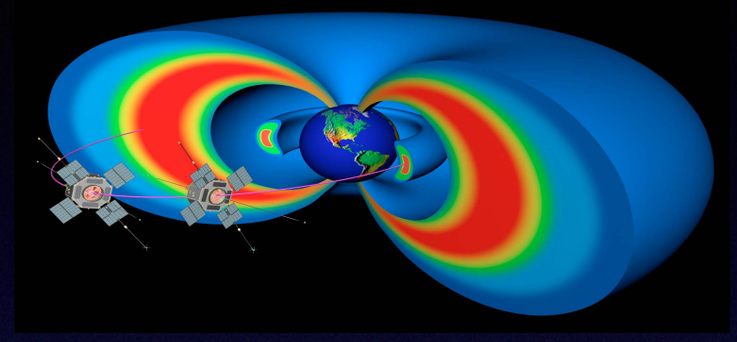

- D_{LL} drives inward diffusion, faster at large L
- Whistler losses faster than replacement by diffusion in slot region
- Those particles that reach low L have lifetimes of years
- Note balance at L=2.8 for this (low!) 1st adiabatic invariant

(W. Johnston GEM tutorial; after Lyons and Thorne, 1973)

Fast Radiation Belt Energization

- Inner edge of the outer belt
- Highly relativistic e- increases immediately in **minutes** at L* = 4.5 after substorm injection of 100 keV particles (not shown)
- 4.5 MeV fluxes increase 90x over ~5 hours
- VLF power increases 100x, pumped by 50-100 keV injected particles

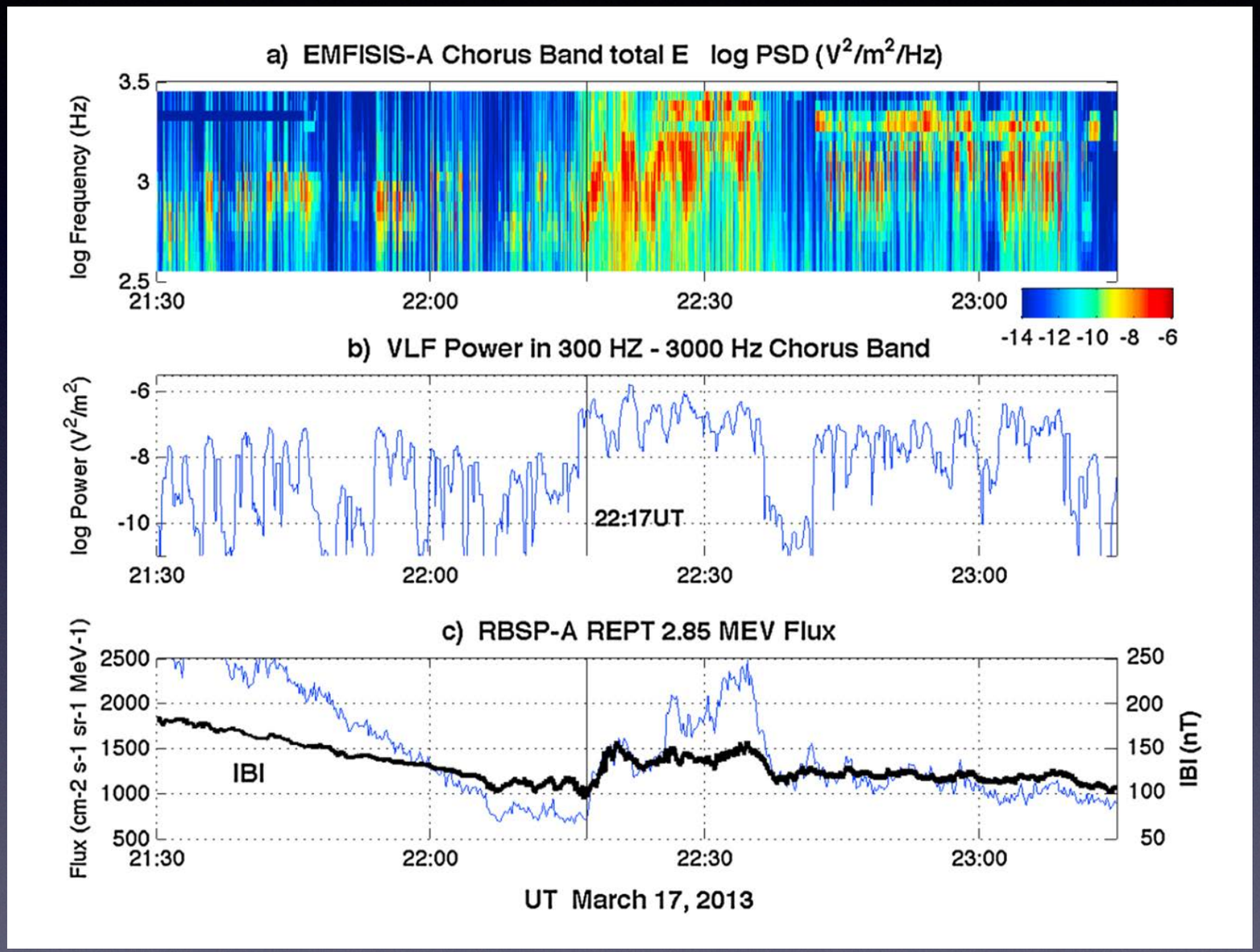

Prompt energization still takes place **outside** the plasmapause

Foster et al, 2014
also Reeves et al, 2013

The ‘Impenetrable Barrier’

Van Allen Probes: Three Years’ Observations of Ultra-Relativistic Electrons

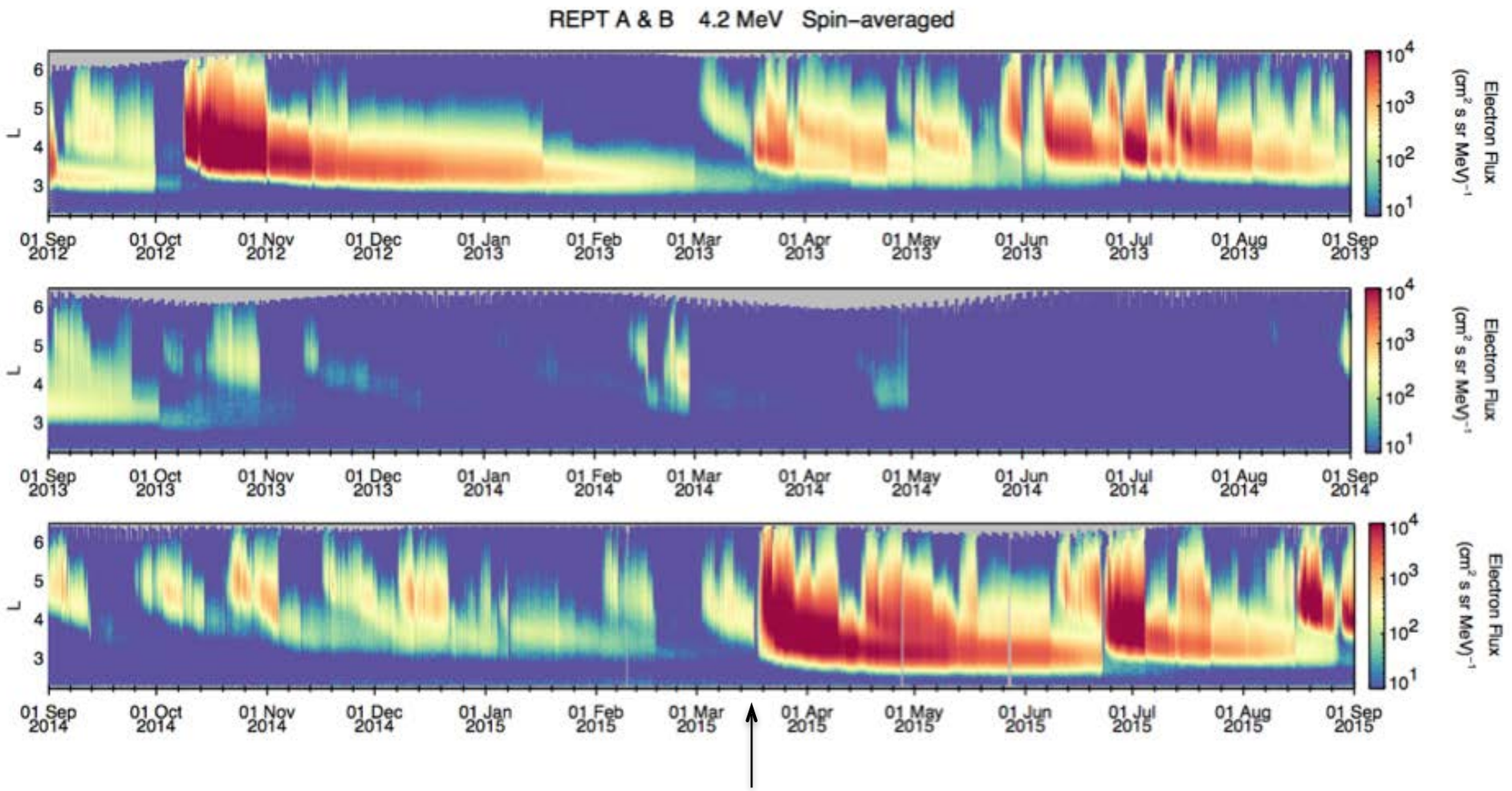

Baker et al, 2014

GIZMODO + Follow

Be Thankful For the Invisible Belt That Saves Earth From Radiation

Kelsey Campbell-Dollaghan
11/26/14 6:00pm · Filed to: EARTH

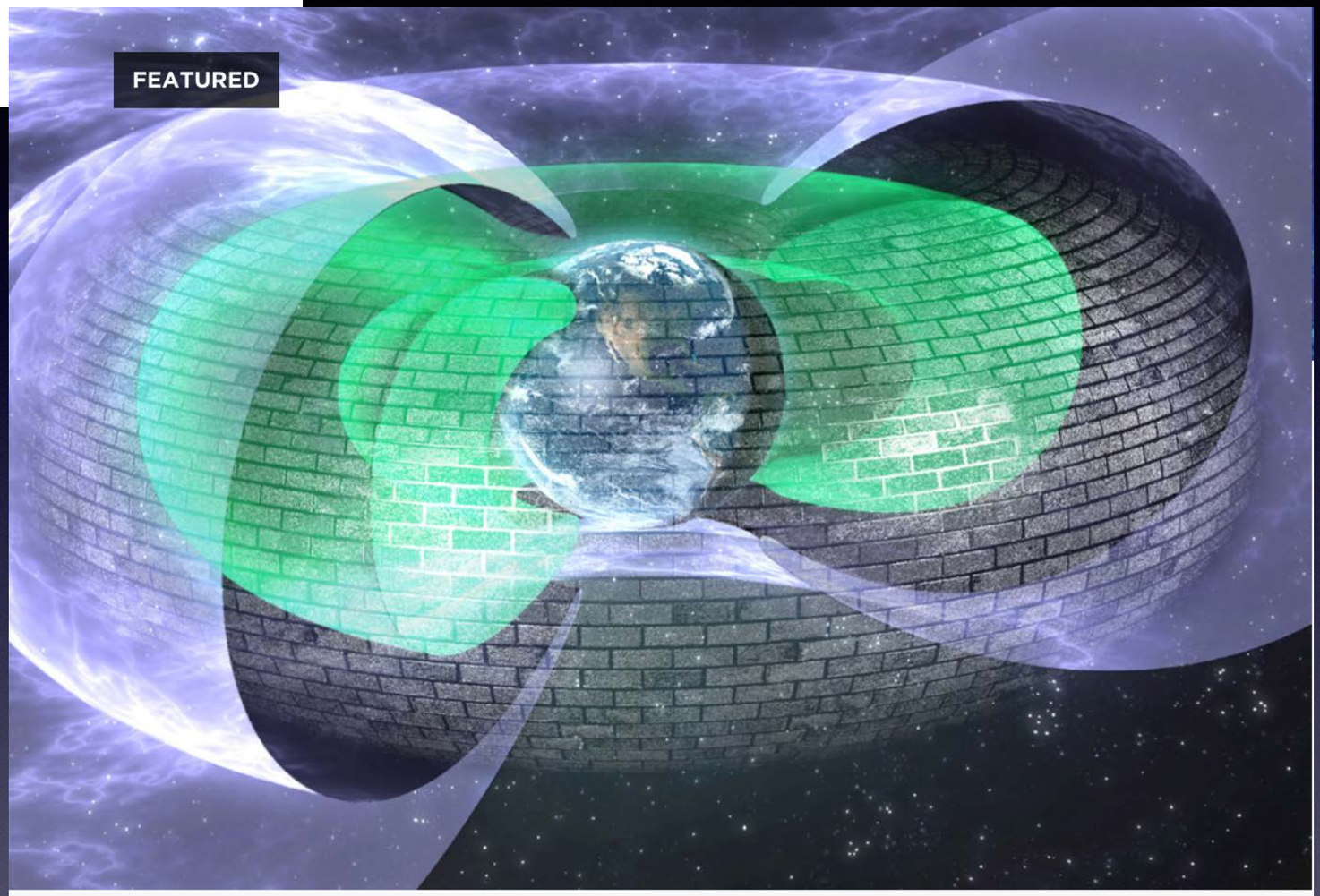

NOVEMBER 27, 2014

Scientists Discover Impenetrable Star Trek-Like 'Force Field' Surrounding Earth

The Press Tries
Its Hand at
The 'Impenetrable Barrier'

The ‘Impenetrable Barrier’

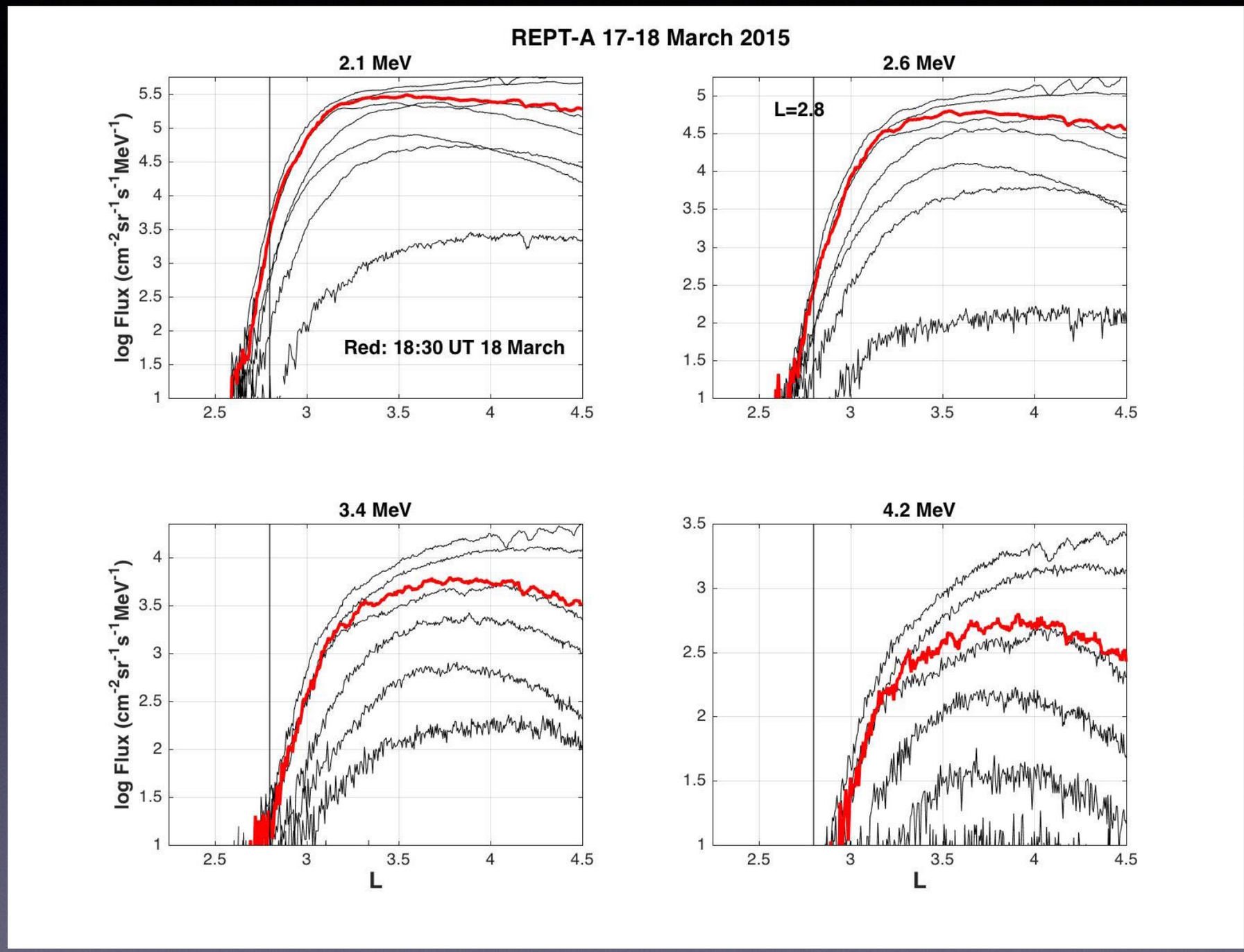

Is this simply the plasmapause location?

Foster et al, 2016

The ‘Impenetrable Barrier’ and the Plasmapause

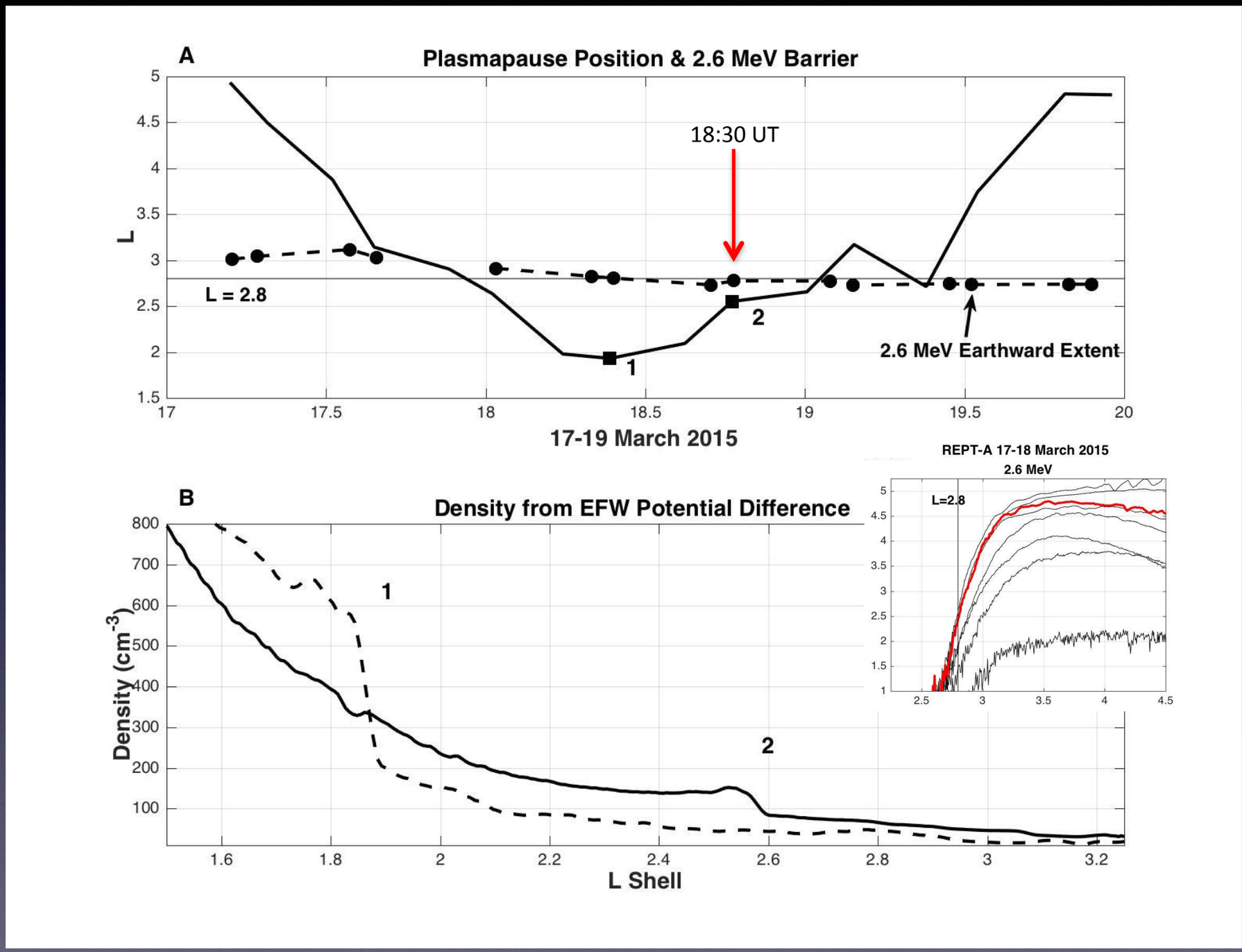

No, it’s not the plasmapause location.

Foster et al, 2016

VLF Transmitters

The large negative radial density gradients deflect the ray inward, but as the ray moves in and encounters markedly reduced gradients, the curvature of the earth's field deflects the ray outward. Upon entering the region of high gradient the ray will again be refracted inward, and the process will be repeated. The result is that the ray is trapped by the density gradient and its path oscillates about the direction of earth's field.

Gradient trapping
Helliwell, 1965

Inan and Bell, 1977

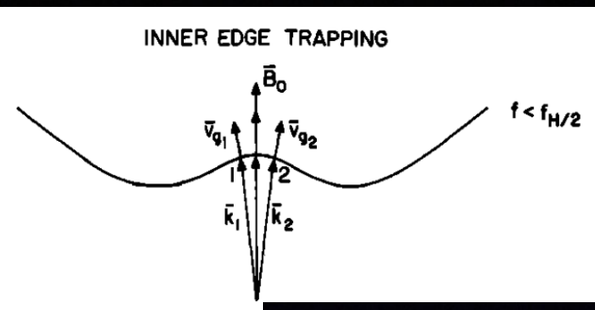

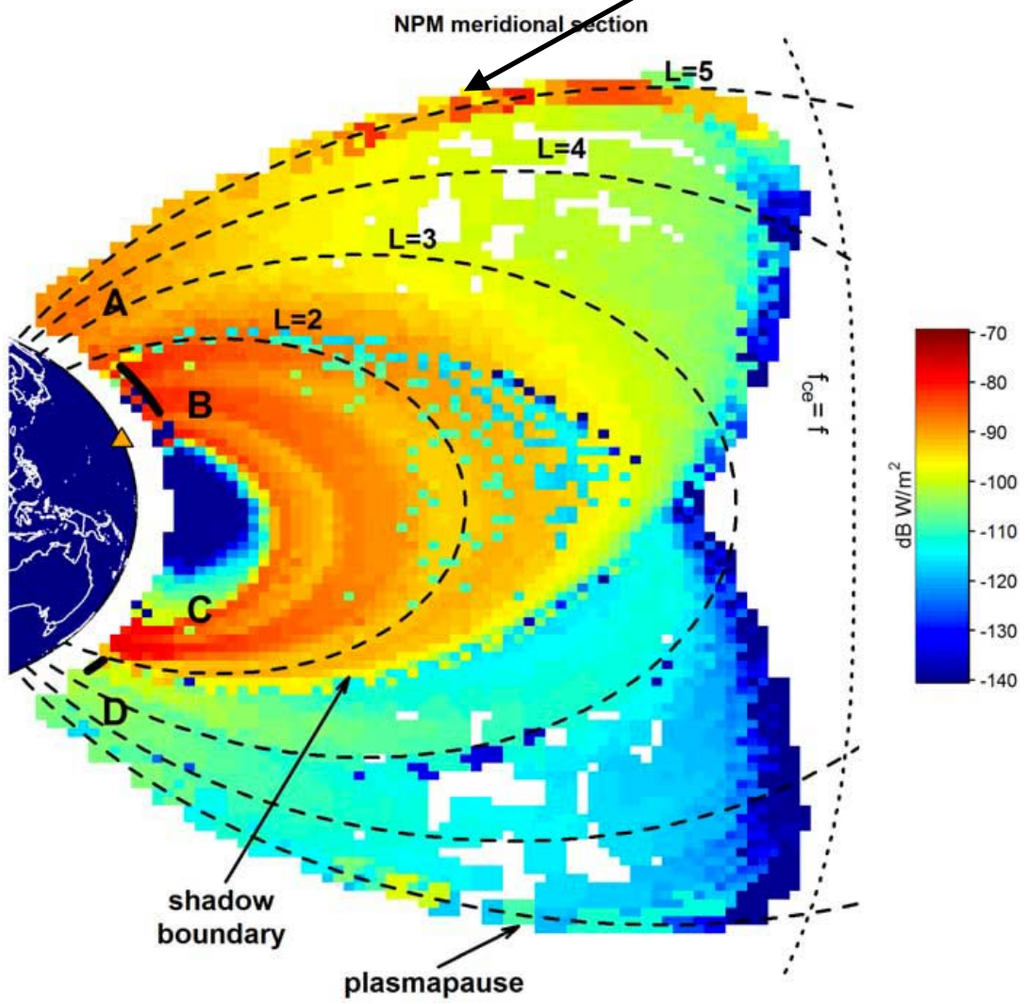

Model

Propagation of VLF Waves in Inner Magnetosphere

The VLF Bubble

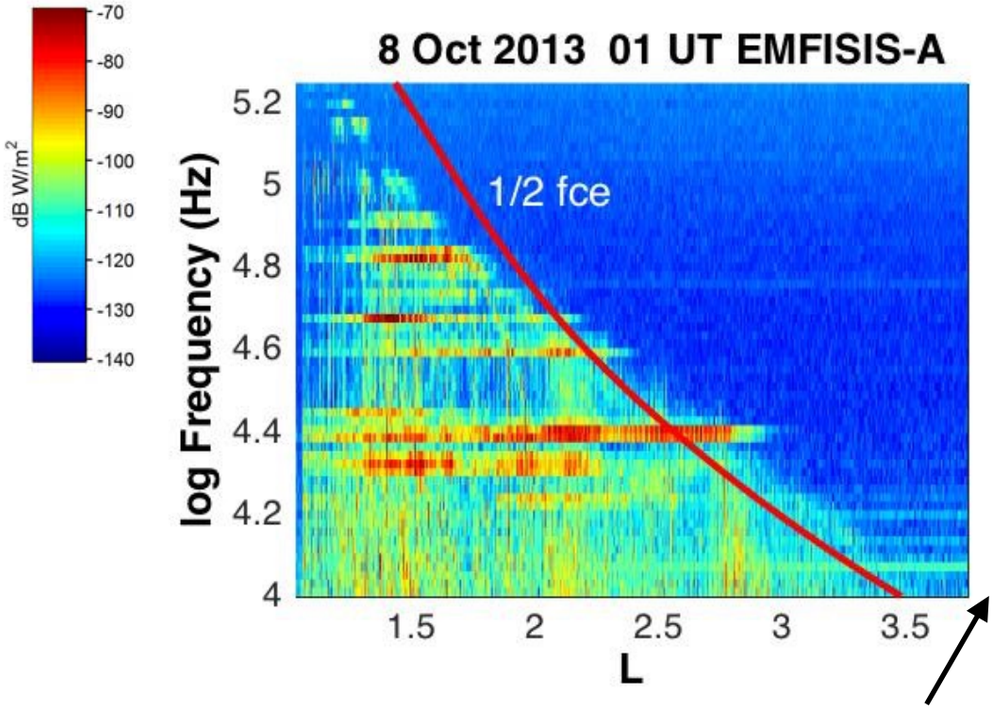

Observations

Plasmapause/PBL

Meridional section of power flux predicted by AFRL's VLF Propagation Code in the plasmasphere due to NPM transmissions. The transmitter is marked by a triangle. Note the prominent shadow boundary in the conjugate hemisphere. An analogous boundary (not visible) exists in the transmitter hemisphere. [Starks et al, 2009]

VLF Transmitters

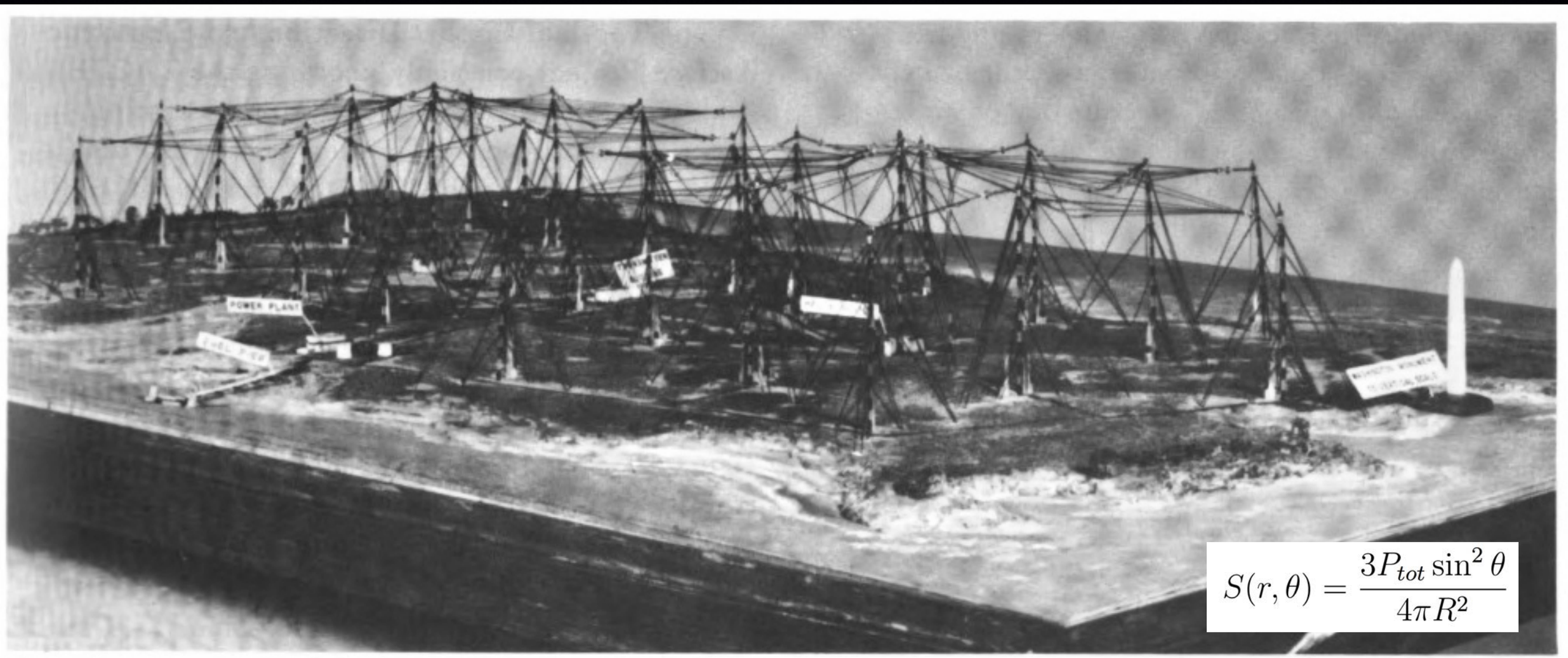

Figure 5. Antenna system of VLF transmitter, Cutler, Maine.

VLF Transmitters

Table 2. VLF Transmitter Call Signs, Frequency, Geographic Coordinates, Output Power, and Geomagnetic *L* Shells

Transmitter	Frequency (kHz)	Latitude	Longitude	Estimated Power (kW)	*L* Shell (2008)
NRK, Iceland	37.5	63° 51′ N	22° 28′ W	100	5.5
NLK, Seattle	24.8	48° 12′ N	121° 55′ W	250	2.9
NDK, North Dakota	25.2	46° 22′ N	98° 20′ W	500	3.3
NAA, Maine	24.0	44° 39′ N	67° 17′ W	1000	2.9
GQD, Anthorn	22.1	54° 53′ N	03° 17′ W	60	2.7
HWU, Rosnay	22.6	46° 43′ N	01° 15′ E	200	1.8
DHO, Ramsloh	23.4	53° 05′ N	07° 37′ E	300	2.4
ICV, Tavolara Island	20.27	40° 55′ N	09° 45′ E	50	1.5
NWC, NW Cape	19.8	21° 49′ S	114° 10′ E	1000	1.4
NTS, Woodside	18.6	38° 29′ S	146° 56′ E	25	2.4
NPM, Hawaii	21.4	21° 26′ N	158° 09′ W	500	1.2
NAU, Puerto Rico	40.75	18° 25′ N	67° 09′ W	125	–
JAP, Ebino	22.2	32° 03′ N	130° 50′ E	100	1.2

(Rodger, 2009)

VLF Resonance with Ultrarelativistic Particles?

Kulkarni et al 2008
VLF TX modeling

Ambient density = 1000 cm-3 @ L=2.8 (plasmasphere)

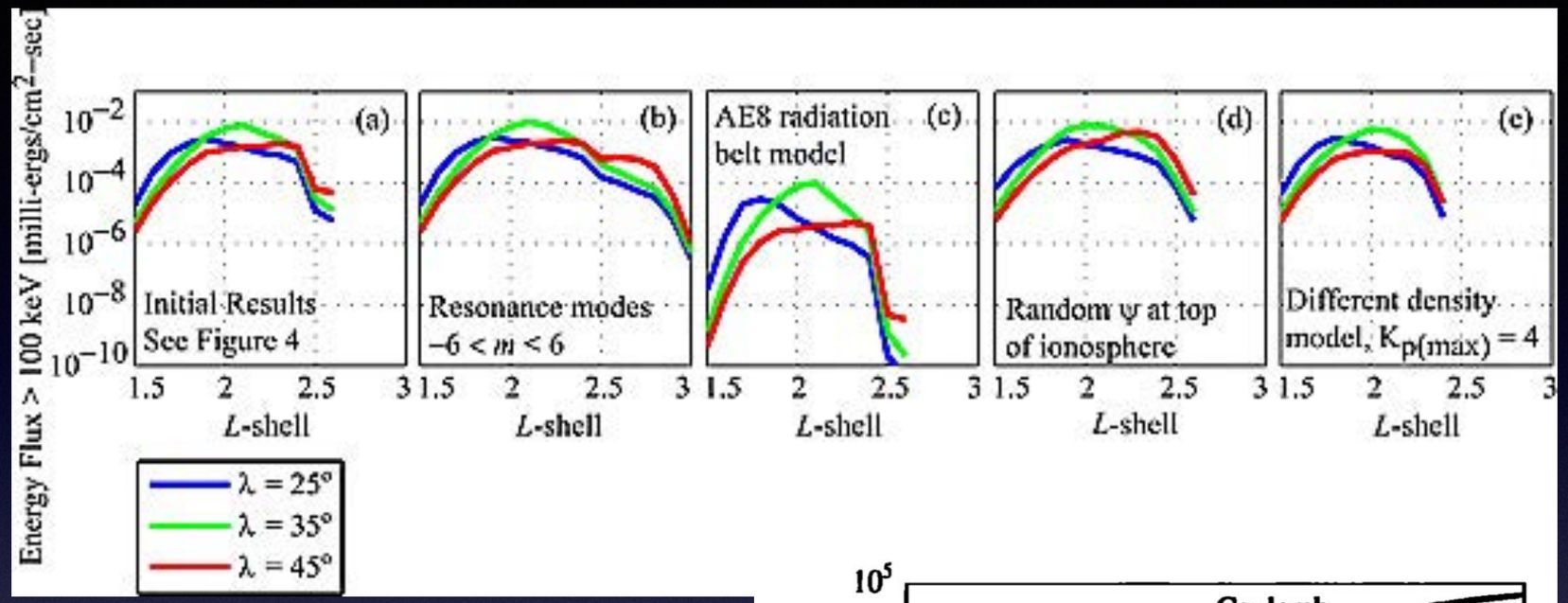

Note that 17.1 and 22.3 kHz VLF transmitter frequencies cannot resonate at the equator beyond L = 2.4 and 2.2, respectively, due to propagation characteristics and an increase in wave absorption as the wave frequency approaches the electron gyrofrequency <…>
Higher-frequency VLF waves should provide the most effective scattering at the lowest value of L, while low frequency (~500 Hz) plasmaspheric hiss should dominate in the outer zone (L >_ 3.0)

Abel and Thorne 1998

All these calculations done INSIDE the plasmasphere

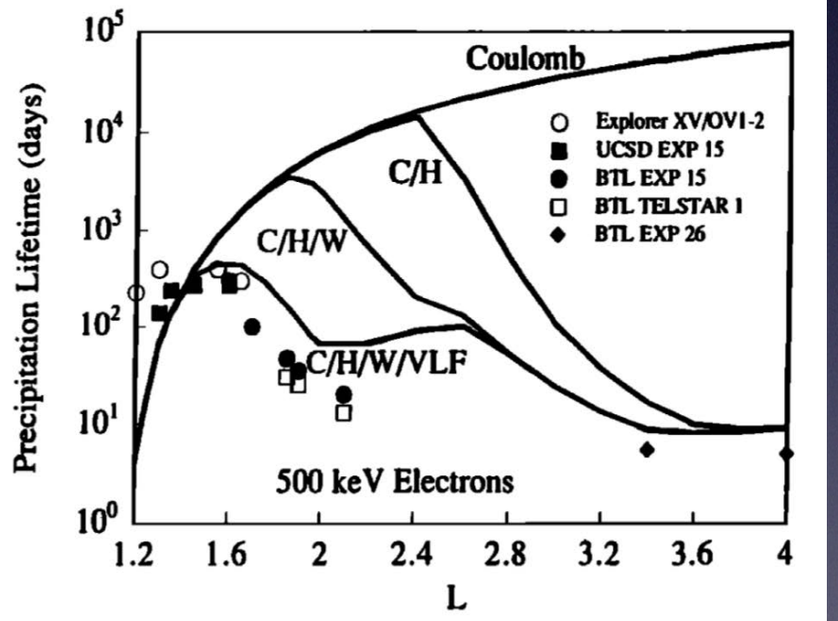

Figure 9. Precipitation lifetime calculations for 500 keV electrons for scattering due to Coulomb collisions (C), Coulomb and plasmaspheric hiss (C/H), Coulomb, plasmaspheric hiss and lightning-generated whistlers (C/H/W), and with all scattering mechanisms included (C/H/W/VLF). Observed decay rates are included for comparison.

VLF Transmitters: In-situ Measurements

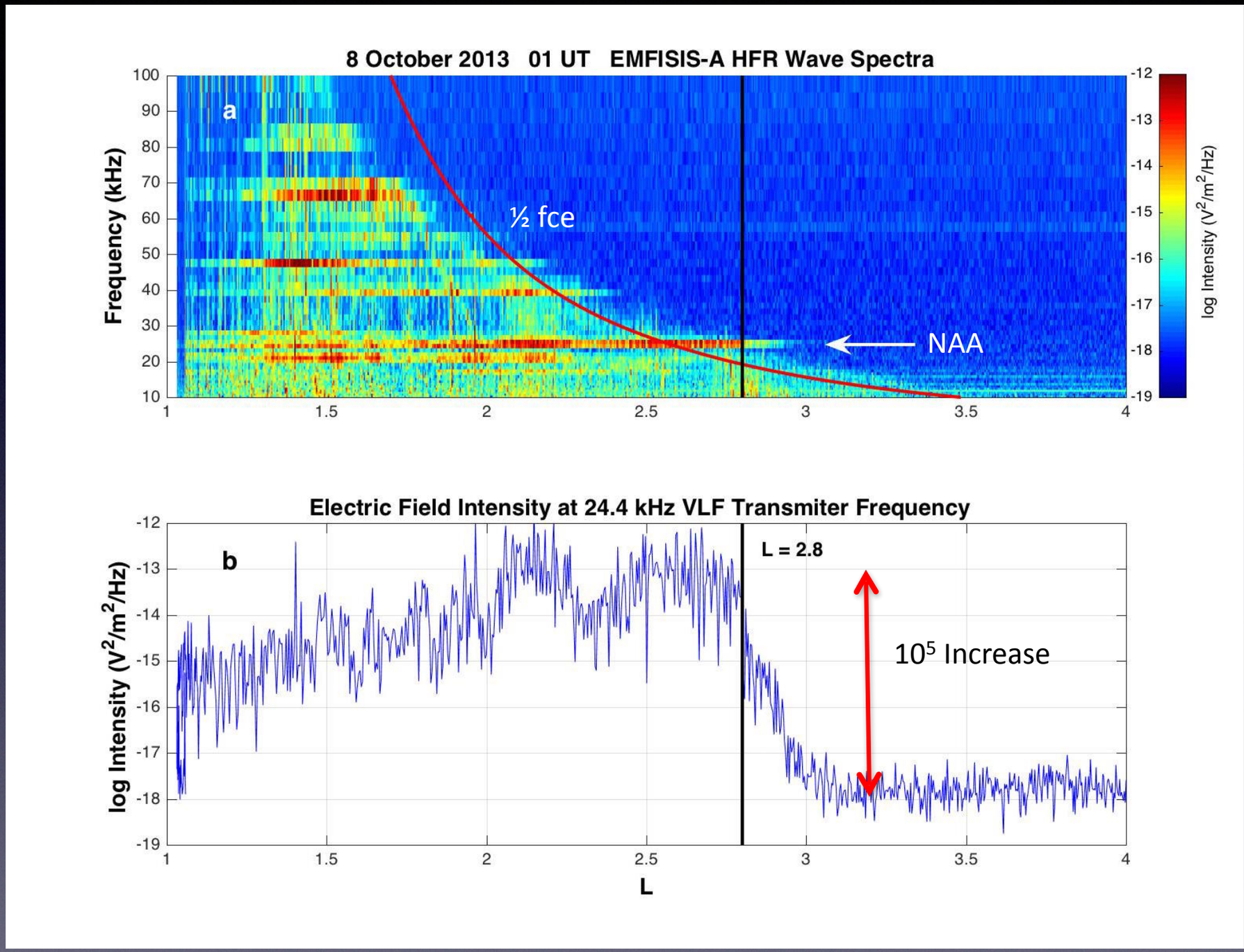

Foster et al, 2016

VLF Transmitters Interact With Natural Chorus

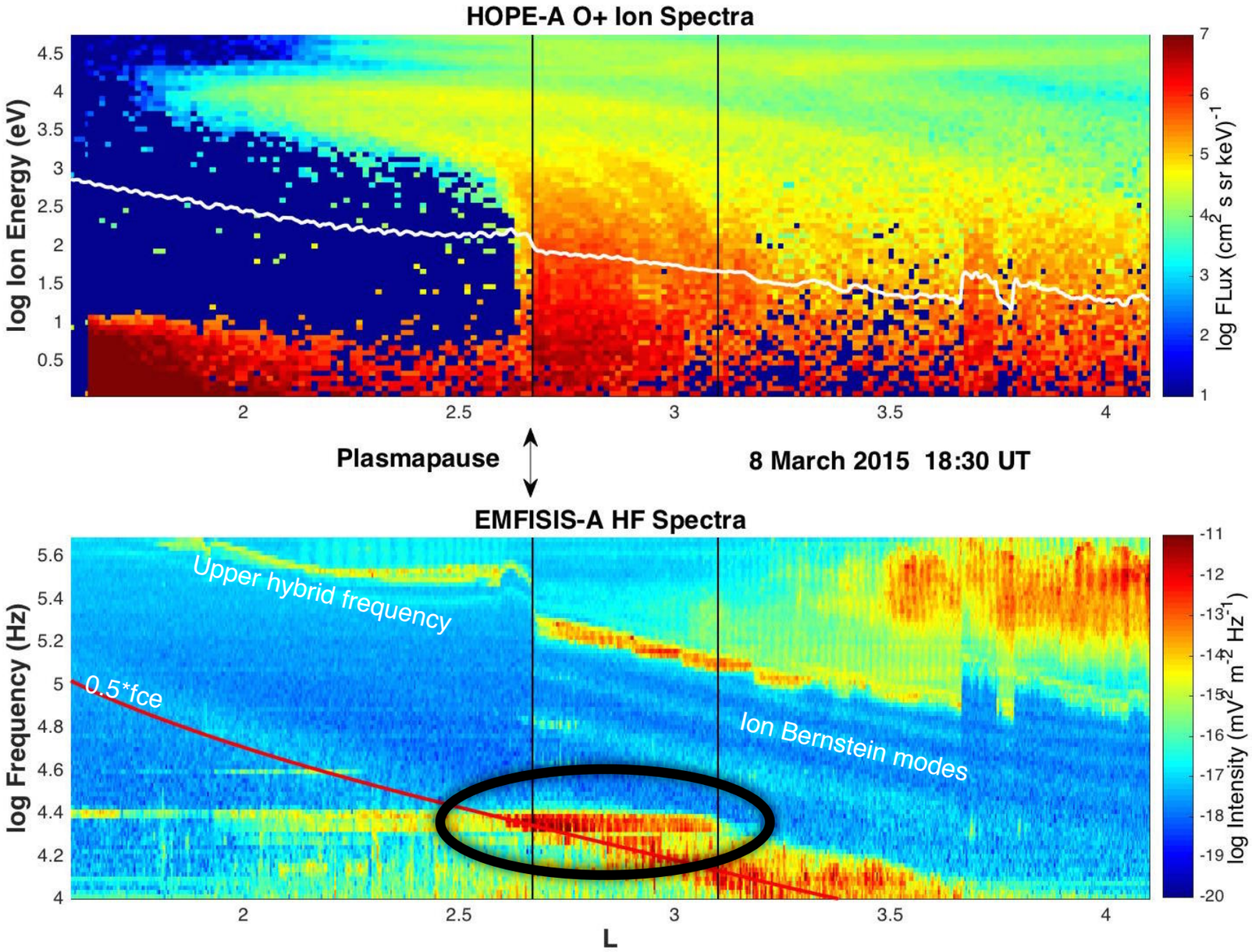

It is likely that VLF TX stimulates significant whistler wave growth outside the plasmasphere

e.g. Foster and Rosenberg, 1976

The VLF transmitter signal encounters a band of natural chorus emissions at 1⁄2 fce immediately beyond the plasmapause

Foster et al, 2016

VLF Wave-Particle Interactions: Enhanced Loss

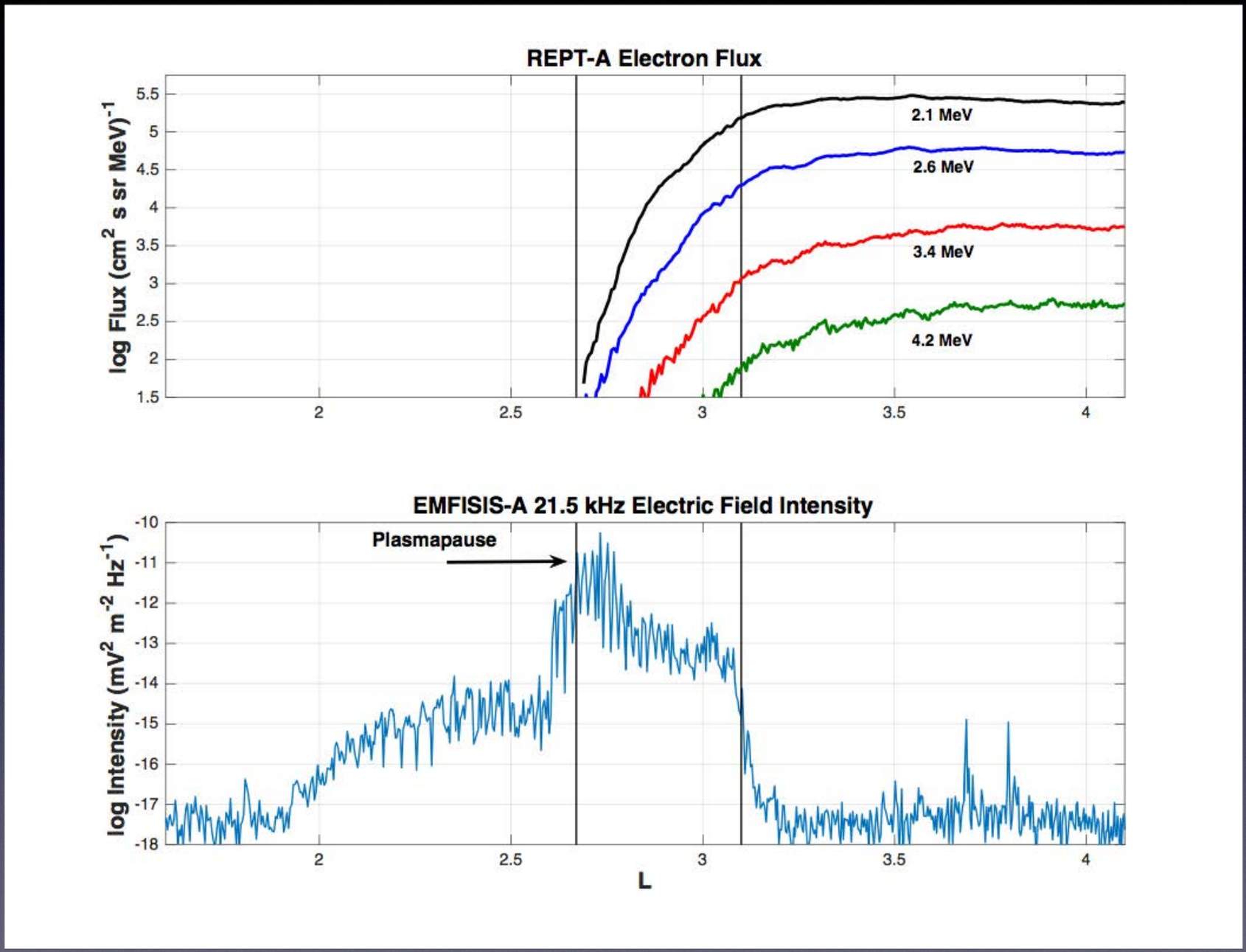

Foster et al, 2016

Cyclotron Resonance for Relativistic Particles

$$\omega - k_{\parallel} v_{\parallel} = -n\omega_{ce}/\gamma$$
$$\gamma = (1 - v^2/c^2)^{-\frac{1}{2}}$$

Cyclotron resonance:
note dependence on pitch angle, energy

$$n^2 = 1 - \frac{X}{1 - \frac{\frac{1}{2}Y^2 \sin^2\theta}{1-X} \pm \frac{1}{1-X}\left(\frac{1}{4}Y^4 \sin^4\theta + Y^2 \cos^2\theta\,(1-X)^2\right)^{1/2}}$$

Appleton-Hartree propagation equation in a cold, collisionless plasma

$$X = \omega_{pe}^2/\omega^2$$

$$Y = \omega_{ce}/\omega$$

Direct dependence on plasma density, wave normal angle
(determines roots of equation)

Wave-Particle Resonance at the ‘Impenetrable Barrier’

- Resonance conditions change drastically when cold plasma density drops outside plasmasphere
- VLF is resonant with UR electrons at the barrier location (60 deg PA)
- 700 Hz is resonant with UR electrons at the barrier location (15 deg PA)

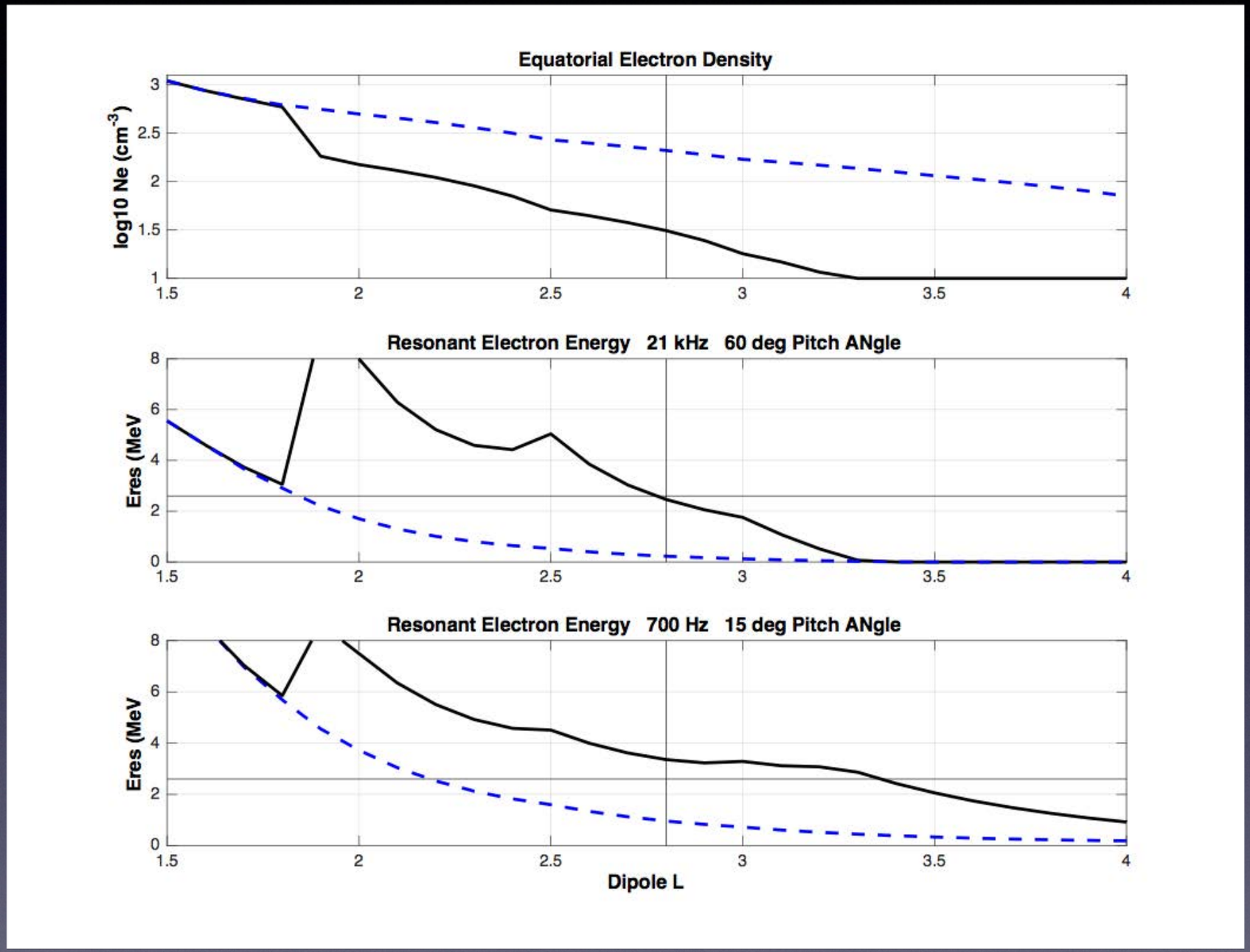

Foster et al, 2016

Barriers, Bubbles, and Plasmapause: The Big Picture

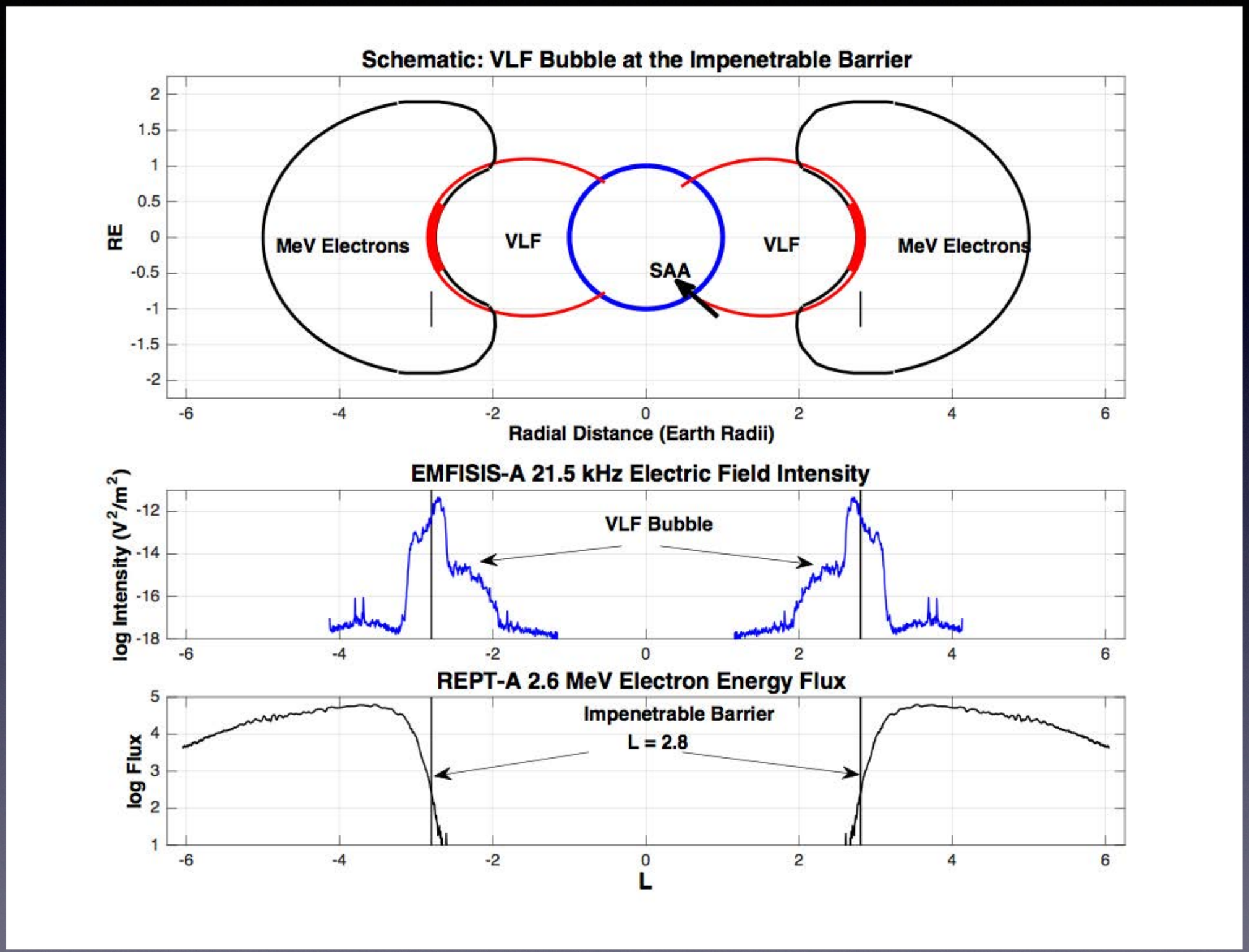

Foster et al, 2016

Summary

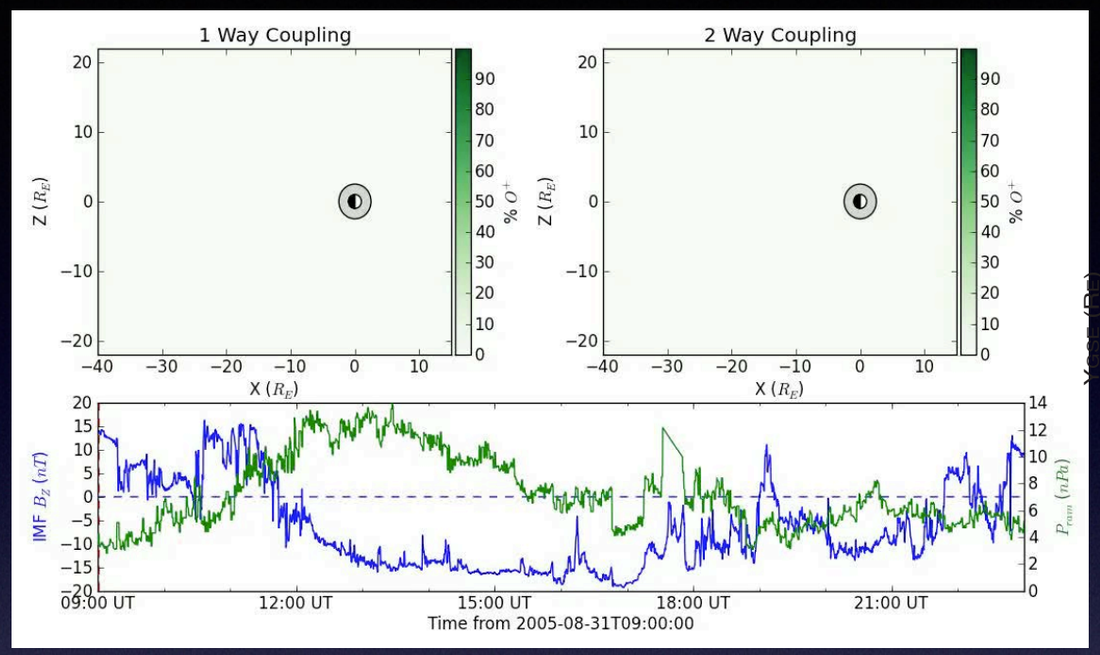

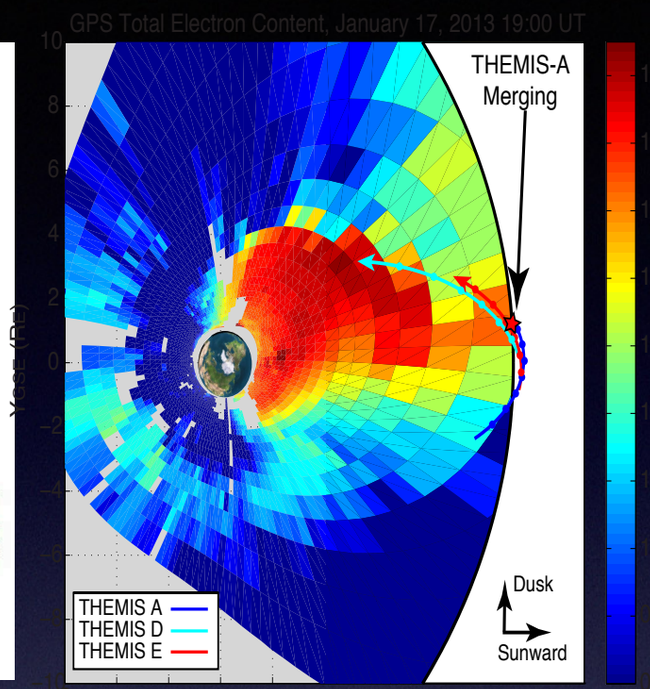

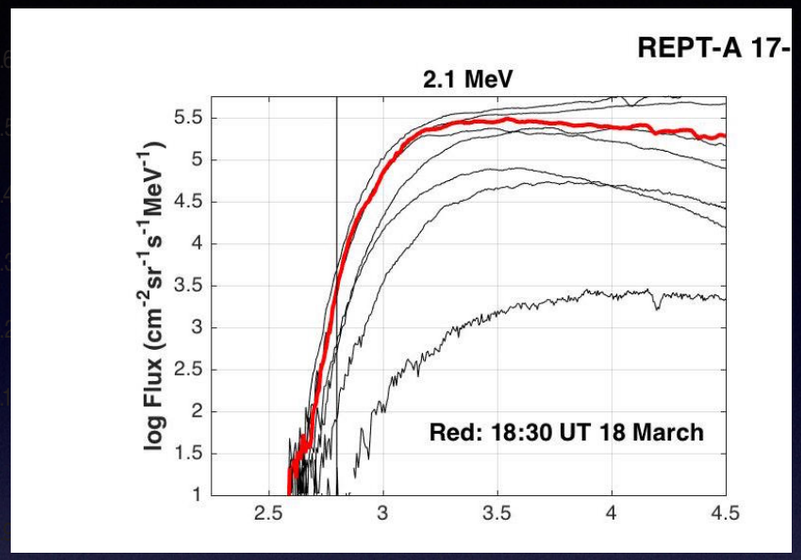

Cold plasma sources in the ionosphere are large

Cold plasma sources are transported through geospace

Cold plasma influence on fundamental processes is significant

Thanks for your attention!